

ISSN : 2165-4069(Online)

ISSN : 2165-4050(Print)



IJARAI

International Journal of  
Advanced Research in Artificial Intelligence

Volume 2 Issue 4

[www.ijarai.thesai.org](http://www.ijarai.thesai.org)

A Publication of  
The Science and Information Organization



# INTERNATIONAL JOURNAL OF ADVANCED RESEARCH IN ARTIFICIAL INTELLIGENCE



THE SCIENCE AND INFORMATION ORGANIZATION

[www.thesai.org](http://www.thesai.org) | [info@thesai.org](mailto:info@thesai.org)



# Editorial Preface

## *From the Desk of Managing Editor...*

"The question of whether computers can think is like the question of whether submarines can swim." — Edsger W. Dijkstra, the quote explains the power of Artificial Intelligence in computers with the changing landscape. The renaissance stimulated by the field of Artificial Intelligence is generating multiple formats and channels of creativity and innovation.

This journal is a special track on Artificial Intelligence by The Science and Information Organization and aims to be a leading forum for engineers, researchers and practitioners throughout the world.

The journal reports results achieved; proposals for new ways of looking at AI problems and include demonstrations of effectiveness. Papers describing existing technologies or algorithms integrating multiple systems are welcomed. IJARAI also invites papers on real life applications, which should describe the current scenarios, proposed solution, emphasize its novelty, and present an in-depth evaluation of the AI techniques being exploited. IJARAI focusses on quality and relevance in its publications.

In addition, IJARAI recognizes the importance of international influences on Artificial Intelligence and seeks international input in all aspects of the journal, including content, authorship of papers, readership, paper reviewers, and Editorial Board membership.

The success of authors and the journal is interdependent. While the Journal is in its initial phase, it is not only the Editor whose work is crucial to producing the journal. The editorial board members, the peer reviewers, scholars around the world who assess submissions, students, and institutions who generously give their expertise in factors small and large— their constant encouragement has helped a lot in the progress of the journal and shall help in future to earn credibility amongst all the reader members.

I add a personal thanks to the whole team that has catalysed so much, and I wish everyone who has been connected with the Journal the very best for the future.

**Thank you for Sharing Wisdom!**

**Managing Editor**  
**IJARAI**  
**Volume 2 Issue 4 April 2013**  
**ISSN: 2165-4069(Online)**  
**ISSN: 2165-4050(Print)**  
**©2013 The Science and Information (SAI) Organization**

# Editorial Board

**Peter Sapaty - Editor-in-Chief**

**National Academy of Sciences of Ukraine**

Domains of Research: Artificial Intelligence

**Alaa F. Sheta**

**Electronics Research Institute (ERI)**

Domain of Research: Evolutionary Computation, System Identification, Automation and Control, Artificial Neural Networks, Fuzzy Logic, Image Processing, Software Reliability, Software Cost Estimation, Swarm Intelligence, Robotics

**Antonio Dourado**

**University of Coimbra**

Domain of Research: Computational Intelligence, Signal Processing, data mining for medical and industrial applications, and intelligent control.

**David M W Powers**

**Flinders University**

Domain of Research: Language Learning, Cognitive Science and Evolutionary Robotics, Unsupervised Learning, Evaluation, Human Factors, Natural Language Learning, Computational Psycholinguistics, Cognitive Neuroscience, Brain Computer Interface, Sensor Fusion, Model Fusion, Ensembles and Stacking, Self-organization of Ontologies, Sensory-Motor Perception and Reactivity, Feature Selection, Dimension Reduction, Information Retrieval, Information Visualization, Embodied Conversational Agents

**Liming Luke Chen**

**University of Ulster**

Domain of Research: Semantic and knowledge technologies, Artificial Intelligence

**T. V. Prasad**

**Lingaya's University**

Domain of Research: Bioinformatics, Natural Language Processing, Image Processing, Robotics, Knowledge Representation

**Wichian Sittiprapaporn**

**Maharakham University**

Domain of Research: Cognitive Neuroscience; Cognitive Science

**Yaxin Bi**

**University of Ulster**

Domains of Research: Ensemble Learning/Machine Learning, Multiple Classification Systems, Evidence Theory, Text Analytics and Sentiment Analysis

---

## Reviewer Board Members

- **Alaa Sheta**  
Electronics Research Institute (ERI)
- **Albert Alexander**  
Kongu Engineering College
- **Amir HAJJAM EL HASSANI**  
Université de Technologie de Belfort-Monbéliard
- **Amit Verma**  
Department in Rayat & Bahra Engineering College, Mo
- **Antonio Dourado**  
University of Coimbra
- **B R SARATH KUMAR**  
Lenora College of Engineering
- **Babatunde Opeoluwa Akinkunmi**  
University of Ibadan
- **Bestoun S.Ahmed**  
Universiti Sains Malaysia
- **Chien-Peng Ho**  
Information and Communications Research Laboratories, Industrial Technology Research Institute of Taiwan
- **David M W Powers**  
Flinders University
- **Dimitris Chrysostomou**  
Democritus University
- **Dr.Dhananjay R Kalbande**  
Mumbai University
- **Francesco Perrotta**  
University of Macerata
- **Frank Ibikunle**  
Covenant University
- **Grigoras Gheorghe**  
"Gheorghe Asachi" Technical University of Iasi, Romania
- **Guandong Xu**  
Victoria University
- **Haibo Yu**  
Shanghai Jiao Tong University
- **Jatinderkumar R. Saini**  
S.P.College of Engineering, Gujarat
- **Krishna Prasad Miyapuram**  
University of Trento
- **Luke Liming Chen**  
University of Ulster
- **Marek Reformat**  
University of Alberta
- **Md. Zia Ur Rahman**  
Narasaraopeta Engg. College, Narasaraopeta
- **Mokhtar Beldjehem**  
University of Ottawa
- **Monji Kherallah**  
University of Sfax
- **Nitin S. Choubey**  
Mukesh Patel School of Technology Management & Eng
- **Rajesh Kumar**  
National University of Singapore
- **Rajesh K Shukla**  
Sagar Institute of Research & Technology-Excellence, Bhopal MP
- **Rongrong Ji**  
Columbia University
- **Said Ghoniemy**  
Taif University
- **Samarjeet Borah**  
Dept. of CSE, Sikkim Manipal University
- **Sana'a Wafa Tawfeek Al-Sayegh**  
University College of Applied Sciences
- **Saurabh Pal**  
VBS Purvanchal University, Jaunpur
- **Shahaboddin Shamshirband**  
University of Malaya
- **Shaidah Jusoh**  
Zarqa University
- **Shrinivas Deshpande**
- **SUKUMAR SENTHILKUMAR**  
Universiti Sains Malaysia
- **T C.Manjunath**  
HKBK College of Engg
- **T V Narayana Rao**  
Hyderabad Institute of Technology and Management
- **T. V. Prasad**

Lingaya's University

- **Vitus S.W Lam**  
Domains of Research
- **VUDA Sreenivasarao**  
St. Mary's College of Engineering &  
Technology
- **Vishal Goyal**
- **Wei Zhong**  
University of south Carolina Upstate
- **Wichian Sittiprapaporn**  
Mahasarakham University
- **Yaxin Bi**

University of Ulster

- **Yuval Cohen**  
The Open University of Israel
- **Zhao Zhang**  
Deptment of EE, City University of Hong  
Kong
- **Zne-Jung Lee**  
Dept. of Information management, Huafan  
University
- **Zhigang Yin**  
Institute of Linguistics, Chinese Academy of  
Social Sciences

# CONTENTS

**Paper 1: Comparison between Linear and Nonlinear Models of Mixed Pixels in Remote Sensing Satellite Images Based on Cierniewski Surface BRDF Model by Means of Monte Carlo Ray**

*Authors: Kohei Arai*

**PAGE 1 – 7**

**Paper 2: E-Learning System Utilizing Learners' Characteristics Recognized Through Learning Processes**

*Authors: Kohei Arai, Anik Nur Handayani*

**PAGE 8 – 12**

**Paper 3: Method for Car in Dangerous Action Detection by Means of Wavelet Multi Resolution Analysis Based on Appropriate Support Length of Base Function**

*Authors: Kohei Arai, Tomoko Nishikawa*

**PAGE 13 – 17**

**Paper 4: Geography Markup Language: GML Based Representation of Time Serie of Assimilation Data and Its Application to Animation Content Creation and Representations**

*Authors: Kohei Arai*

**PAGE 18 – 22**

**Paper 5: Improvement of Automated Detection Method for Clustered Microcalcification Based on Wavelet Transformation and Support Vector Machine**

*Authors: Kohei Arai, Indra Nugraha Abdullah, Hiroshi Okumura, Rie Kawakami*

**PAGE 23 – 28**

**Paper 6: A Simulated Multiagent-Based Architecture for Intrusion Detection System**

*Authors: Onashoga S. Adebukola, Ajayi O. Bamidele, Akinwale A. Taofik*

**PAGE 29 – 38**

**Paper 7: Applying Inhomogeneous Probabilistic Cellular Au-tomata Rules on Epidemic Model**

*Authors: Wesam M. Elsayed, Ahmed H. El-bassiouny, Elsayed F. Radwan*

**PAGE 39 – 47**

**Paper 8: Fusion of Saliency Maps for Visual Attention Selection in Dynamic Scenes**

*Authors: Jiawei Xu, Shigang Yue*

**PAGE 48 – 58**

**Paper 9: Web-based Expert Decision Support System for Tourism Destination Management in Nigeria**

*Authors: Yekini Nureni Asafe, Adetoba Bolaji, Aigbokhan Edwin Enaholo, Oluwafemi Olubukola*

**PAGE 59 – 63**

**Paper10: Category Decomposition Method for Un-Mixing of Mixels Acquired with Spaceborne Based Visible and Near Infrared Radiometers by Means of Maximum Entropy Method with Parameter Estimation Based on Simulated Annealing**

*Authors: Kohei Arai*

**PAGE 64 – 69**

# Comparison Between Linear and Nonlinear Models of Mixed Pixels in Remote Sensing Satellite Images Based on Cierniewski Surface BRDF Model by Means of Monte Carlo Ray Tracing Simulation

Kohei Arai

Graduate School of Science and Engineering  
Saga University  
Saga City, Japan

**Abstract**—Comparative study on linear and nonlinear mixed pixel models of which pixels in remote sensing satellite images is composed with plural ground cover materials mixed together, is conducted for remote sensing satellite image analysis. The mixed pixel models are based on Cierniewski of ground surface reflectance model. The comparative study is conducted by using of Monte Carlo Ray Tracing: MCRT simulations. Through simulation study, the difference between linear and nonlinear mixed pixel models is clarified. Also it is found that the simulation model is validated.

**Keywords**—Monte Carlo simulation; ray tracing method; mixed pixel model; surface model;

## I. INTRODUCTION

All land pixels in remote sensing images are essentially mixed pixels that consist of multiple ground cover materials. Currently, there are two types of models aiming to untangle these contributions: linear and non-linear mixture models. The linear mixture models assume negligible interactions among distinct ground cover materials while the nonlinear mixture models assume that incident solar radiation is scattered within the scene itself and that these interaction events may involve several types of ground cover materials.

R. Singer and T. B. McCord (1979) [1], B. Hapke (1981) [2] and R. N. Clark and T. I. Roush (1984) [3] proposed linear mixture models while R. Singer (1974) [4], B. Nash and J. Conel (1974) [5] proposed nonlinear mixture models for the mixed pixels containing different mineral resources. Meanwhile, C. C. Borel and S. A. Gerst (1994) [6] proposed another nonlinear mixture model for vegetated areas. These nonlinear mixture pixel models, however, did not take into consideration the influence of topographic features or the influence of multiple scattering in the atmosphere. Meanwhile, Cierniewski proposed a surface model which consists of two dimensional array of ellipsoidal shapes of elements [7]. One of the specific features of the Cierniewski's surface model is representation of Bi-Directional Reflectance Function: BRDF. Although there are some nonlinear mixture models, there is no nonlinear mixed pixel model taking into account BRDF of the surface in concern.

A nonlinear mixture model for the interpretation of mixed pixels in remote sensing satellite images is proposed. The proposed model is a Monte Carlo Ray-Tracing: MCRT model that takes into account interactions among the ground cover materials (multiple reflections among the materials on the surface) [8]. The proposed model also takes into account topographic features (slope) of the ground surface. As an example, Top of the Atmosphere: TOA radiance of mixed pixels based on the proposed nonlinear model is compared to that of the conventional linear model.

This paper proposes a nonlinear mixed pixel model that takes into account topographic features of the surface and multiple scattering in the atmosphere. Furthermore, the proposed nonlinear mixed pixel model takes into account interactions among ground cover materials separated by different distances and having different shapes. Since multiple scattering interactions in three dimensional media are not so easy to solve using the radiative transfer equation, the proposed mixture model is based on Monte Carlo Ray-Tracing: MCRT.

Section 2 describes the proposed nonlinear mixed pixel model together with details of the MCRT algorithm. Section 3 presents experimental results showing the influence of multiple scattering interactions between trees, the shape of the trees, the slope of the terrain, and the atmospheric optical depth. Finally, the model derived TOA radiance is compared between linear and nonlinear models.

## II. PROPOSED MODEL

### A. Monte Carlo Ray-Tracing:MCRT Simulation Model

Nonlinear mixture model and brief description of Monte Carlo Ray-Tracing model: MCRT. Nonlinear mixing model proposed here is composed with more than two ground cover materials and is based on the MCRT model. In order to take into account the geographical feature, slope of the ground surface can be changed. Also any ground cover materials can be set for the ground surface together with different shape of ground cover materials. The simulation with MCRT model is called MCRT Simulation, MCRTS (Arai, 2005) [9]. In MCRTS, 50 by 50 by 50km of simulation cell size is assumed.



The ground surface is composed with two planes, surface A and B, with the different slopes,  $\alpha$  and  $\beta$  and with surface reflectance,  $\Gamma_A$  and  $\Gamma_B$  as is shown in Figure 1. a and b show IFOV on the ground for the surface A and B.

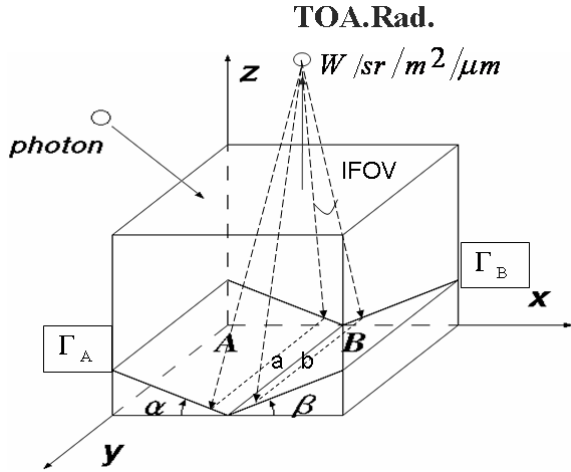


Fig.1. Nonlinear mixed pixel model based on Monte Carlo Ray-Tracing Simulation model with 50x50x50km cell and two ground surfaces (The pixels situated along with border between two surface are mixed pixels).

A photon is put in the simulation cell from the top of the cell with the incidence angle that depends on the specified solar zenith angle. The position of which the photon is put in is changed by time by time in accordance with the uniformly distributed random numbers which are generated by Mersenne Twister<sup>1</sup>.

Depending on the optical depth of the atmosphere, free travel length  $L$  of photon is determined as follows,

$$L = -L_0 \log(Rnd) \quad (1)$$

$$L_0 = \frac{h}{\tau_{all}} \quad (2)$$

where  $L_0$  is called free travel length, denoting the average distance of interaction of a photon from one position to another.  $Rnd$  is uniformly distributed random numbers ranges from 0 to 1.  $h$  denotes the physical height of the atmosphere (50km in this case) while  $\tau_{all}$  denotes the optical depth of the atmosphere which is determined as follows,

$$\tau_{all} = \tau_{aero} + \tau_{mol} \quad (3)$$

where the subscript *aero* is associated with aerosols while *mol* with molecules. Here, it is assumed that atmosphere consists of aerosols and air molecules. Because the wavelength in concern ranges from 450 to 1050nm so that optical depth of ozone and water vapors are assumed to be

negligible except 936nm of water vapor absorption band. A small absorption due to ozone is situated from 500 to 650nm around.

The photon meets aerosol particles or molecule when the photon travels in the atmosphere then scattering due to the aerosols or molecules occurs. The probability of the collision to the aerosols or molecules depends on their optical depths. If the endpoint of photon travel is in the atmosphere, the photon meets aerosol or molecule. The probability of the photon meets aerosol is  $\tau_{aero} / \tau_{all}$  while that of the photon meets molecule is  $\tau_{mol} / \tau_{all}$ . In accordance with the phase function of aerosols or molecules, the photon is scattered. Strength of scattering as a function of scattering angle  $\theta$  is determined by the phase function,  $P(\theta)$ , the Rayleigh for molecules, equation (4) and Heyney-Greestein function, equation (5) (it is just an approximation function of which the phase function is monotonically decreasing) for aerosols. Actual phase function can be determined with MODTRAN 4.0 of Mie code with the measured refractive index of aerosols through field experiments. By using uniformly distributed random numbers, scattering direction is determined. The phase function as  $P(\theta)$ , where  $\theta$  is the angle between the incident direction and the scattering direction.

For molecules, the Rayleigh phase function is as follows,

$$P(\theta) = (3/4)(1 + \cos^2 \theta) \quad (4)$$

while that for aerosols, we use the Heyney-Greenstein approximation function of the following,

$$P(\theta) = \frac{1 - g_\lambda^2}{(1 + g_\lambda^2 - 2g_\lambda \cos \theta)^{3/2}} \quad (5)$$

where  $g_\lambda$  is the asymmetry factor of the aerosol phase function which depends on the wavelength of the radiation and the compositions, sizes, and the shapes of the aerosol particles.

In the calculation of TOA radiance, the number of photons,  $N$  which comes out from the top of the atmosphere within the angle range which corresponds to the Instantaneous Field of View: IFOV of the sensor in concern is used thus the normalized TOA radiance,  $Rad$  is determined as follows,

$$Rad = \frac{\mu_0 \mu \Delta \mu}{2} \left( \frac{N}{N_{total}} \right) \quad (6)$$

where  $\mu_0 = \cos \theta_0$ ,  $\mu = \cos \theta$ ,  $\theta_0$  is the solar zenith angle and  $\theta$  is a viewing solid angle.  $\Delta \mu$  is a view solid angle, i.e., FOV (field of view).  $N_{total}$  is the number of photons which are put in the cell in total. If you multiply solar irradiance to  $Rad$  in unit of (W/m<sup>2</sup>/sr/ $\mu$ m), then the TOA radiance in the same unit is calculated.

The input parameters are determined by field experimental data. They are (1) Material reflectance which is albedo of the entire ground cover material, (2) Background surface material

<sup>1</sup> Mersenne Twister (MT), <http://www.math.sci.hiroshima-u.ac.jp/~m-mat/MT/mt.html>

reflectance, (3) Material-material distance, (4) Optical depth of aerosol and molecule, (5) Solar zenith and azimuth angles, (6) IFOV of the sensor, (7) Sensor direction (view zenith angle) and height. On the other hand, output parameters include TOA radiance and ten groups of photons. They are (1) Photons that are put in the atmosphere from the top of cell in total, (2) Photons that are come from the top of the cell within the range of IFOV, (3) Photons that are reflected by material, (4) Photons that are absorbed by material, (5) Photons that are reflected on the background, (6) Photons that are absorbed on the background, (7) Photons that are scattered by aerosols, (8) Photons that are absorbed by aerosols, (9) Photons that are scattered by molecules and (10) Photon that are absorbed by molecule. A photon equation must be formed, that is, the number of put-in-photons must be equal to the sum of come-out-photons which are come-out from the top of cell and the photons which are absorbed by aerosols and molecules, material and background. Each simulation has proved this equation.

From the results from the preliminary MCRTS with a plenty of input parameters, it is concluded that 700,000 of put-in-photons would be enough for the MCRTS in many cases.

**B. Surface Model**

Figure 2 shows Cierniewski surface Bi-Directional Reflectance Distribution Function: BRDF model based ground surface model.

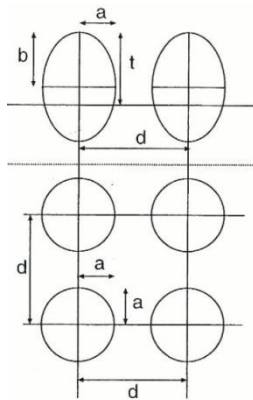


Fig.2. Cierniewski based ground surface model (Side view: above, Top view: bottom)

The proposed model is composed with two dimensional array of ellipsoidal shape of elements. These elements are shaped with ellipsoidal shape (shorter radius of “a” and longer radius of “b”) and are two dimensionally aligned with the interval of “d”. These surfaces are situated on the ground surface in the defined space of MCRT model. The sun, sensor onboard remote sensing satellites are situated as shown in Figure 3.

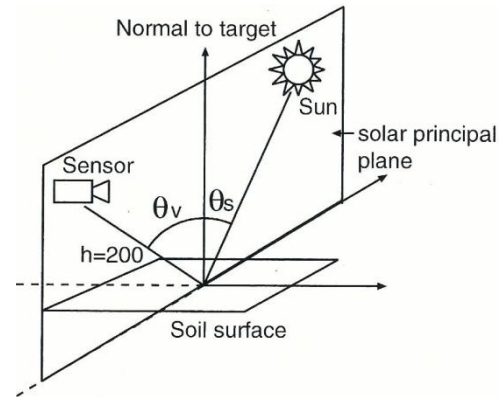


Fig.3. Geometric relations among the sun, sensor, and ground surface (soil surface)

In the principal plane among the sun, sensor, and the point of ground cover target on ground surface, solar zenith angle, observation zenith angle, slant range, and Instantaneous Field of View: IFOV are defined as shown in Figure 4.

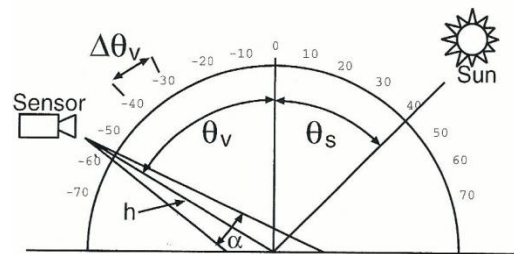


Fig.4. Definitions of solar zenith angle, observation zenith angle, slant range, and Instantaneous Field of View: IFOV

These surface models are situated left and right ground surface with the designated slopes separately for linear model while these surfaces are situated with the same slopes interactively for nonlinear model as shown in Figure 5. Geometric relation for these mixed pixel models are shown in Figure 6.

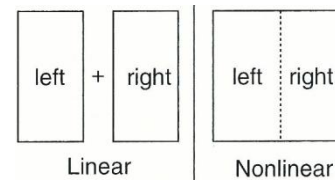
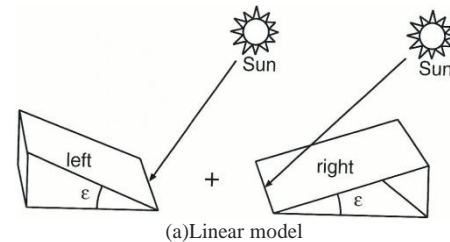


Fig.5. Linear and Nonlinear mixed pixel models



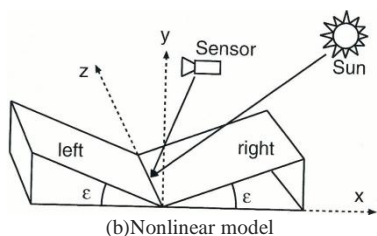


Fig.6. Linear and nonlinear mixed pixel models

### III. EXPERIEMNTS

#### A. Comparison to Cierniewski Surface Model

Slope zero of flat surface is assumed to be simulated. Table 1 shows the parameters for the simulation. All the simulation studies hereafter are conducted at the wavelength of 500nm. Figure 7 shows an example of the Bi-Directional Reflectance Function: BRDF with slope zero surface.

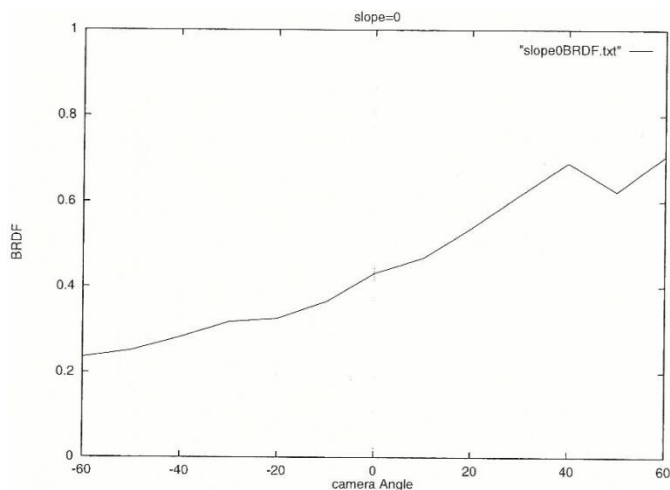


Fig.7. BRDF of the slope zero surface based on proposed surface model derived from the MCRT simulation

TABLE I. GIVEN PARAMETRS FOR THYE PROPOSED SURFACE MODEL

(a)Geometric relations among the sun, sensor and ground target

$\theta_s$	41.0	h	200
$\theta_v$	$-60^\circ \sim 60^\circ$	$\epsilon$	$0^\circ$
$\Delta_v$	10	$\Delta_\epsilon$	$0^\circ$
$\alpha$	4		

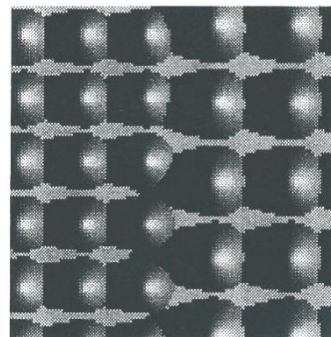
(b)Parameters for ellipsoid

	left	right
a	2.5	2.0
b	5.0	4.0
d	5.4	4.2
t	5.0	4.0

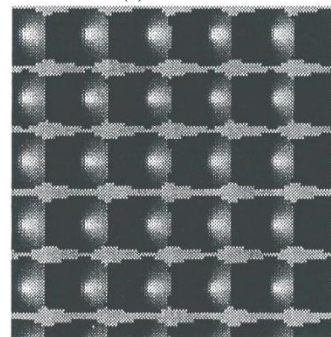
There is the hot spot at around 40 degree of observation angle (camera angle) because of solar zenith angle is 41 degree.

#### B. Comparison between Linear and Nonlinear Mixture Model of the Mixed Pixels in Concern

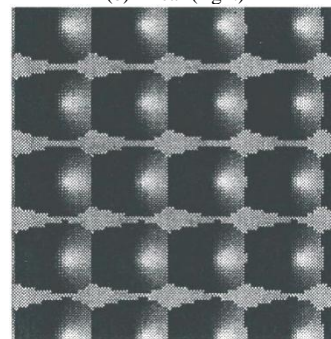
Figure 8 (a) shows how the surface of nonlinear mixture model looks like while Figure 8 (b) and (c) shows, respectively, how the surface of linear mixture model looks like (Top view).



(a)Nonlinear



(b)Linear (right)



(c)Linear (left)

Fig.8. Examples of outlooks of the surface with ellipsoidal shapes of elements based surfaces for linear and nonlinear mixed pixel models.

Nonlinear mixed pixel model assumes the flat surface of Figure 8 (a) of pixel with half mixing ratios for each surface. Then, MCRT simulation is conducted once. On the other hand, linear mixed pixel model assumes the flat surface of the linear right (Figure 8 (b)) and the linear left Figure 8 (c)), separately. Then, MCRT simulation result for each surface is combined together after MCRT simulation.

BRDF derived from the MCRT simulation with the linear and nonlinear surface mixture models is shown in Figure 9.

The parameters for this simulation are shown in Table 2. Hot spot is situated at around observation angle of 40 degree. The difference between linear and nonlinear models is quite small.

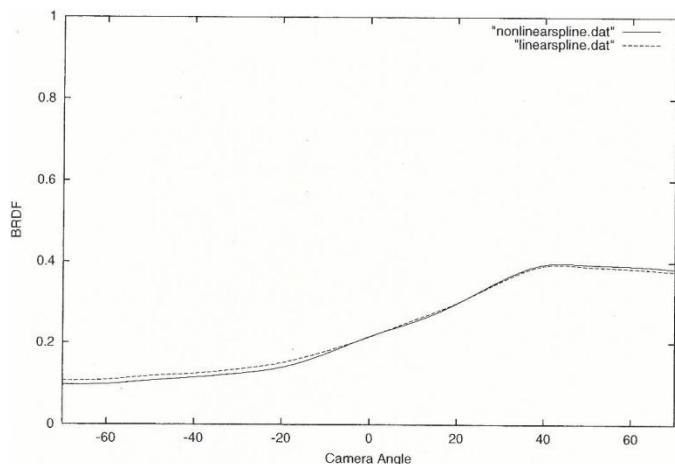


Fig.9. BRDF derived from the MCRT simulation with the linear and nonlinear surface mixture models

TABLE II. GIVEN PARAMETERS FOR THYE PROPOSED SURFACE MODEL

(a)Geometric relations among the sun, sensor and ground target

$\theta_s$	36.9	h	200
$\theta_v$	-70° ~ 70°	$\epsilon$	0°
$\Delta_v$	10	$\Delta_\epsilon$	0°
$\alpha$	4		

(b)Parameters for ellipsoid

	left	right
a	1.4	1.9
b	8.5	11.5
d	2.6	3.2
t	4.1	4.5

Dotted line in Figure 9 shows linear model derived BRDF while solid line shows nonlinear model derived BRDF. Linear model derived BRDF is little bit greater than that of nonlinear model derived BRDF. Due to multiple reflection between two slopes, BRDF decreases for the nonlinear mixture surface model.

### C. TOA Radiance Comparison between Linear and Nonlinear Mixture Models

Top of the Atmosphere: TOA radiance ( $W/cm^2/str$ ) is estimated based on MCRT simulation with the parameters of Table 2 as functions of optical depth of atmospheric molecule and aerosol. The MCRT simulation is conducted with the parameters shown in Table 2 except observation angle. The designated observation angle is zero of zenith angle, nadir view. Figure 10 (a) and (b) shows the difference between linear and nonlinear mixture surface models derived TOA radiances for the surface reflectance of 0.2 (a) and 0.4 (b), respectively. The vertical axis of Figure 10 shows nonlinear model based TOA radiance minus linear model based TOA radiance. TOA radiance depends on the reflectance significantly. These results are compared to those derived from MODTRAN 4. Both TOA radiances show good coincidence. Therefore, the proposed simulation model is validated.

The parameters for surface model of ellipsoidal shapes are changed. The TOA radiance with surface reflectance of 0.4 differences between linear and nonlinear models is shown in Figure 11 for aerosol optical depth of 0.1 and molecule optical depth of 0.1. Figure 11 (a) shows the case that the parameter “a” is changed for left slope with keeping the parameter “a” for right slope at 1.9. The parameters for Figure 11 (b) to (i) are shown below,

- (b)Left a=1.4, right a=1.1-2.1
- (c)Left b=10.9-11.5, right b=11.5
- (d)Left b=8.5, right b=7.9-8.9
- (e)Left d=2.2-3.2, right d=3.2
- (f)Left d=2.6, right d=2.8-3.6
- (g)left t=3.7-4.5, right t=4.5
- (h)Left t=4.1, right t=4.1-4.9
- (i) $\epsilon=0-20$  degree,  $t=0.0, n0.5, 1.0$ , aerosol optical depth=0.2, and molecule optical depth=0.2 where  $\epsilon$  denotes slope angle of the surface in concern.

The vertical axis of Figure 11 shows nonlinear mixture model based TOA radiance minus linear mixture model based TOA radiance.

In comparison to linear and nonlinear mixture models derived TOA radiance as a function of b is not so significant comparing to those for the parameter a. On the other hand, the parameters of d and t are significant. Meanwhile, surface slope is much significant in particular for the slope angle is much larger than 15 degree.

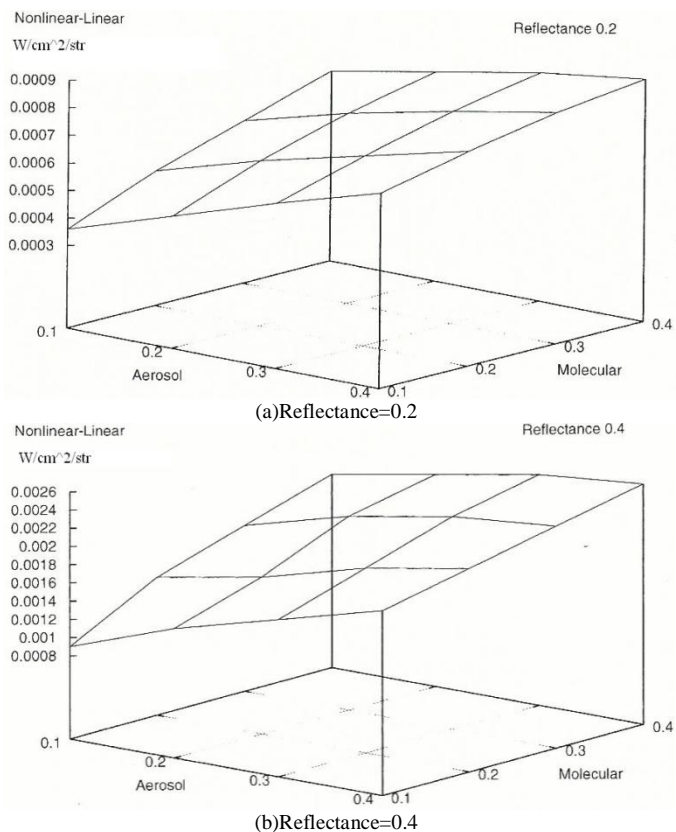
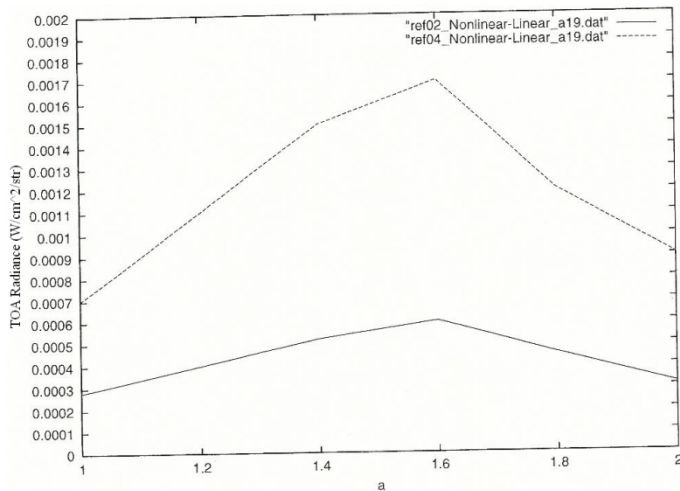
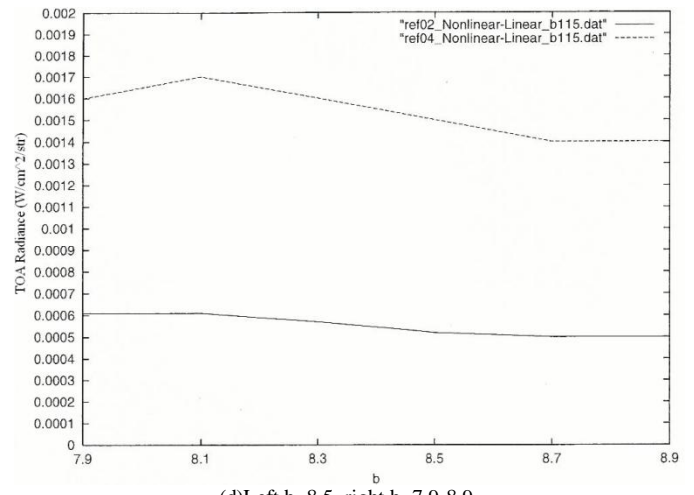


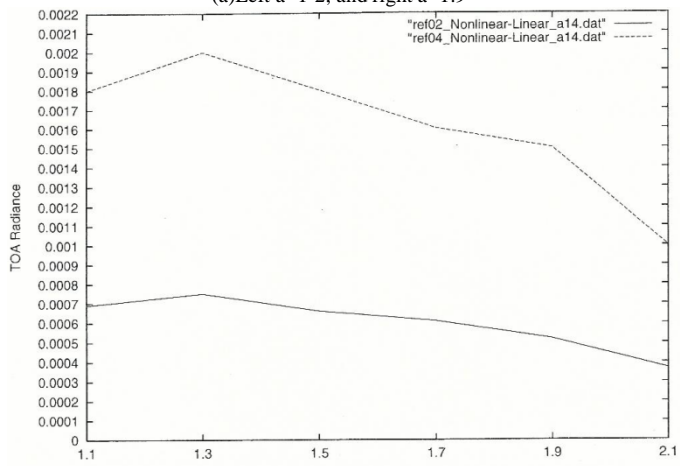
Fig.10. Estimated TOA radiances as function of aerosol and molecule optical depth as well as surface reflectance.



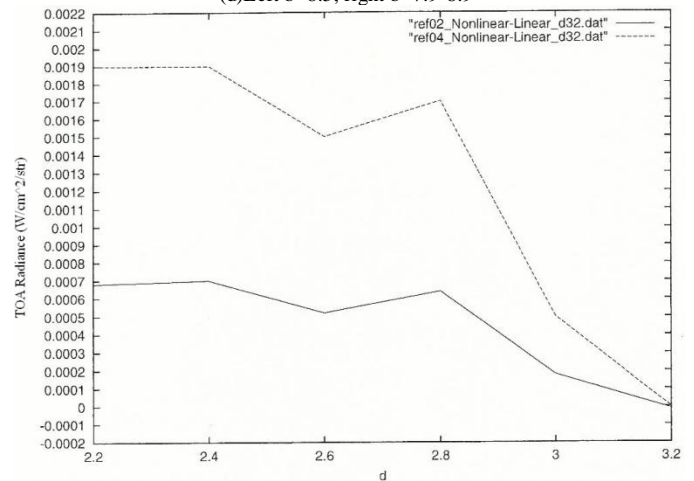
(a) Left a=1-2, and right a=1.9



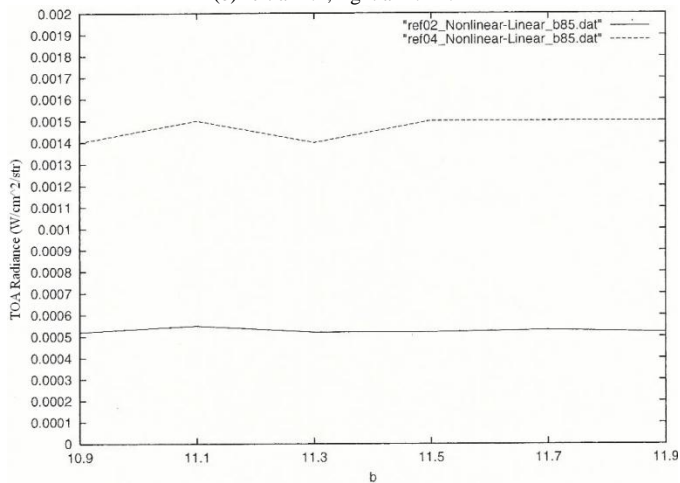
(d) Left b=8.5, right b=7.9-8.9



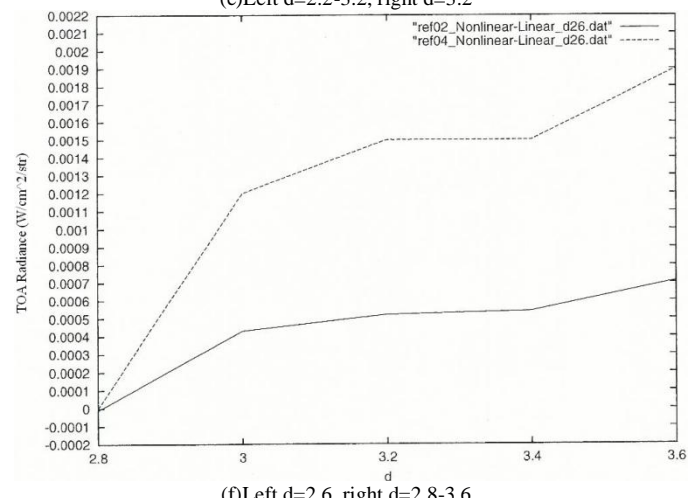
(b) Left a=1.4, right a=1.1-2.1



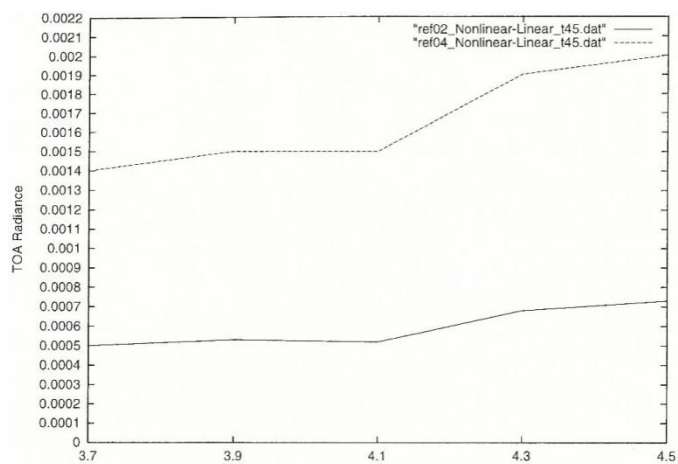
(e) Left d=2.2-3.2, right d=2.8-3.2



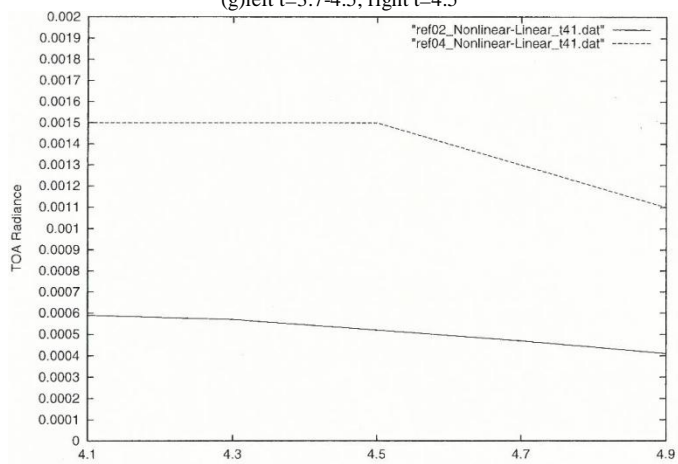
(c) Left b=10.9-11.5, right b=11.5



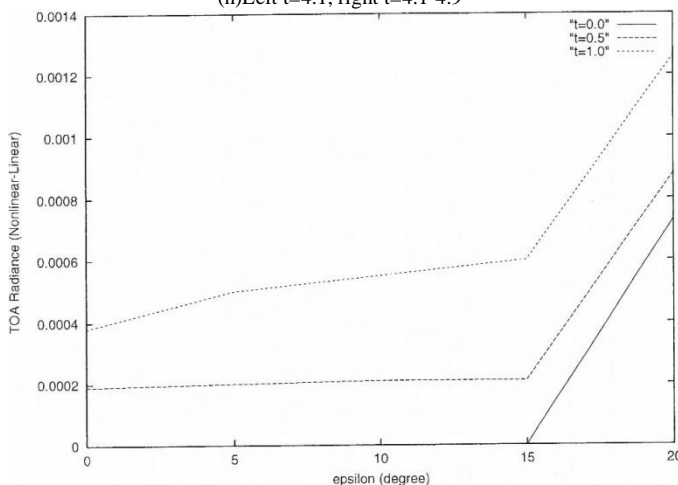
(f) Left d=2.6, right d=2.8-3.6



(g)left t=3.7-4.5, right t=4.5



(h)Left t=4.1, right t=4.1-4.9



(i) $\epsilon=0-20$  degree,  $t=0.0, 0.5, 1.0$ , aerosol optical depth=0.2, and molecule optical depth=0.2

Fig.11. TOA radiance difference between linear and nonlinear mixture models

#### IV. CONCLUSION

Comparative study on linear and nonlinear mixed pixel models of which pixels in remote sensing satellite images is

composed with plural ground cover materials mixed together, is conducted for remote sensing satellite image analysis. The mixed pixel models are based on Cierniewski of ground surface reflectance model.

The comparative study is conducted by using of Monte Carlo Ray Tracing: MCRT simulations. Through simulation study, the difference between linear and nonlinear mixed pixel models is clarified. Also it is found that the simulation model is validated.

In comparison to linear and nonlinear mixture models derived TOA radiance as a function of  $b$  is not so significant comparing to those for the parameter  $a$ . On the other hand, the parameters of  $d$  and  $t$  are significant. Meanwhile, surface slope is much significant in particular for the slope angle is much larger than 15 degree.

#### ACKNOWLEDGMENT

The author would like to thank Mis. Reiko Inagaki for her efforts through experiments and simulations.

#### REFERENCES

- [1] R.Singer and T.B.McCord, Mars; Large scale mixing of bright and dark surface materials and implications for analysis of spectral reflectance, Proc., 10<sup>th</sup> Lunar and Planetary Sci., Conf., 1835-1848, 1979.
- [2] B.Hapke, Bidirection reflectance spectroscopy, I. Theory, Journal of Geophysical Research, 86, 3039-3054, 1981.
- [3] R.N.Clark and T.I.Roush, Reflectance spectroscopy: Quantitative analysis techniques for remote sensing applications, Journal of Geophysical Research, 89, B7, 6329-6340, 1984.
- [4] R.Singer, Near infrared spectral reflectance of mineral mixtures: Systematic combinations of pyroxenes olivine and iron oxides, Journal of Geophysical Research, 86, 7967-7982, 1974.
- [5] B.Nash and J.Conel, Spectral reflectance systematic for mixtures of powdered hypersthene, labradorite and ilmenite, Journal of Geophysical Research, 79, 1615-1621, 1974.
- [6] C.C.Borel and S.A.Gerst, Nonlinear spectral mixing models for vegetative and soils surface, Remote Sensing of the Environment, 47, 2, 403-416, 1994.
- [7] J.Cierniewski, Geometrical modelling of soil bi-directional reflectance in the optical domain, Bougucki Scientific Publishers, 1999.
- [8] K.Arai, Fundamental Theory on Remote Sensing, Gakujutu-tosho-Shuppan, Publishing Co. Ltd., 2001.
- [9] Arai, K, Lecture Notes on Remote Sensing, Morikita-Shuppan, Co.Ltd., 2005

#### AUTHORS PROFILE

**Kohei Arai**, He received BS, MS and PhD degrees in 1972, 1974 and 1982, respectively. He was with The Institute for Industrial Science and Technology of the University of Tokyo from April 1974 to December 1978 also was with National Space Development Agency of Japan from January, 1979 to March, 1990. During from 1985 to 1987, he was with Canada Centre for Remote Sensing as a Post Doctoral Fellow of National Science and Engineering Research Council of Canada. He moved to Saga University as a Professor in Department of Information Science on April 1990. He was a councilor for the Aeronautics and Space related to the Technology Committee of the Ministry of Science and Technology during from 1998 to 2000. He was a councilor of Saga University for 2002 and 2003. He also was an executive councilor for the Remote Sensing Society of Japan for 2003 to 2005. He is an Adjunct Professor of University of Arizona, USA since 1998. He also is Vice Chairman of the Commission "A" of ICSU/COSPAR since 2008. He wrote 30 books and published 322 journal papers

# E-Learning System Utilizing Learners' Characteristics Recognized Through Learning Processes with Open Simulator

## Overcoming Weak Points through Dialogs with Avatars in Open Simulator in Learning Processes

Kohei Arai

Graduate School of Science and Engineering  
Saga University  
Saga City, Japan

Anik Nur Handayani

Graduate School of Science and Engineering  
Saga University  
Saga City, Japan

**Abstract**—E-learning system utilizing learners' characteristics which is recognized through learning processes with Open Simulator for overcoming weak points is proposed. Through dialogs with avatars in the Open Simulator, it is possible to understand learners' weak points. Using learners' characteristics, most appropriate subjects and achievement tests are provided by the proposed e-learning system. Experimental results show that the proposed e-learning system is much effective than the conventional e-learning system without utilizing learners' characteristics.

**Keywords**—e-learning system; Q/A System; Open Simulator; learners' characteristics;

### I. INTRODUCTION

Studies over the years are shown that students had actively and more interactively involved in a classroom discussion or self studies increases by as much as 20%. Meanwhile, IT technology has been seen a tool to encourage student involvement. Today, a large number of portable game consoles and network devices could be representative. Also the blending of those devices is getting popular. It illustrates familiar scenario for today learners.

Virtual worlds such as OpenSimulator require a level of meta-cognition in relation to functioning within them, the translation of movement and actions via an interface medium make the learning such as real learning.

This proposed e-learning system will assist the students in the learning process through the Q/A system utilizing avatar using OpenSim as Virtual Education opportunities. There are some related research works. The paper discusses a case study which aims to make research projects more engaging for middle school students by incorporating a variation to the traditional gallery walk workflow [1].

They collect research posters and transfer the media into the shared a virtual world. Present collaborative cheerleading method among virtual world users and sensory effect is using wearable haptic wrist guard for providing more interactive and immersive [2].

Describing the use of OpenSimulator as a platform for enhanced learning concepts incorporate a variety of desirable attributes [3].

The following section describes the proposed Q/A system utilizing e-learning system with OpenSimulator of avatar followed by some experiments. Then conclusion is described with some discussions.

### II. PROPOSED Q/A SYSTEM UTILIZING E-LEARNING SYSTEM WITH OPENSIM OF AVATAR

#### A. Problem Statements

There are some knowhow,

- a) How to developing and connecting user avatar and avatar system by using OpenSimulator
- b) How to developing Q/A in the system
- c) How to connecting avatar system with the knowledge base (i.e. Wikipedia Online)
- d) How to parsing the question
- e) How to gain the Q/A pair to the knowledge database

Namely,

- a) Starting with installing, setup user, setup region and grid,
  - b) Developing Q/A system for collaborative virtual learning
  - c) By using LSL HTTP request using Linden Scripting Language (LSL) and Wikipedia API (Application Protocol Interface) using LSL is used for creating interactive content in Second Life.
- (4)To get keyword

(5)Gain the Q/A activity to the knowledge database (external database)

OpenSimulator is an open source server platform for hosting virtual worlds. It is compatible with the client

for Second Life and can host alternative worlds with differing feature sets with multiple protocols. Open Simulator has the following features,

- 1) Supports online, multi-user 3D environments as small as 1 simulator or as large as thousands of simulators.
  - 2) Supports 3D virtual spaces of variable size within one single instance.
  - 3) Supports multiple clients and protocols - access the same world at the same time via multiple protocols.
  - 4) Supports clients that create 3D content in real time.
  - 5) Supports in world scripting using a number of different languages, including LSL/OSSL, C# and VB.NET.
- where LSL = The Linden Scripting Language (LSL) is used for creating interactive content in Second Life.

Only the single open simulator is used for the proposed Q/A system utilizing e-learning system with OpenSim of avatar.

### B. Q/A System

Referring to the Question Answering Systems: A survey → Ali Mohamed Nabil Alam, Mohamed Hassan Haggag (IJRRIS Sept. 2012), the following Q/A system is created. Process flow of Q/A is shown in Figure 1. Q/A system consists Question processing, Information processing, and answer processing as follows,

#### 1. Question Processing

1) *Question Analysis:* Identifying the focus can be done using pattern matching (pengenalan pola) rules, based on the question type classification

2) *Question Classification:* The question is classified by its type: what, who, when, where, why and how.

3) *Question Reformulation:* The process of extracting keywords such as stop word lists

#### 2. Information Processing

##### 1) Information Retrieval:

Information retrieval systems are usually evaluated based on two metrics – precision and recall. Precision refers to the ratio of relevant documents returned to the total number of documents returned. Recall refers to the number of relevant documents returned out of the total number of relevant documents available in the document collection being searched.

2) *Paragraph Filtering:* the most relevant documents should contain the question keywords

##### 3) Paragraph Ordering:

Same word sequence score: the number of words from the question that are recognized in the same sequence within the current paragraph window.

#### 3. Answer Processing

1) *Answer identification:* The recognition of the answer type returned by the parser creates a candidate answer

2) *Answer extraction:* The parser enables the recognition

of the answer candidates in the paragraphs. So, once an answer candidate has been identified.

#### 3) Answer validation:

Confidence in the correctness of an answer can be increased in a number of ways.

We use specific knowledge sources to check answers.

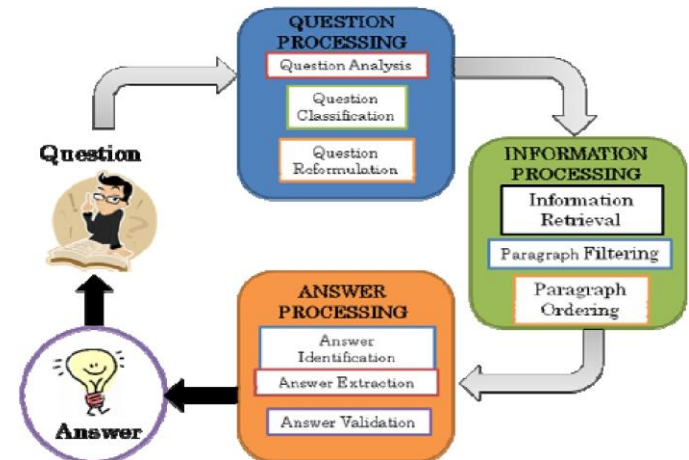


Fig. 1. Process flow of the proposed Q/A system

### C. System Block Diagram

Figure 2 shows system block diagram of the proposed system. The proposed system is based on Client Server model. There are two avatar systems, one is in the server and the other one is in the client. Both avatars can communicate each other as well as in between client user avatars. Thus the question raised from one user can be shared with all users. The server side avatar is always listening to the question and answer among users using LSL. HTTP request using LSL and PHP for keyword parsing and querying search and JSON/XML output respond. All the questions and answers are archived in the knowledge base system. OpenSimulator 0.7.2 creates the basic avatar clothing/body parts set (a ruth) for each avatar so they should be editable separately by each user.

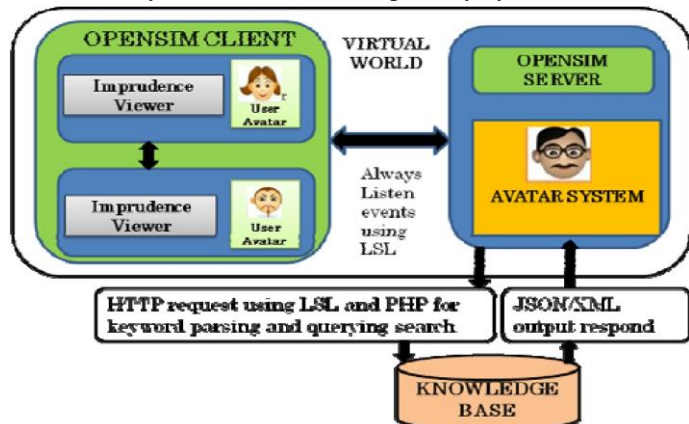


Fig. 2. System block diagram of the proposed system.



Figure 3 shows system architecture.

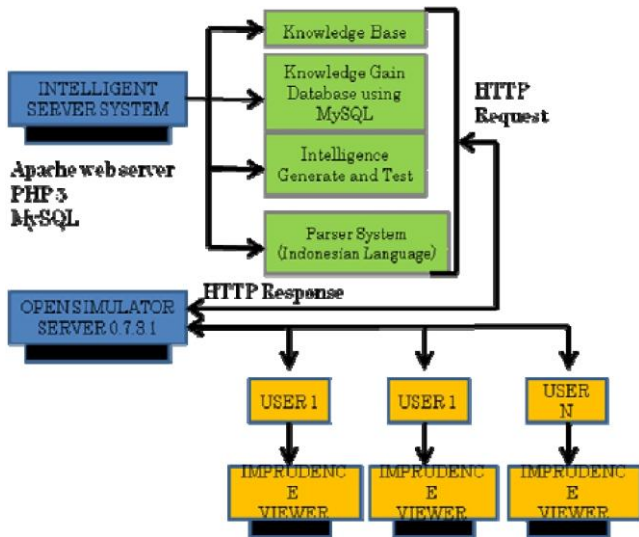


Fig. 3. Proposed system architecture

In the system architecture level, internet interface can be done with Apache web server with web design by PHP 5. Knowledge base system is based on MySQL. Also, Knowledge base is realized by using Wikipedia API (Application Protocol Interface). Results send in xml format, xml convert to readable format using PHP. Internet/Local Communication using HTTP Protocol (HTML Post Method) with the following procedure,

- HTML Post Method →
- Get → is basically for getting data
- Post → storing updating data or ordering product

#### D. Proposed Learning Procedure

Avatar in the server side has huge knowledge base which contains questions and correct answers through the previous learning processes by users. Avatar in the server side, also can present most appropriate answer which is extracted from the database to the question which is raised from users. These processes are archived every time user makes a question as knowledge.

Furthermore, server side avatar has the capability for characterization of users. In other word, knowledge base is created and updated by user by user. Users learn subjects in a collaborative manner. They can make a question and also can respond to it. These answers are qualified by server side avatar through Wikipedia API. Thus user answers and Wikipedia answers are evaluated and most appropriate answer is provided to the user who makes the question. These correct and most appropriate answers are archived in the database in the knowledge base system.

Specific user makes specific mistakes. Such this fact is a user's character. Server side avatar knows user's character through characterization from the aforementioned learning processes. Thus server side avatar makes corrections when user makes mistakes. Also server side avatar knows users'

difficulties. Therefore, avatar makes a plenty of questions for the difficult subjects for the specific users.

### III. IMPLEMENTATION AND EXPERIMENTS

#### A. Implimentation

Open Simulator 0.7.2 can be installed easily. Also PHP, Apache, MySQL are installed easily together with LSL and Wikipedia API. Knowledge base contains questions and answers as well as evaluation results of quality of answers which are evaluated using LSL and Wikipedia API. The knowledge base is composed with tables included in MySQL of database as shown in Figure 4. Figure 4 (a) shows example of questions and answers retrieved result while Figure 4 (b) shows example of retrieved result of correct answers. Figure 4 (c) shows example of the history of achievement test results. It can be done by student by student, by subject by subject, by stage by stage, etc. The table contains field, type, null key default, and extra for the data of knowledge, question, and answer. Using MySQL command, all the questions and correct answers are retrieved. Also it can be referred the history of achievement test results by subject by subject.

#### B. Avatar Design

Figure 5 shows examples of avatar designed for the proposed system specifically.

```

mysql> show table;
ERROR 1064 (42000): You have an error in your SQL syntax; check the manual that corresponds to your MySQL server version for the right syntax to use near '' at line 1
mysql> show tables;
+-----+
| Tables_in_delta |
+-----+
| mon             |
| ririki           |
+-----+
2 rows in set (0.00 sec)

mysql> show fields from mon;
+-----+
| Field | Type          | Null | Key | Default | Extra |
+-----+
| kanoku | text          | NO   |     |          |       |
| mon    | varchar(10)  | NO   |     |          |       |
| mondai | text         | NO   |     |          |       |
| kaitou | text         | NO   |     |          |       |
+-----+
4 rows in set (0.00 sec)
    
```

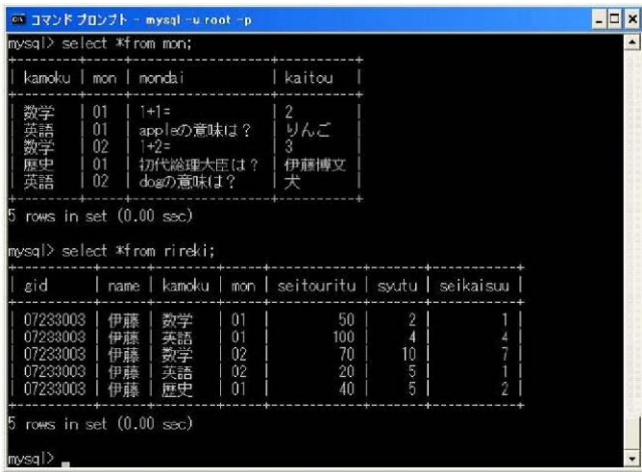
(a)Database content by question and answer

```

+-----+
| Field | Type          | Null | Key | Default | Extra |
+-----+
| kanoku | text          | NO   |     |          |       |
| mon    | varchar(10)  | NO   |     |          |       |
| mondai | text         | NO   |     |          |       |
| kaitou | text         | NO   |     |          |       |
+-----+
4 rows in set (0.00 sec)

mysql> show fields from ririki;
+-----+
| Field | Type          | Null | Key | Default | Extra |
+-----+
| sid   | varchar(10)  | NO   |     |          |       |
| name  | text         | NO   |     |          |       |
| kanoku | text         | NO   |     |          |       |
| mon    | varchar(10)  | NO   |     |          |       |
| seitouritu | double      | NO   |     |          |       |
| svutu | int(11)      | NO   |     |          |       |
| seikaisu | int(11)     | NO   |     |          |       |
+-----+
7 rows in set (0.00 sec)
    
```

(b)Correct answer retrieval



(c) Achievement test result history by subject by

Fig. 4. subject Figure 4 Database contents

It can be done with the following procedure,

- 1) Click the Inventory Button
- 2) Create -> New Clothes -> Shirt, Pants, etc
- 3) Create -> New Body Parts -> Hair, Shape, etc
- 4) Edit those from the inventory
- 5) Wear them

An update: SecondLife: SL has since removed the default "Ruth" avatar and replaced it with a set of pre-built custom avatars. If there is ever an issue with your current avatar under either OpenSimulator or SL, your avatar is displayed as a particle cloud effect. OpenSimulator maintains a default avatar very similar to what "Ruth" looked like, however, for additional custom avatars, one would need to build a repository of avatar clothes and body parts (in their server's database, available to all, or in that particular user's inventory alone).



(a) Designed fundamental avatar



(b) Client user avatars



(c) Server avatar

Fig. 5. Designed avatars.

### C. Implementation and Experimental Result

Q/A system implementation result are shown in Table 1. Q/A system are completed without any trouble.

Experiments of learning performance test with and without avatar are conducted. Three subjects, History, Mathematics, and English reading are prepared. The effectiveness of avatar can be evaluated with achievement test by ten of undergraduate students of Saga University. In accordance with the experimental results, approximately 10% of improvement is observed for e-learning system with avatar in comparison to that without avatar. The improvements are different by subject by subject. The avatar is effective for the subject of history followed by English reading and mathematics. Although concrete answer can be easily prepared for history and English reading, it is rather difficult to prepare concrete answer for the mathematics subject

TABLE I. Result from Q/A system installation

QA Components	Question Processing	Document Processing	Answer Processing
Question Analysis	√		
Question Classification	√		
Question Reformulation	√		
Information Retrieval		√	
Paragraph Filtering		√	
Paragraph Ordering		√	
Answer Identification			√
Answer Extraction			√
Answer Validation			√

#### IV. CONCLUSIONS

E-learning system utilizing learners' characteristics which is recognized through learning processes with Open Simulator for overcoming weak points is proposed. Through dialogs with avatars in the Open Simulator, it is possible to understand learners' weak points. Using learners' characteristics, most appropriate subjects and achievement tests are provided by the proposed e-learning system. Experimental results show that the proposed e-learning system is much effective than the conventional e-learning system without utilizing learners' characteristics.

As the results, the following conclusions are obtained,

- 1) *In this proposed research we focus on collaborative question answer activities in the networked virtual world environment.*
- 2) *With the avatar system that connects to the knowledge database, could assist student in providing answers.*
- 3) *QA based collaborative learning could be done much attractively than the conventional QA system through Avatars in virtual learning.*

#### ACKNOWLEDGMENT

The authors would like to thank Mr. Kazauma Itoh of Saga University and the students of State University of Malang, Indonesia who contributed to the experiments.

#### REFERENCES

- [1] Joshua Schendel, Chang Liu, David Chelberg, Teresa Franklin. 2008. Virtual Gallery Walk, an Innovative Outlet for Sharing Student Research Work in K-12 Classrooms. 38<sup>th</sup> Frontiers in Education Conference.
- [2] Changhyeon Lee, Hye, Min Choi, Yong-Moo Kwon. 2010. Networked Collaborative Group Cheerleading Technology. International Symposium on Ubiquitous Virtual Reality.
- [3] Walter Ridgewell, Vive Kumar, Oscar Lin. 2011. OpenSim Virtual World as Platform for Enhanced Learning Concepts. 11<sup>th</sup> IEEE International Conference on Advanced Learning Technologies.

#### AUTHORS PROFILE

**Kohei Arai**, He received BS, MS and PhD degrees in 1972, 1974 and 1982, respectively. He was with The Institute for Industrial Science and Technology of the University of Tokyo from April 1974 to December 1978 also was with National Space Development Agency of Japan from January, 1979 to March, 1990. During from 1985 to 1987, he was with Canada Centre for Remote Sensing as a Post Doctoral Fellow of National Science and Engineering Research Council of Canada. He moved to Saga University as a Professor in Department of Information Science on April 1990. He was a councilor for the Aeronautics and Space related to the Technology Committee of the Ministry of Science and Technology during from 1998 to 2000. He was a councilor of Saga University for 2002 and 2003. He also was an executive councilor for the Remote Sensing Society of Japan for 2003 to 2005. He is an Adjunct Professor of University of Arizona, USA since 1998. He also is Vice Chairman of the Commission "A" of ICSU/COSPAR since 2008. He wrote 30 books and published 322 journal papers

# Method for Car in Dangerous Action Detection by Means of Wavelet Multi Resolution Analysis Based on Appropriate Support Length of Base Function

Kohei Arai

Graduate School of Science and Engineering  
Saga University  
Saga City, Japan

Tomoko Nishikawa

Graduate School of Science and Engineering  
Saga University  
Saga City, Japan

**Abstract**—Multi-Resolution Analysis: MRA based on the mother wavelet function with which support length differs from the image of the automobile rear under run is performed, and the run characteristic of a car is searched for. Speed, deflection, etc. are analyzed and the method of detecting vehicles with high accident danger is proposed. The experimental results show that vehicles in a dangerous action can be detected by the proposed method.

**Keywords**—Change detection; MRA; support length of mother wavelet

## I. INTRODUCTION

There are strong demands on detection of the cars in dangerous actions in particular on freeways, highways at which high speed cars are passing through. Most of the freeways, highways equip cameras at some intervals to monitor traffic flow and detect such dangerous cars. Traffic flow monitoring with camera acquired car images is relatively easy to measure. It, however, is not so easy to detect dangerous cars. If dangerous cars are detected, then some cautions may be made with loud speaker to the dangerous cars and the surrounding cars to prevent car accidents.

Temporal change detections can be done with moving pictures by using differential operators such as Sobel, Prewitz, Laplacian, etc. [1]. It, however, is affected by the noises included in the moving pictures. Differential operators enhance noises usually. On the other hands, discrete wavelet transformation based Multi Resolution Analysis: MRA [2]-[8] allows spatio-temporal change detection with a variety of parameters, order and support length of base function of wavelet, shift and magnification of wavelet function, and levels of wavelet transformations. By tuning the parameters, appropriate MRA can be formed for detection of dangerous cars. There is another approach for car tracking method based on Kalman filter [9]. Also wavelet parameter estimation method is proposed [10]. Therefore, these object tracking and

object trajectory analysis for drivers' behavior estimation can be done after the detection of dangerous cars.

The following section describes the proposed method for detection of dangerous cars followed by some experiments. Then conclusion is described with some discussions.

## II. PROPOSED METHOD

### A. Discrete Wavelet Transformation

Discrete wavelet transformation for the given time series of scalar variables,  $\eta_i$  are defined in equation (1) with square matrix,  $C_n$  (wavelet transformation matrix) which consists of low wavelet frequency component coefficients,  $p_i$  and high wavelet frequency component coefficients,  $q_i$ .

$$C_n \begin{bmatrix} \eta_1 \\ \eta_2 \\ \vdots \\ \eta_n \end{bmatrix} \quad (1)$$

Then the given time series of scalar variables can be divided into two parts, low frequency and high frequency components. There is a variety of wavelet transformation matrix with the different parameters of the order and the support length of the base function. For instance, the wavelet transformation matrix for the 8<sup>th</sup> order and two of the support length is shown in equation (2). In the case of the wavelet transformation matrix for the 8<sup>th</sup> order with two support length is expressed in equation (3).

In the case of Daubechies base function, the wavelet transformation matrix with two of the support length can be calculated with equation (4) while that with four of the support length can be calculated with equation (5). Meanwhile, the wavelet transformation matrix with the arbitrary support length, (sup) can be calculated with equation (6).

$$C_8^{[2]} \begin{bmatrix} \eta_1 \\ \eta_2 \\ \eta_3 \\ \eta_4 \\ \eta_5 \\ \eta_6 \\ \eta_7 \\ \eta_8 \end{bmatrix} = \begin{bmatrix} p_0 & p_1 & & & & & & \\ q_0 & q_1 & & & & & & \\ & & p_0 & p_1 & & & & \\ & & q_0 & q_1 & & & & \\ & & & & p_0 & p_1 & & \\ & & & & q_0 & q_1 & & \\ & & & & & & p_0 & p_1 \\ & & & & & & q_0 & q_1 \end{bmatrix} \begin{bmatrix} \eta_1 \\ \eta_2 \\ \eta_3 \\ \eta_4 \\ \eta_5 \\ \eta_6 \\ \eta_7 \\ \eta_8 \end{bmatrix} \quad (2)$$

$$= \begin{bmatrix} p_0x_1 + p_1x_2 \\ q_0\eta_1 + q_1\eta_2 \\ p_0\eta_3 + p_1\eta_4 \\ q_0\eta_3 + q_1\eta_4 \\ p_0\eta_5 + p_1\eta_6 \\ q_0\eta_5 + q_1\eta_6 \\ p_0\eta_7 + p_1\eta_8 \\ q_0\eta_7 + q_1\eta_8 \end{bmatrix}$$

$$C_8^{[4]} \begin{bmatrix} \eta_1 \\ \eta_2 \\ \eta_3 \\ \eta_4 \\ \eta_5 \\ \eta_6 \\ \eta_7 \\ \eta_8 \end{bmatrix} = \begin{bmatrix} p_0 & p_1 & p_2 & p_3 & & & & \\ q_0 & q_1 & q_2 & q_3 & & & & \\ & & p_0 & p_1 & p_2 & p_3 & & \\ & & q_0 & q_1 & q_2 & q_3 & & \\ & & & p_0 & p_1 & p_2 & p_3 & \\ & & & q_0 & q_1 & q_2 & q_3 & \\ p_2 & p_3 & & & p_0 & p_1 & & \\ q_2 & q_3 & & & q_0 & q_1 & & \end{bmatrix} \begin{bmatrix} \eta_1 \\ \eta_2 \\ \eta_3 \\ \eta_4 \\ \eta_5 \\ \eta_6 \\ \eta_7 \\ \eta_8 \end{bmatrix} \quad (3)$$

$$= \begin{bmatrix} p_0\eta_1 + p_1\eta_2 + p_2\eta_3 + p_3\eta_4 \\ q_0\eta_1 + q_1\eta_2 + q_2\eta_3 + q_3\eta_4 \\ p_0\eta_3 + p_1\eta_4 + p_2\eta_5 + p_3\eta_6 \\ q_0\eta_3 + q_1\eta_4 + q_2\eta_5 + q_3\eta_6 \\ p_0\eta_5 + p_1\eta_6 + p_2\eta_7 + p_3\eta_8 \\ q_0\eta_5 + q_1\eta_6 + q_2\eta_7 + q_3\eta_8 \\ p_0\eta_7 + p_1\eta_8 + p_2\eta_1 + p_3\eta_2 \\ q_0\eta_7 + q_1\eta_8 + q_2\eta_1 + q_3\eta_2 \end{bmatrix}$$

$$\begin{aligned} (C_n^{[2]})^T C_n^{[2]} &= I_n \\ p_0 + p_1 &= \sqrt{2} \\ q_0 &= p_1 \\ q_1 &= -p_0 \\ 0^0 q_0 + 1^0 q_1 &= 0 \end{aligned} \quad (4)$$

$$\begin{aligned} (C_n^{[4]})^T C_n^{[4]} &= I_n \\ p_0 + p_1 + p_2 + p_3 &= \sqrt{2} \\ q_0 &= p_3 \\ q_1 &= -p_2 \\ q_2 &= p_1 \\ q_3 &= -p_0 \\ 0^0 q_0 + 1^0 q_1 + 2^0 q_2 + 3^0 q_3 &= 0 \\ 0^1 q_0 + 1^1 q_1 + 2^1 q_2 + 3^1 q_3 &= 0 \end{aligned} \quad (5)$$

$$\begin{aligned} (C_n^{[sup]})^T C_n^{[sup]} &= I_n \\ \sum_{j=0}^{sup-1} p_j &= \sqrt{2} \\ q_j &= (-1)^j p_{(sup-1)-j} \quad (j = 0, 1, 2, \dots, (sup-1)) \\ \sum_{j=0}^{sup-1} j^r q_j &= 0 \quad \left( r = 0, 1, 2, \dots, \left( \frac{sup}{2} - 1 \right) \right) \end{aligned} \quad (6)$$

### B. Multi Resolution Analysis: MRA

The input data of scalar variables can be transformed to high (H) and low (L) wavelet frequency components with the wavelet transformation matrix. This Discrete Wavelet Transformation: DWT is called as the first level of DWT. L component can be divided into H and L components. This DWT is called as the second level of DWT. Furthermore, these transformations can be repeatedly applied to the L components again. These DWT is called as decomposition. The level is corresponding to the frequency components. In other words, arbitrary frequency component can be extracted with the different level of wavelet frequency component.

Because of the  $C^T C = C^{-1} C$ , it is possible to reconstruct original input data of scalar variables with the all levels of H components and the highest level of L component. This process is called with reconstruction, or Inverse Discrete Wavelet Transformation: IDWT.

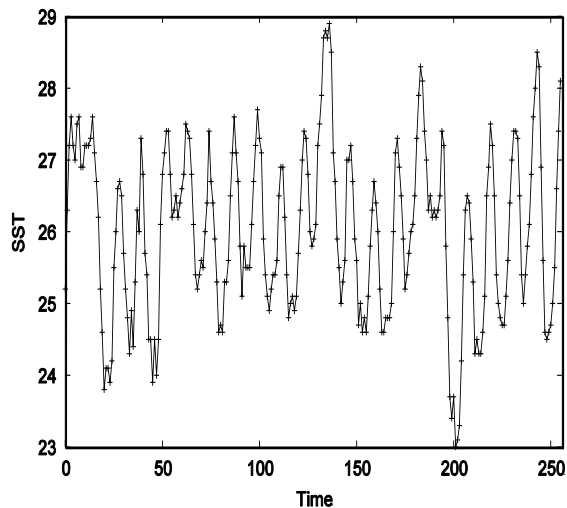
DWT and IDWRT can also be defined to the two dimensional image data as well as three dimensional moving pictures. Furthermore, these can be applied to arbitrary dimensional data  $f$  as follows,

$$(fC)^T (C^T) \dots C^T \quad (7)$$

For instance, DWT divides two dimensional input data into LL, HL, LH, and HH. The first and the second characters denote horizontal and vertical directions, respectively.

### C. Effect of the Support Length

In order to clarify the effect of the support length, relatively calmly changed Southern Oscillation Index: SOI is compared to relatively rapidly changed SOI which are shown in Figure 1 (a) and (b), respectively. DWT is applied at once (first level) to the data with the different support length. After that IDWT is applied to the transformed wavelet frequency component with L component only. Root Mean Square Error: RMSE between the reconstructed data and the original data is evaluated. The results are shown in Figure 2.



(a) Relatively calm

(b) Relatively rapid

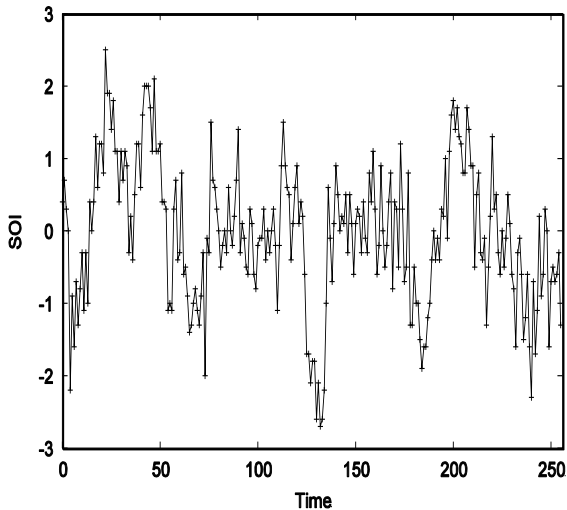
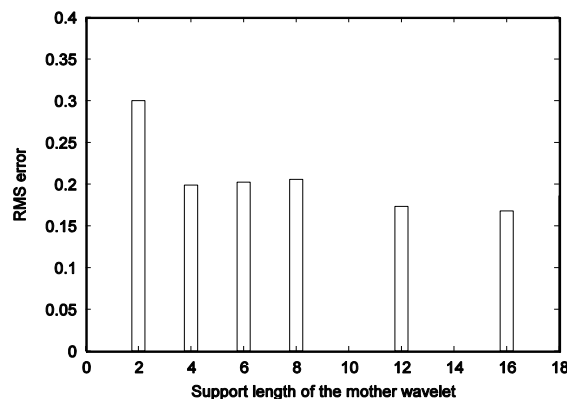
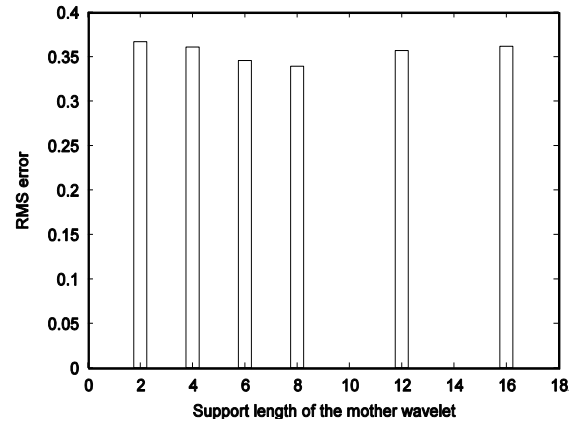


Fig. 1. Two different types of time series of data



(a) Relatively calm



(b) Relatively rapid

Fig. 2. Root Mean Square error between original and reconstructed time series data through DWT with different support length (2-16) of mother wavelet.

RMSE is represented reproducibility without high frequency component. Therefore, it is said that long support length (16) is appropriate for relatively calmly changed time series of data in terms of reproducibility while around 8 of support length is suitable for relatively rapidly changed data. Consequently, there is an appropriate support length depending on how rapidly changed the input time series data.

#### D. Method for Dangerous Car Detection

Using moving pictures acquired with traffic flow monitoring cameras, dangerous car can be detected. In order to detect car, edge detection method is applied to the moving pictures. Edges can be detected by the process of which 3D DWT (decomposition) is applied to the original moving pictures, then IDWT (reconstruction) is applied to the decomposed wavelet frequency components without LLL component which results in enhancement of high frequency component (edge enhancement). Therefore, spatial-temporal changes can be detected.

It is well known that the tail of car in dangerous actions used to be vibrated (slipping and sliding motion) with around a couple of Hz in horizontal direction. It is possible to detect such actions (direction and vibration frequency component) by using the aforementioned DWT and IDWT processes. Therefore, dangerous car detection is capable.

### III. EXPERIMENTS

#### A. Data Used

Example of the moving picture for the car in dangerous action is shown in Figure 3. Image size is 128 by 128 pixels while the quantization bit is 8. Meanwhile, the frame rate is 8 frames per second. This moving picture is acquired with traffic flow monitor camera for four second.

This moving picture is downloaded from the site of <http://www.youtube.com/watch?v=COdILcgGUQ>.

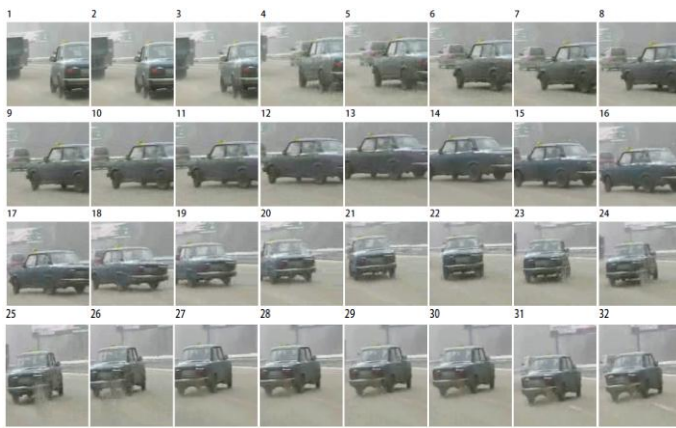


Fig. 3. Original moving picture of the car in a dangerous action from the site of <http://www.youtube.com/watch?v=COdLcgGUQ>.

### B. Effect of Support Length

Spatial-temporal change detection is performed for the example of moving picture by using the proposed method with the different support length of base function of Daubechies mother wavelet. Figure 4 shows the resultant images.

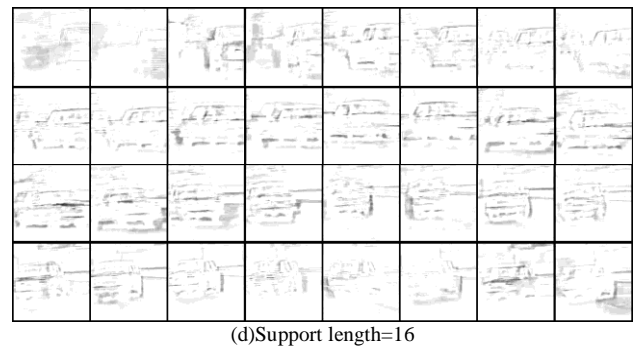
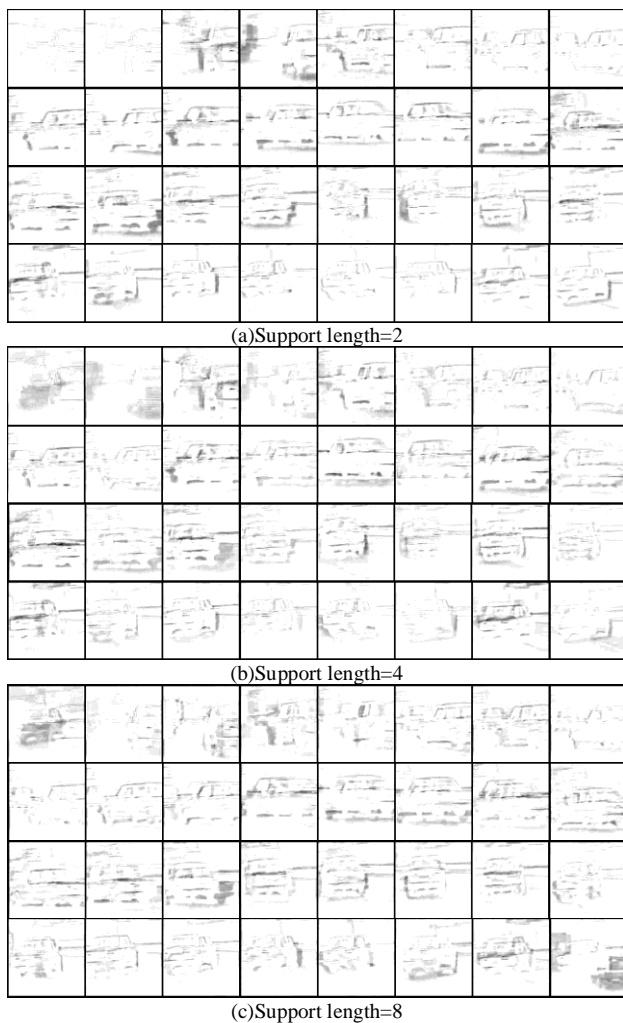


Fig. 4. Moving parameter estimation through 3D wavelet transformation with the different support length of 2, 4, 8, and 16 of Daubechies mother wavelet.

From Figure 4, it is found that dangerous actions can be detected at 23 frame number and after. Due to the fact that the frequency component derived from the proposed method is a couple of Hz, it is found that this car is in dangerous actions after 23 frames.

In comparison of these detected edges and spatial-temporal changes, it is found that 8 of support length would be best followed by 16 and 4 and 2.

### C. Detected Spatio-Temporal Changed Pixels

Through binarization of the Figure 4 with the appropriate threshold, spatial-temporal changed pixels can be detected. Figure 5 shows the number of the detected spatial-temporal changed pixels with the threshold of 128 and 64, respectively.

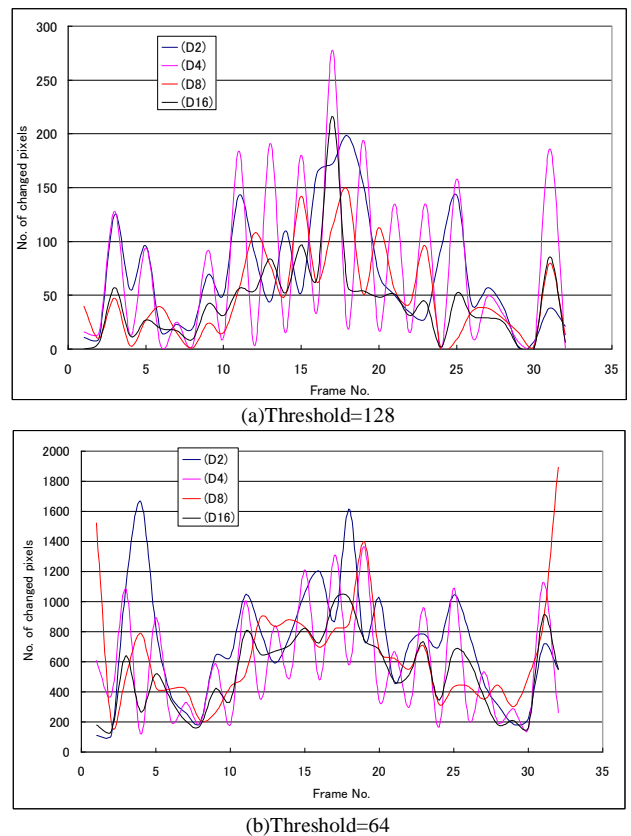


Fig. 5. The number of detected change pixels through the proposed method with the different support length of mother wavelet (Daubechies).

Figure 5 (a) shows that there are two peaks situated at around 12 to 23 frame and at around 25 to 28 frame. It also shows the hunching of the number changed pixels for small support length. This is caused by the influence due to shorter support length. In accordance with increasing of support length, this hunching effect is getting small. Therefore, longer support length is better than shorter support length in terms of spatial-temporal change detection. It is obvious that the number of detected changed pixels for the threshold is 64 is greater than that of the threshold is 128 by approximately 5.6 times.

#### IV. CONCLUSION

Multi-Resolution Analysis: MRA based on the mother wavelet function with which support length differs from the image of the automobile rear under run is performed, and the run characteristic of a car is searched for. Speed, deflection, etc. are analyzed and the method of detecting vehicles with high accident danger is proposed. The experimental results show that vehicles in a dangerous action can be detected by the proposed method with the different support length of wavelet base function.

#### ACKNOWLEDGMENT

The authors would like to thank Dr. Kaname Seto for his suggestions and comments for this study.

#### REFERENCES

- [1] K.Arai, Lecture Note on Wavelet Analysis, Kindai-Kagakusha Publishing Co. Ltd., 2006.
- [2] Fundamental Theory on Wavelet Analysis, Morikita-Shuppan Publishing Inc., 2000.
- [3] K.Arai, Kaname Seto, Method for moving characteristics estimation of 3D objects by means of wavelet analysis, Journal of Visualization Society of Japan, 24, Suppl.1, 2004.
- [4] K.Arai, Kaname Seto, Tomoko Nishikawa, Method for moving characteristics estimation of rotation and acceleration based on wavelet

analysis, Journal of Visualization Society of Japan, 26, Suppl.1, 145-148, 2006.

- [5] Corbett J., Leduc J.-P., and Kong M., Analysis of de-formational transformations with spatio-temporal continuous wavelet transforms, in Proceedings of IEEE-ICASSP, 1999.
- [6] Duval-Destin M. and Murenzi R., Spatio-temporal wavelets: Applications to the analysis of moving patterns, Progress in Wavelet Analysis and Applications, Editions Frontières, Gif-sur-Yvette, France, 1993.
- [7] J.-P.Leduc, F.Mujica, R.Murenzi, and M.J.T.Smith, Spatio temporal Wavelets: A Group-Theoretic Construction For Motion Estimation And Tracking. Siam J. Appl. Math. Society for Industrial and Applied Mathematics 61.2, 596-632, 2000.
- [8] F.Mujica, J.-P.Leduc, R.Murenzi and M.J.T.Smith, A New Motion Parameter Estimation Algorithm Based on the Continuous Wavelet Transform IEEE Transactions on Image Processing, 9, 5, 873-888, 2000.
- [9] Bing Wang, Rong Chun Zhao, Motion tracking using the continuous wavelet transform and EKF models, Proceedings of the International Computer Congress 2004, 155-161, World Scientific Publishing Co. Pte. Ltd., 2004.
- [10] Brault P., A New Scheme For Object-Oriented Video Compression And Scene Analysis, Based On Motion Tuned Spatio-Temporal Wavelet Family And Trajectory Identification, IEEE-ISSPIT03, 2003.

#### AUTHORS PROFILE

**Kohei Arai**, He received BS, MS and PhD degrees in 1972, 1974 and 1982, respectively. He was with The Institute for Industrial Science and Technology of the University of Tokyo from April 1974 to December 1978 also was with National Space Development Agency of Japan from January, 1979 to March, 1990. During from 1985 to 1987, he was with Canada Centre for Remote Sensing as a Post Doctoral Fellow of National Science and Engineering Research Council of Canada. He moved to Saga University as a Professor in Department of Information Science on April 1990. He was a councilor for the Aeronautics and Space related to the Technology Committee of the Ministry of Science and Technology during from 1998 to 2000. He was a councilor of Saga University for 2002 and 2003. He also was an executive councilor for the Remote Sensing Society of Japan for 2003 to 2005. He is an Adjunct Professor of University of Arizona, USA since 1998. He also is Vice Chairman of the Commission "A" of ICSU/COSPAR since 2008. He wrote 30 books and published 322 journal papers.



# Geography Markup Language: GML Based Representation of Time Serie of Assimilation Data and Its Application to Animation Content Creation and Representations

Kohei Arai<sup>1</sup>

Graduate School of Science and Engineering  
Saga University  
Saga City, Japan

**Abstract**—Method for Geography Markup Language: GML based representation of time series of assimilation data and its application to animation content creation and representations is proposed. It is validated the proposed method with NCEP/GDAS assimilation data. Also usefulness of the proposed interpolation method with tweening method is confirmed for unequal time interval of the time series data.

**Keywords**—assimilation data; GML; NCEP/GDAS; tweening method of interpolation

## I. INTRODUCTION

Geography Markup Language: GML<sup>1</sup> is proposed by Open GIS Consortium: OGC<sup>2</sup> and is International Standardization Organization: ISO standard of open Geographic Information System: GIS [1],[2]. It is available to represent 3D GIS data with GML and also to represent time series of 3D imagery data. On the other hands, four dimensional assimilation data is available for four dimensional meteorological data representations such as NCEP/GDAS<sup>3</sup>, NASA/DAO<sup>4</sup>, etc. It allows visual perceptions and manipulations. Therefore, the proposed method may be useful for such purposes with the four dimensional assimilation data.

GML based representation is based on client/server system essentially. Therefore, the required assimilation data have to be searched and downloaded. Assimilation data search starts with meta<sup>5</sup> search followed by actual assimilation data. Therefore, data search procedure is required for implementations. Also interpolation method is required for equalization of time intervals between assimilation data because the assimilation data is unequal time interval of data. Tweening<sup>6</sup> method is employed for interpolation. Thus the equal time interval of assimilation can be represented and manipulated smoothly.

The following section describes the proposed method followed by implementation and experiments. Then conclusion is described together with some discussions.

## II. PROPOSED METHOD

### A. Open GIS

Open GIS is proposed by Open GIS Consortium: OGC. Open GIS allows collection of geographical data and information through internet in terms of distributed data servicing system based on client server model. Conceptual configuration of Open GIS is shown in Figure 1.

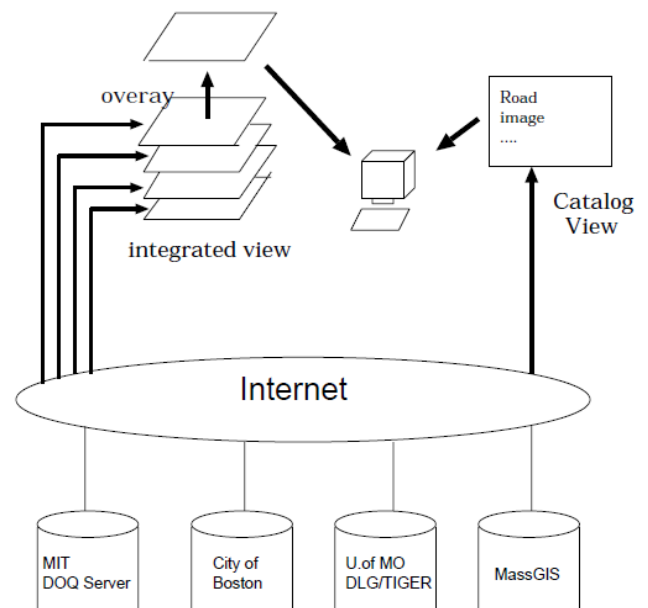


Fig. 1. Conceptual configuration of Open GIS system

Meanwhile, abstracted specification of Open GIS is shown in Table 1. On the other hand, implementation specification is shown in Table 2. Implementation specification includes simple feature, catalog, grid coverage, web map service interface, Geography Markup Language: GML, web feature service, etc. Essentially, Open GIS system is web based GIS

<sup>1</sup> <http://www.opengeospatial.org/standards/gml>

<sup>2</sup> <http://www.opengeospatial.org/>

<sup>3</sup> <http://www.mmm.ucar.edu/mm5/mm5v3/data/gdas.html>

<sup>4</sup> <http://gmao.gsfc.nasa.gov/>

<sup>5</sup> <http://ja.wikipedia.org/wiki/%E3%83%A1%E3%82%BF%E3%83%87%E3%83%BC%E3%82%BF>

<sup>6</sup> <http://en.wikipedia.org/wiki/Inbetweening>

system. GML is XML<sup>7</sup> based data description language for geographical data.

TABLE I. SPECIFICATION OF OPEN GIS SYSTEM

Topic 0	Overview
Topic 1	Feature Geometry
Topic 2	Spatial Reference Systems
Topic 3	Location Geometry
Topic 4	Stored Function and Interpolation
Topic 5	The OpenGIS Feature
Topic 6	The Coverage Type
Topic 7	Earth Imagery
Topic 8	Relations Between Features
Topic 9	Accuracy
Topic 10	Feature Collections
Topic 11	Metadata
Topic 12	The OpenGIS Service Architecture
Topic 13	Catalog Services
Topic 14	Semantics and Information Communities
Topic 15	Image Exploitation Services
Topic 16	Image Coordinate Transformation Services

TABLE II. IMPLEMENTATION SPECIFICATION OF OPEN GIS

OpenGIS Simple Features Specification (for OLE/COM,CORBA,SQL)
OpenGIS Catalog Services Implementation Specification
OpenGIS Grid Coverages Implementation Specification
OpenGIS Coordinate Transformation Services Implementation Specification
OpenGIS Web Map Service Interfaces Implementation Specification
OpenGIS Geography Markup Language Implementation Specification
OpenGIS Web Feature Service Implementation Specification
OpenGIS Filter Encoding Implementation Specification
OpenGIS Styled Layer Descriptor Implementation Specification

B. Process Flow of the Proposed System

Figure 2 shows process flow of the proposed GIS animation and representation based n Open GIS. First, client makes search request for date, region, layer, altitude spatially and temporally. Meta data, then, is searched from the server. After that, search results are down loaded from the server. It is not always that the time interval is constant. In order to demonstrate animation of assimilation data, it is better to show equal time interval of assimilation data periodically. Server provided assimilation data, however, are unequal time interval of time series data. Therefore, some interpolation is required for conversion from unequal time interval of data to equal time interval data. Tweening is utilized for the conversion. Tweening algorithm is as follows,

Assuming two data point values, A and B, i-th tweening point,  $T_i$  is expressed by equation (1)

$$T_i = A + i * (B - A) / N \tag{1}$$

where N denotes the number of tweening points. Tweening points of the simplest case are shown in Figure 2. In Figure 2, there are only two adjacent data (line in this case). The line

which connects middle points of the two adjacent lines is called tweening (in between line). Thus interpolations can be done between two adjacent data.

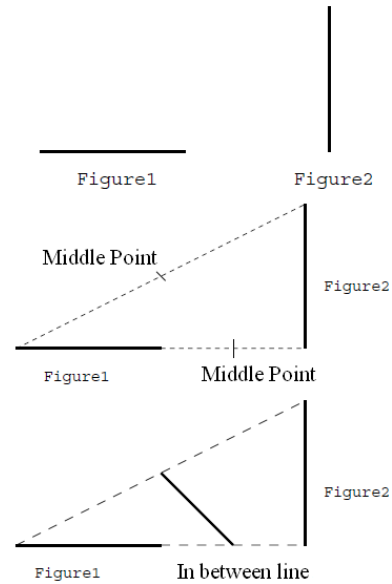


Fig. 2. Tweening Algorithm

Equal time interval of assimilation data file format is converted to GIF<sup>8</sup> for animation. Then animated assimilation data can be represented.

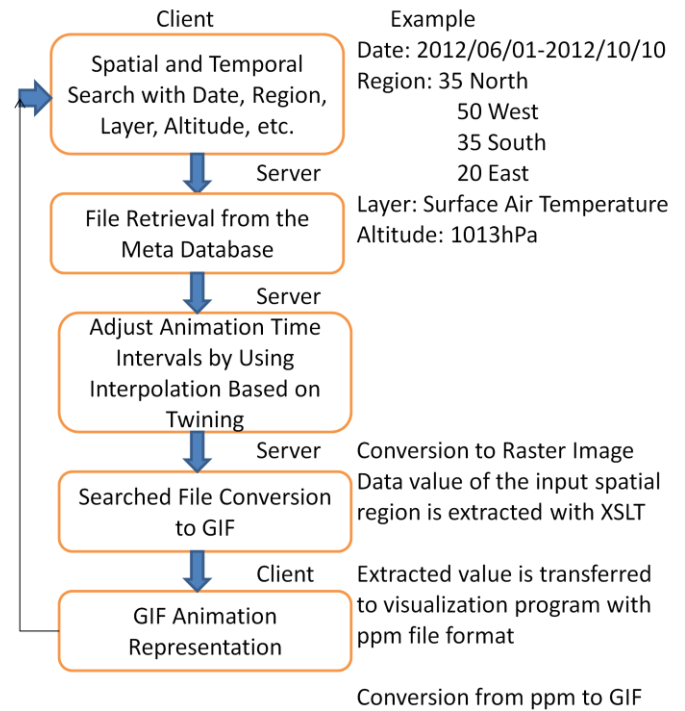


Figure 2 Process flow of the proposed GIS animation and representation based on Open GIS

<sup>7</sup> [http://ja.wikipedia.org/wiki/Extensible\\_Markup\\_Language](http://ja.wikipedia.org/wiki/Extensible_Markup_Language)

<sup>8</sup> <http://www.tohoho-web.com/wwwgif.htm>

### C. Example of GIS Representation with NVIS of GRASS

Retrieved GIS data can be represented with NVIS<sup>9</sup> of GRASS<sup>10</sup> software. GRASS is Free Open Source Software: FOSS of GIS. In the GRASS, there is NVIS for GIS representations.

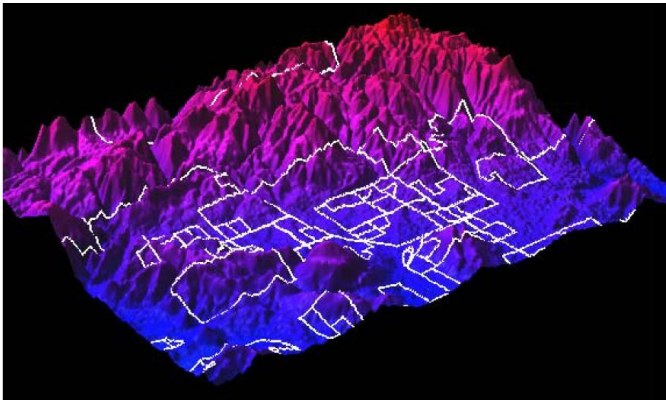


Fig. 3. Example of GIS representation with NVIS of GRASS software

### D. Assimilation Data

NCEP (National Center for Environmental Prediction)/GDAS (Global Data Assimilation Model) has 360 by 181 of meshed data of air temperature, relative humidity, cloud fraction, ozone mixing ratio, etc. at the number of altitudes which are predicted every 6 hours a day. NCEP/GDAS is described with GRIB format<sup>11</sup> and can be read with wgrib<sup>12</sup> of command. Example of NCEP/GDAS of air temperature on the surface is shown in Figure 4. Also example of NCEP/GDAS data of surface air temperature in GML expression is shown in Figure 5.

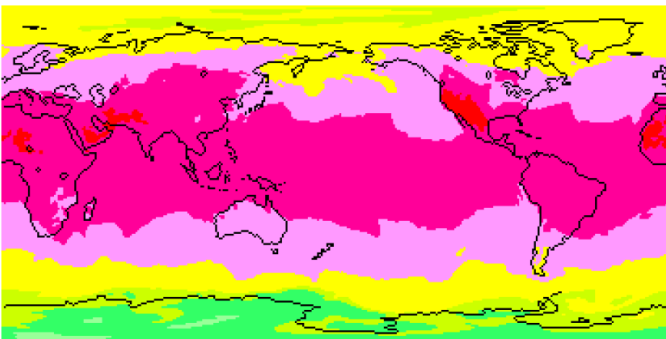


Fig. 4. Example of NCEP/GDAS assimilation data of surface air temperature

## III. EXPERIEMENT

### A. Meta Data Search and Assimilation Data Search

Web design is conducted for meta data and assimilation data search. Figure 6 shows the designed web interface of search engine. In this example, the entire query is input from the dialog box in the Figure 6.

The entire query is listed in Table 3. Meanwhile, the ranges for the query parameters are listed in Table 4. Through this web interface, the meta data and the assimilation data in concern can be retrieved with the entire query of attributed parameter for the assimilation data in concern. Then retrieved data is obtained as shown in Figure 7.

```
<?xml version="1.0"?>
<GdasDataModel>

  <name>NCEP 1-degree Global Data Assimilation Model</name>
  <Parameter>Temperature</Parameter>
  <Unit>K</Unit>
  <altitude>1000</altitude>
  <boundeBy>
    <Box>
      <coord><X>-179.0</X><Y>90.0</Y></coord>
      <coord><X>180.0</X><Y>-90.0</Y></coord>
    </Box>
  </boundeBy>

  <DataElement>
    <Point>
      <coord><X>-179.0</X><Y>90.0</Y></coord>
    </Point>
  </DataElement>

  <DataElement>
    <Point>
      <coord><X>-179.0</X><Y>90.0</Y></coord>
    </Point>
    <DataValue>266.000000</DataValue>
  </DataElement>

  <DataElement>
    <Point>
      <coord><X>-178.0</X><Y>90.0</Y></coord>
    </Point>
    <DataValue>266.000000</DataValue>
  </DataElement>
  .....
  .....

  <DataElement>
    <Point>
      <coord><X>180.0</X><Y>-90.0</Y></coord>
    </Point>
    <DataValue>241.100000</DataValue>
  </DataElement>

  <Time>2001-6-01-00</Time>
</GdasDataModel>
```

Fig. 5. Example of NCEP/GDAS data of surface air temperature in GML expression

<sup>9</sup> <http://nvisinc.com/index.php>

<sup>10</sup> <http://grass.fbk.eu/>

<sup>11</sup> <http://en.wikipedia.org/wiki/GRIB>

<sup>12</sup> <http://www.cpc.ncep.noaa.gov/products/wesley/wgrib.html>

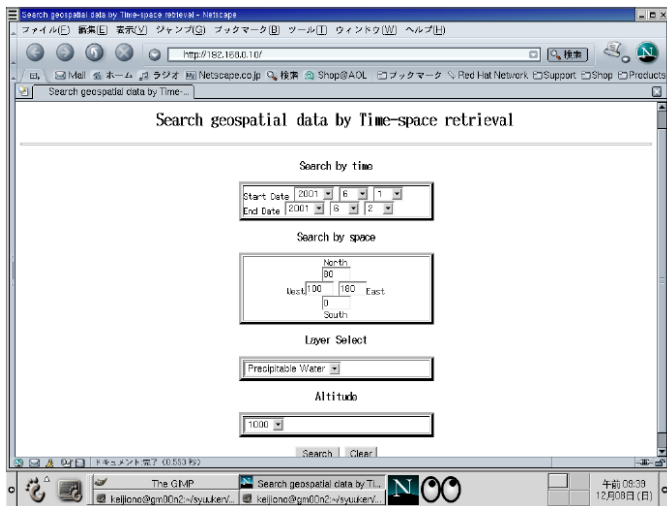


Fig. 6. Designed web interface for meta data search and assimilation data search

TABLE III. ALL THE QUERIES FOR SEARCHING META DATA AND ASSIMILATION DATA

Title	Value
Date	Year
	Month
	Day
	Hour
	Minute
	Second
Region	East end
	West end
	North end
	South end
Coordinate System	Latitude resolution
	Longitude resolution
	Unit of geographical coordinate
	Map projection
Object type	
Layer name	
Altitude	
File name	
File location	
Format	

B. Retrieved Assimilation Data

Example of the retrieved assimilation data is shown in Figure 8. Figure 8 (a) shows the retrieved surface relative humidity while Figure 8 (b) shows that of surface air temperature. Retrieved assimilation data are obtained by altitude by altitude and by time by time. Since the altitude

interval and the time interval is not equal as shown in Figure 9, interpolation is required in space and time domains. Tweening algorithm is utilized for the interpolations.

TABLE IV. RANGES FOR THE QUERY PARAMETERS

Date	2001/06/01-2010/05/31
Geographical region	North Boundary(-90-90 degree)
	South Boundary(-90-90 degree)
	East Boundary(-180-180 degree)
	West Boundary(-180-180 degree)
Layer Name	Air temperature, Relative Humidity, Total Column Ozone, Cloud Fraction, Precipitable Water
Altitude	1013-100hPa

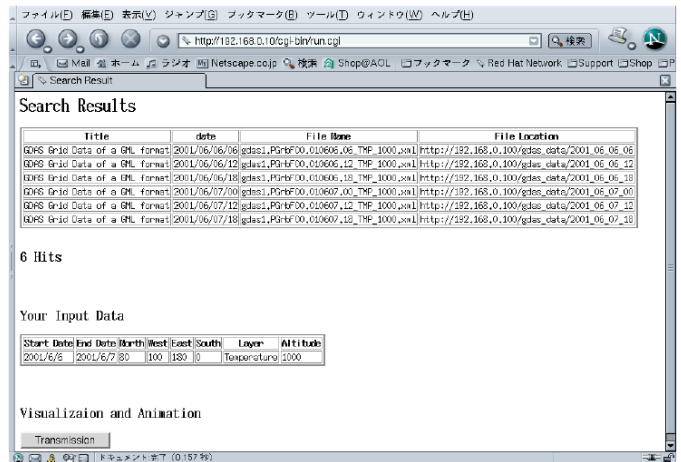
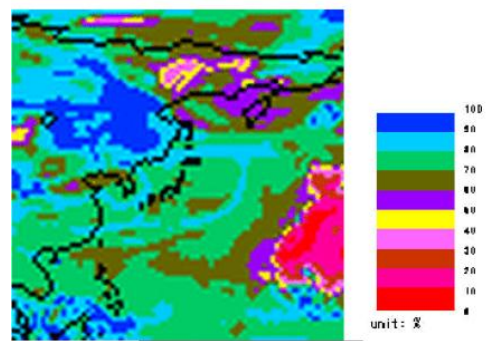


Fig. 7. Example of retrieved assimilation data.

Relative Humidity: 1000 mb

date : 2001/6/6 -> 2001/6/7

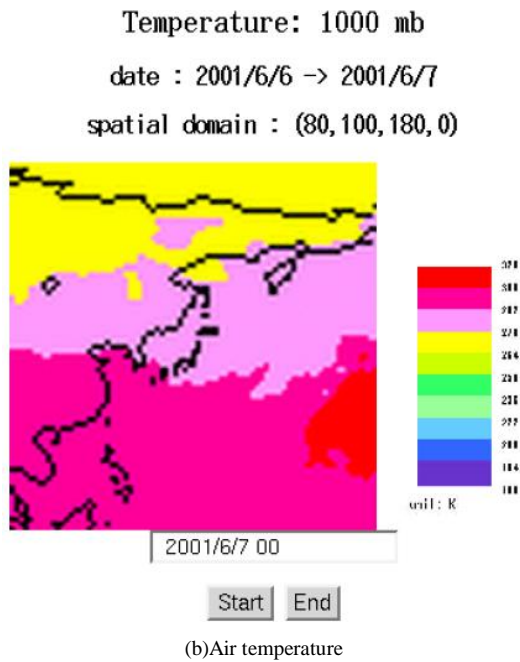
spatial domain : (80, 100, 180, 0)



2001/6/7 06

Start End

(a)Relative humidity



(b)Air temperature

Fig. 8. Example of retrieved assimilation data

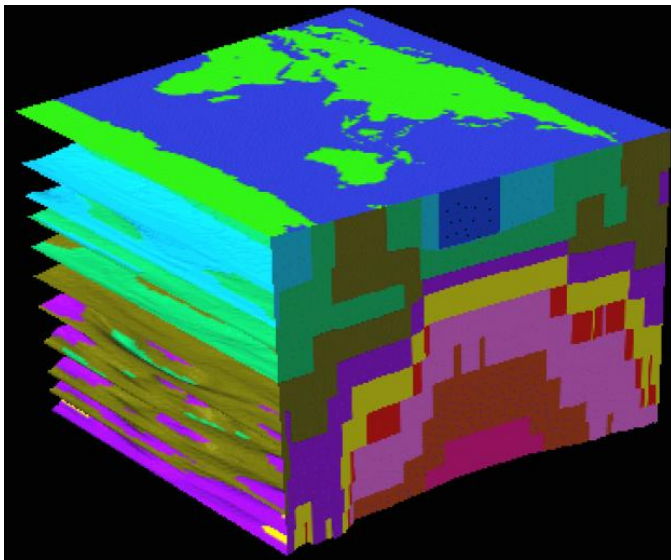


Fig. 9. Example of four dimensional assimilation data with equal space and time intervals which is derived from those with unequal space and time intervals through tweening algorithm of interpolation

After that, these assimilation data format is converted to GIF format for animation representations. Thus animation of four dimensional assimilation data representation can be done as shown in Figure 10.

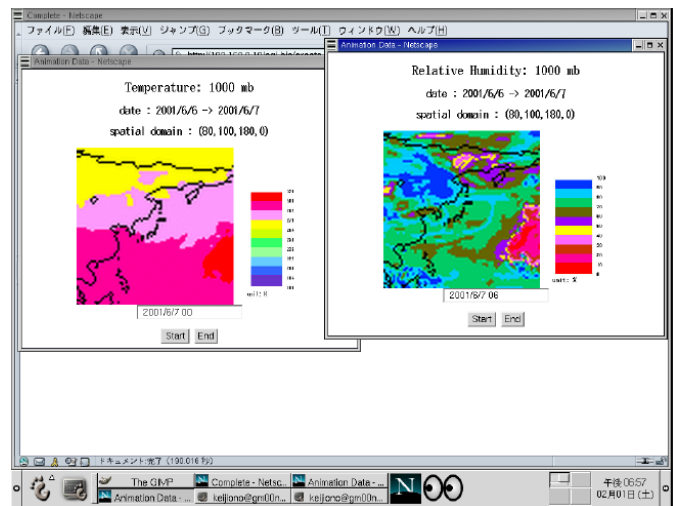


Fig. 10. example of the animation of four dimensional assimilation data representation

#### IV. CONCLUSION

Method for Geography Markup Language: GML based representation of time series of assimilation data and its application to animation content creation and representations is proposed. It is validated the proposed method with NCEP/GDAS assimilation data. Also usefulness of the proposed interpolation method with tweening method is confirmed for unequal time interval of the time series data.

#### ACKNOWLEDGMENT

The author would like to thank Mr. Keiji Ono for his effort to implement GIS system and to conduct the experiment with four dimensional assimilation data.

#### REFERENCES

- [1] K.Arai, Java based methods for remote sensing satellite imagery data processing, Morikita Publishing Co. Ltd., 2001.
- [2] Kohei Arai, Chapter 4: A sea surface temperature estimation method for ocean areas and seasons using a GIS as Neural Network, Sediment and Ecohydraulics INTERCOH 2005, T.Kusuda, H.Yamanishi, J.Spearman and J.Z.Gailani, Edt. Elsevier, ISBN:978-0-444-53184-1, 43-51, 2008.

#### AUTHORS PROFILE

**Kohei Arai**, He received BS, MS and PhD degrees in 1972, 1974 and 1982, respectively. He was with The Institute for Industrial Science, and Technology of the University of Tokyo from 1974 to 1978 also was with National Space Development Agency of Japan (current JAXA) from 1979 to 1990. During from 1985 to 1987, he was with Canada Centre for Remote Sensing as a Post Doctoral Fellow of National Science and Engineering Research Council of Canada. He was appointed professor at Department of Information Science, Saga University in 1990. He was appointed councilor for the Aeronautics and Space related to the Technology Committee of the Ministry of Science and Technology during from 1998 to 2000. He was also appointed councilor of Saga University from 2002 and 2003 followed by an executive councilor of the Remote Sensing Society of Japan for 2003 to 2005. He is an adjunct professor of University of Arizona, USA since 1998. He also was appointed vice chairman of the Commission "A" of ICSU/COSPAR in 2008. He wrote 30 books and published 332 journal papers

# Improvement of Automated Detection Method for Clustered Microcalcification Based on Wavelet Transformation and Support Vector Machine

Kohei Arai, Indra Nugraha Abdullah, Hiroshi Okumura, Rie Kawakami  
Graduate School of Science and Engineering  
Saga University  
Saga City, Japan

**Abstract**—The main problem that corresponding with breast cancer is how to deal with small calcification part inside the breast called microcalcification (MC). A breast screening examination called mammogram is provided as preventive way. Mammogram image with a considerable amount of MC or called clustered MC has been a problem for the doctor and the radiologist. Particularly, when they should determine correctly the region of interest. This work is an improvement work from the previous work. It utilizes the Daubechies D4 wavelet as a feature extractor and the SVM classifier as an effective binary classifier. The escalating point shown with 84.44% of classification performance, 90% of sensitivity and 91.43% of specificity.

**Keywords**—Automated Detection Method; Mammogram; Clustered Microcalcification; Wavelet; SVM; Standard Deviation.

## I. INTRODUCTION

Breast cancer is the uncontrolled growth of breast cells caused by a genetic abnormality. Mostly breast cancer starts from lobules cells, glands or milk producer, and duct cells. Duct cells are parts that transporting milk from the lobules to the nipple. A tumor can be categorized into two main types. First is benign type with characteristic nearly similar with the normal one in appearance such as slow growth, will not spread to the other body parts. The second is a malignant type with vice versa characteristics from benign type.

Based on the Globocan, an international World Health Organization agency for cancer located in France, breast cancer is the most frightening cancer for women in the world, and become the most common cancer both in developing and developed regions. In 2008 estimated 1.38 million new cancer cases diagnosed, the proportion of breast cancer was 23% of all cancers.

TABLE I. SUMMARY OF BREAST CANCER INCIDENCE AND MORTALITY WORLDWIDE IN 2008

Region	Cases	Deaths
World	1384	458
Africa Region	68	37
American Region	320	82
East Mediterranean Region	61	31
Europe Region	450	139
South-East Asia Region	203	93

Western Pacific Region	279	73
------------------------	-----	----

In table 1, we can notice to all regions, the rates of mortality are extraordinarily high and obviously there is no region in the world that has not affected with this cancer. The most worrisome region is Europe region with the number of incidence case and mortality case are 450 and 139, respectively. That means the rate of mortality in this region is 0.308 and made this rate is similar to the rate of the world region, which is 0.331.

In order to overcome this problem, every woman needs to concern about their health through various continuous tests. Breast cancer tests covering screening tests, diagnostic tests, and monitoring tests. In this study, we will focus on the test in screening tests called Mammograms, the most valuable tool not only to screen the cancer, but also to diagnose and evaluate.

Mammogram can read any signs of abnormality such as asymmetry of shape, irregular areas, clusters of small microcalcification (MC) and area of skin thickening. Commonly, the radiologist also operates a Computer Aided Diagnosis (CAD) system. This system will analyze the digital format of mammogram, and the result is a mammogram with any markers in the suspicious areas. The difficulty for the system is to discover clustered extra small calcifications in the form of clusters called with clustered MC.

Abdallah et.al [2] reported the efficient technique to detect the ROI using multi-branch standard deviation analysis and resulting the promising result which more than 98% of true positive (TP) cases. Papadopoulos et.al [3] had proposed the work consists of three stages, first was the cluster detection stage, second stage was the feature extraction stage, and the final stage was the classification stage. In the final stage, they were comparing neural network (NN) and support vector machine (SVM). Accomplished that performance of the SVM was greater than the NN. The most current one is Tieu et.al [4] detected the clustered MC based on the analysis of the their texture. Selection process had done via labeling method of the image that obtained from subtraction the smoothing image from the contrast enhance image, and classification of features completed by neural network. This method was resulting superfine sensitivity equal with 100% and 87.7% of specificity with proper classification rate 89%.

We also had conducted the similar work. However, previous work's result on classification utilizing neural network was deficient [5]. This system needs a new method to achieve better performance of classification, as well as sensitivity and specificity results. Wavelet transform decompose an image to high and low frequency of data when the MC closely related with the high frequency data. Combination of wavelet transform with the SVM classifier as a powerful tool for classifying binary class can be a guaranteed point to obtain better results. Therefore, we propose Daubechies D4 wavelet coefficient's feature with the SVM.

## II. PROPOSED METHOD

### A. Dataset

Dataset comes from Japanese Society of Computer Aided Medical Imaging Technology. Each image has size 2510 x 2000 pixels with single pixel consist of 10 bits. This dataset has two types of images, one-side of breast and two-side of breast. The following images are shown as sample images from the dataset:

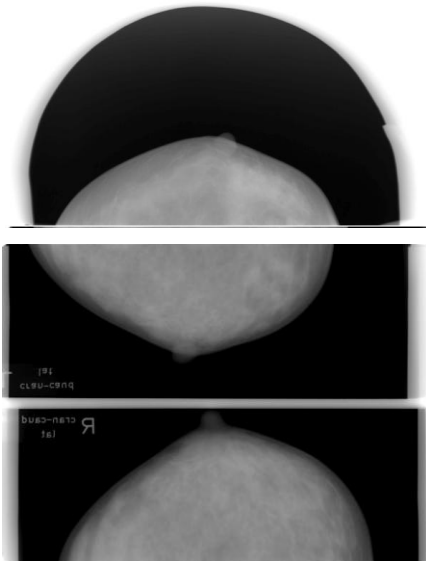


Fig. 1. Samples of mammogram image inside the dataset. One-side of breast (top), two-side of breast (bottom).

There are three categories inside the dataset, normal (N), calcification (C), and tumor (T). However, since the detection for tumor category is easy even using human perception. We only consider two categories that are N and C and inside the C class can be found some numbers of clustered MC. The number of images in C and N categories are 12 images, 33 images, respectively.

### B. Detection of MC and Clustered MC

#### 1) Breast Tissue Detection Based on Texture-based Analysis

In this study, we apply the method that has developed by Tieudeu et.al [4] with modification in one specified area. They are developed the main method by utilizing three methods. First is enhancing the contrast of the original image then

produce an image called contrast enhance image (CI) and the way to get this image become a point of modification. The second is smoothing the original image then produce an image called with smoothed image (SI). The last is subtraction the smoothed image from enhanced image then called with difference image (DI).

This adoption motivated by clustered MC that allied with breast mass can be concluded as a benign or even premalignant cancer. Frequently, MC only associated with extra cell growth inside the breast. This method also can save time and memory processing for further process. Different with the previous study when forming the CI, we are using the histogram equalization method with the aim to spread the most frequent intensity values that make the lower contrast reach a higher contrast. The details are represented by the equation below:

$$prob_n = \frac{\#pixels \text{ intensity } n}{\#pixels}; n = 0, 1, 2 \dots L \quad (1)$$

$$M_i = floor \left( (L) \sum_{n=0}^i prob_n \right) \quad (2)$$

Where  $prob_n$  denotes the normalized histogram for each gray level value,  $n$  is gray level values,  $L$  is maximum gray level value and  $M$  is image matrix.

#### 2) Multi-branch Standard Deviation Analysis

MC related with local maxima pixels in the image. This motivated us to find a correlation between the local maxima and its neighboring pixels. In this study, we conduct an analysis utilizing standard deviation method to find this correlation as reported by Abdallah et.al [2]. Develop a multi-branch point of view become basic needs. It because highly possible if we find a local maxima in one direction and after take a look in a different direction that point is not a local maxima. That critical point provides promising solution to find the clustered MC in one small area. The illustration provided as below:

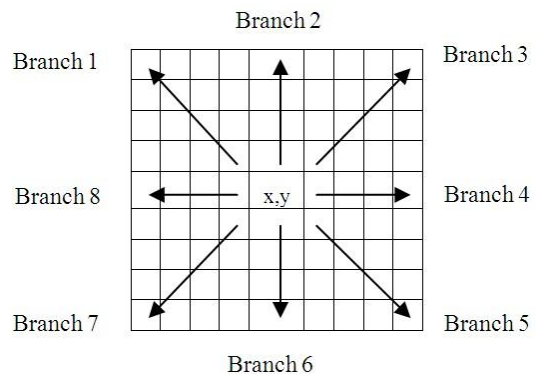


Fig. 2. Multi-branch standard deviation analysis to find MC.

Where  $x, y$  point is an ideal local maxima if from all branches seen as a local maxima. Dissimilar with Abdallah et.al work, we only calculate the standard deviation for the n-brightest pixel only.

At the time that we need to know one point is local

maxima from one branch, the threshold value and the counter needed. While calculating the threshold between the central pixel and its neighbor pixels if the standard deviation greater than the threshold value the counter will be increasing by one, whereupon an ideal local maxima is the point that has a counter value equal with eight. Described with the following equation:

$$STD_i = \sqrt{\frac{\sum_{i=1}^n (Center - x_i)^2}{n}}; \quad i = 1, 2, \dots, 8 \quad (3)$$

Where:

- $STD_i$  = Standard Deviation at branch  $i$
- Center = Cluster center
- $x_i$  = Gray level value at the specified position  $i$
- $n$  = Number of pixels

As said before the counter will have a maximum value 8, that value is equal with a total of branches in this method.

The mammogram image is scanned under 0.1 mm x 0.1 mm, acquired the number of pixels is 10 x 10 pixels/mm. Regarding the size of single MC is under 1 mm, the 9 x 9 window size will be appropriate enough to detect MC. Region of interest (ROI) as a final result of this section has size 128 x 128 which matched with the most clustered MC's size. In this study, one mammogram image represented by one ROI although there is more than one clustered of MC can be found. It is because this system has a purpose as assistance to the doctor and the radiologist when they are facing the clustered MC. Even if only one representation of clustered MC is found still means the patient defined as calcification's patient and need further treatment. Moreover, selection criterion of ROI is the area with the highest number of suspicious local maxima pixels (MC).

### C. Daubechies D4 Wavelet Transform

For  $N \in \mathbb{N}$ , Daubechies wavelet of class D-2N is function  $\psi = {}_N\psi \in L^2(\mathbb{R})$  denoted by

$$\psi(x) := \sqrt{2} \sum_{k=0}^{2N-1} (-1)^k h_{2N-1-k} \phi(2x - k), \quad (4)$$

where  $h_0, \dots, h_{2N-1} \in \mathbb{R}$  are the constant filter coefficients that fulfilling the conditions

$$\sum_{k=0}^{N-1} h_{2k} = \frac{1}{\sqrt{2}} = \sum_{k=0}^{N-1} h_{2k+1}, \quad (5)$$

similarly, for  $l = 0, 1, \dots, N - 1$ ,

$$\sum_{k=2l}^{2N-1+2l} h_k h_{k-2l} = \begin{cases} 1 & \text{if } l = 0, \\ 0 & \text{if } l \neq 0, \end{cases} \quad (6)$$

and where  $\phi = {}_N\phi : \mathbb{R} \rightarrow \mathbb{R}$  is the scaling function, given by the recursive equation

$$\phi(x) = \sqrt{2} \sum_{k=0}^{2N-1} h_k \phi(2x - k) \quad (7)$$

Daubechies orthogonal wavelets of classes D2 - D20 (only even index numbers) are the wavelets that generally used [7]. The index number belongs to the number 2N of coefficient. Single wavelet has a number of vanishing moments equal to half the number of coefficients. In this study we propose to use Daubechies D4 wavelets, it has two vanishing moments. With these vanishing moments D4 can encodes polynomial of two coefficients, for example constant and linear signal components. It will be suitable as a feature extractor for representing clustered MC.

### D. Support Vector Machine

SVM is a powerful tool for data classification. The indicators are the easiness to apply and impose Structural Risk Minimization (SRM). SRM armed the SVM to have strong ability in generalization of data. Its function is to minimize an upper bound on the expected risk. In principle, SVM learns to obtain optimal boundary with maximum margin that able to separate set of objects with different class of membership.

In order to achieve the maximum margin classifier, we have two options. Hard margin and soft margin are the options that totally depend on linearity of the data. Hard margin SVM is applicable to a linearly separable dataset. However, often the data is not linearly separable. Soft margin SVM emerged as its solution [8]. The optimization problem for the soft margin SVM presented as below:

$$\min_{w,b} \frac{1}{2} \|w\|^2 + C \sum_{i=1}^n \xi_i$$

subject to:  $y_i(w^T x_i + b) \geq 1 - \xi_i, \quad \xi_i \geq 0. \quad (8)$

where  $w, C, \xi, b$  are the weight vectors, the penalty of misclassification or margin errors, the margin error, the bias, respectively.

In (8) can lead us to efficient kernel methods approach. A kernel method is an algorithm that depends on the data only through kernel function, which computes a dot product in some possibly high dimensional data. Using the function  $\phi$  training vector the input space  $x$  is mapped into higher dimensional space.  $K(x_i, x_j) = \phi(x_i)^T \phi(x_j)$  is called kernel function. The degree of the polynomial kernel can control the flexibility of resulting classifier [9]. It will be appropriate with this research when we classify the clustered MC and non-clustered MC. Polynomial kernel is shown in following equation:

$$K(x_i, x_j) = (\gamma x_i^T x_j + r)^d, \quad \gamma > 0. \quad (9)$$

where  $\gamma, r, d$  are kernel parameters, and  $i, j$  denote  $i^{th}, j^{th}$  vector in dataset.

In this research, we propose to use Sequential Minimal Optimization (SMO). SMO act as efficient solver of the optimization problem in training of support vector machines. SMO also solves the problems analytically by way of breaks the problems into a series of smallest possible problems.



Despite of this algorithm guaranteed to converge, it used heuristics to choose the pair of multipliers that able to accelerate the rate of converge.

### III. EXPERIMENTS

#### A. Detection of MC

Through the described method, we obtained all images called the CI, SI and DI. From below DI image, we can obviously see the breast tissue area. This area will be the main concern when finding the clustered MC. Through the DI also we obtained efficiency in memory and time processing. As an example, shown with the images below:

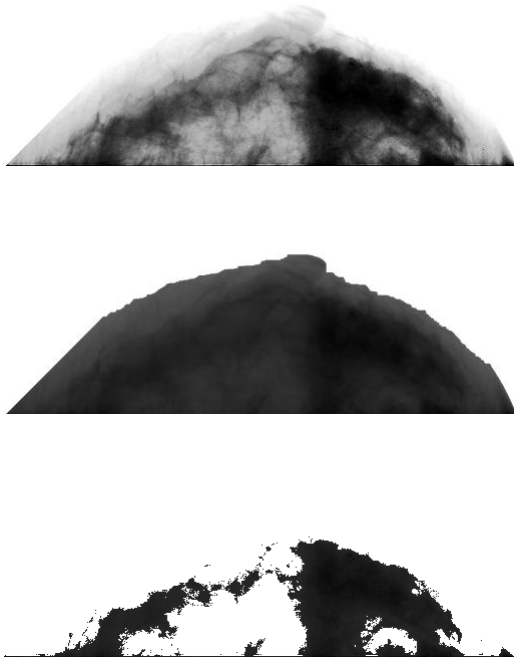


Fig. 3. Sample of the CI, SI and DI images.

Mostly the MCs are detected on this category. It clearly shows that multi-branch standard deviation method with window size  $9 \times 9$  was suitable to detect the clustered MC. The following images show detected MC inside the mammogram image:

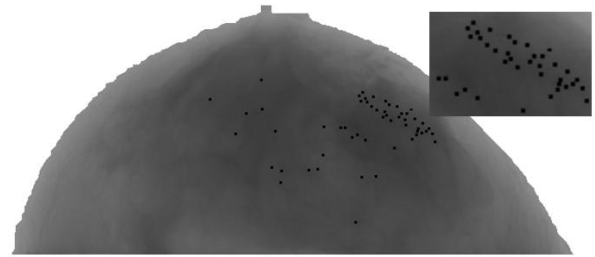
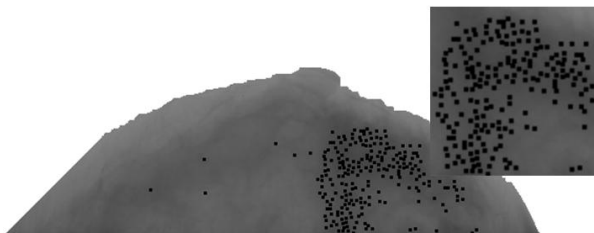


Fig. 4. The samples of detected MC on mammogram images.

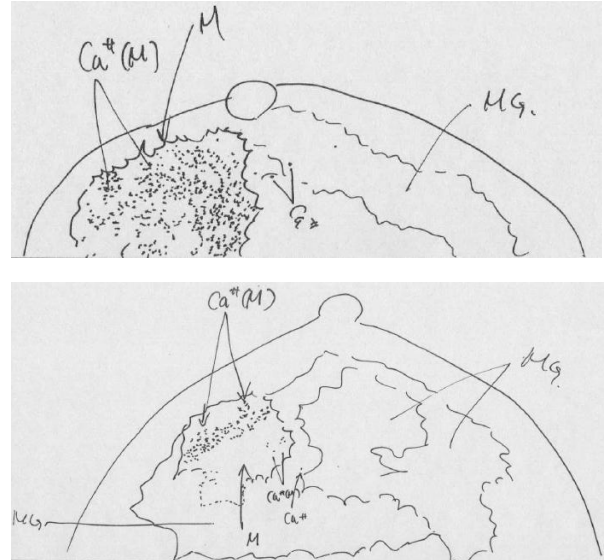


Fig. 5. The sketch images (reverse side with original image) of corresponding mammogram images in Fig. 4

The maximum  $n$  value was 200. It means we only calculate 200-brightest pixels inside the mammogram image. After the experiment, threshold value for MC detection equal with 8 was the maximum threshold value.

#### B. Detection of clustered MC

The size of mammogram image is large, make the efficiency in time and memory processing should be properly considered. As a solution, the ROI selection was not applied pixel-wise detector, but based on  $128 \times 128$  pixels of window-wise detector and moved around the image. The window with the highest number of detected MC will be selected. According to the proposed method, resulting ROI images as presented below:

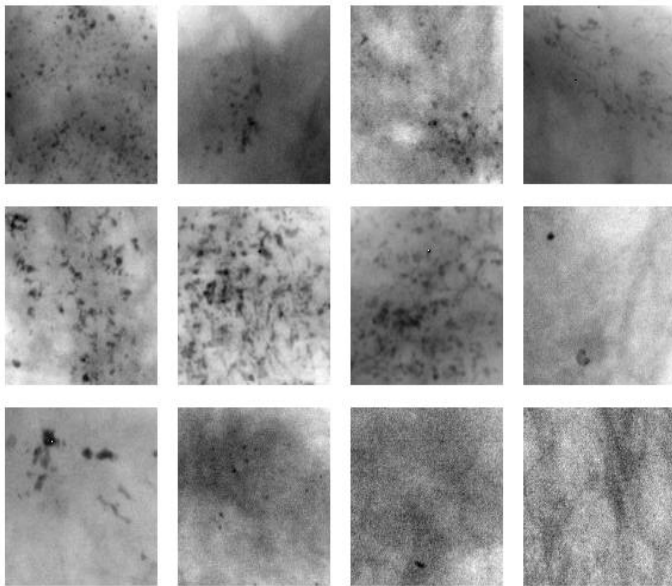


Fig. 6. The detected clustered MC region.

From above image, the system was resulting 12 of clustered MC images. The correct and false detected clustered MC were 9 and 3 images, respectively.

Precisely, true positive (TP), true negative (TN), false positive (FP) and false negative (FN) are the options for diagnosis decision. TP means similarity clustered MC of judgment from an expert and system, TN means similarity a non-clustered MC judgment from an expert and system, FP means a non-clustered MC classified as clustered MC, and last is FN which means a clustered MC classified as a non-clustered MC. After the experiment, the results shown with the following table:

TABLE II. CONFUSION MATRIX

TP	FP
9	3
FN	TN
1	32

At the comparison process, in order to increase the accuracy of ideal clustered MC image, we were involving the sketch image from the doctor as the knowledge base as shown in Fig. 5.

Hereafter let we talk about other parameters that can indicate the system whether is acceptable or not which are sensitivity and specificity. Both parameters are shown as below:

$$\text{Sensitivity} = \frac{TP}{TP+FN}$$

$$\text{Specificity} = \frac{TN}{TN+FP}$$

Previously, we were working with T category as well as N and C categories. However, similar with aforementioned reason, the determination of T category is something effortless. The doctor will find out quickly the mammogram image that considered as a tumor or not. In this study, we were only working with N and C category. Acquired the sensitivity and specificity values are 90% and 91.43%, respectively.

### C. Features Selection

Features selection is based on statistical theory consist of max, mean, variance, standard deviation, coefficient of variation, with two additional features, centroid and 7 Hu moments. These features capture from decomposition result of each detail, approximation, horizontal, vertical, and diagonal details, visualize as shown in Figure.

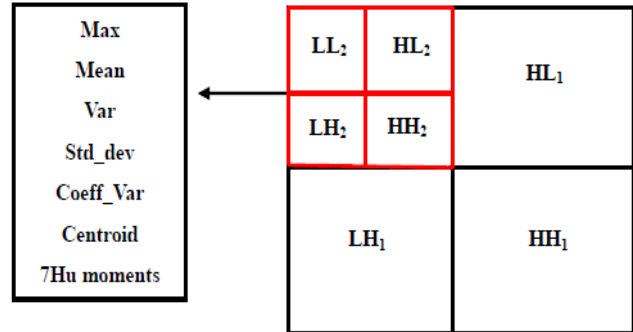


Fig. 7. Features selection from wavelet coefficients.

The mean, variance, and standard deviation are valuable because of their relationships to the normal curve. Variance distribution represents the high frequency data that related with MC. Likewise, max number of wavelet coefficient involved is an additional feature to represent high frequency data. Meanwhile, coefficient of variation shows the extended variability in relation to mean of the population.

The Hu moments are proved to be invariant to the scaling, rotation and reflection. We used centroid to measure contour's centroid of the clustered MC image. From these features, we obtained satisfactory classification results. Approximation included because some of distinct factor that contained in the clustered MC image.

### D. Classification performance

In this part, the data set separated into two parts that are training and testing parts with the data proportion were 74% and 26%, respectively. For training data, we were adding ideal output in the form of ROI from all categories manually to train the classifier and then extracted their features. The below table is classification performance:

TABLE III. CLASSIFICATION RESULT USING DECOMPOSITION IMAGE LEVEL 2 OF DAUBECHIES D4 (IN PERCENT)

Method	L,H,V,D	H,V,D
Training set	95.31	94.53
Supply test set	80	82.22

\*L, V, H, D stand for (approximation image, horizontal, vertical, diagonal details)

TABLE IV. CLASSIFICATION RESULT USING DECOMPOSITION IMAGE LEVEL 3 OF DAUBECHIES D4 (IN PERCENT)

Method	L,H,V,D	H,V,D
Training set	94.53	94.53

Supply test set	84.44	82.22
-----------------	-------	-------

\*L, V, H, D stand for (approximation image, horizontal, vertical, diagonal details)

Even though MC related with high frequency data. We still found small necessity of approximation image. The MC in the form of cluster could well capture while we considered it. Then, the decomposition level 3 of supply test result was resulting more preferable result in comparison with level 2.

The detected MCs that lied in level 3 of the ROI image nearly similar to the sketch result inside the dataset. We decided, not to apply decomposition level 4 because the decomposition result will be a quarter of previous decomposition images, 16x16 pixels image is too small to be recognized by the system.

#### IV. CONCLUSION

In this study, we had improvement in classification result, sensitivity and specificity. In comparison with the previous method, this method was finer. The current classification result was much better indicated by 84.44% compared to 70.8% of result in the previous work. The sensitivity and specificity values were also escalated from 79% and 87% to 90% and 91.43%, respectively. Moreover, this system had the efficiency in time and memory processing in term of detection of breast tissue as well as utilization the SVM classifier.

#### V. FUTURE WORK

The future work that can be developed from this current work is conducting another proper method in single MC detection to obtain superfine clustered MCs. One of the promising methods is Dyadic wavelet transformation with its shift invariant characteristic. That detection is to escalate the sensitivity and specificity performances.

#### REFERENCES

- [1] Songyang Yu and Ling Guan, "A cad system for the automatic detection of clustered microcalcifications in digitized mammograms films," IEEE Transactions on Medical Imaging, Vol 19(2), pp. 115-125, 2000.
- [2] M. H. Abdallah, A. A. Abubaker, R. S. Qahwaji, M. H. Saleh, "Efficient technique to detect the region of interests in mammogram image," Journal of Computer Science, Vol 4(8), pp. 652-662, 2008.
- [3] Papadopoulos A., Fotiadis D.I., Likas A., "Characterization of clustered microcalcifications in digitized mammograms using neural network

and support vector machine", Artificial Intelligence in Medicine Vol. 34, pp. 141-150, 2005.

- [4] A. Tieudeu, C. Daul, A. Kentshop, P. Graebing, D. Wolf, "Texture-based analysis of clustered microcalcifications detected on mammograms," Digital Signal Processing, Vol 22, pp. 124-132, 2011.
- [5] Arai K., Abdullah I.N., Okumura H, "Automated detection method for clustered microcalcification in mammogram image based on statistical textural feature". International Journal of Advanced Research in Artificial Intelligence (IJARAI) Vol. 1(3), pp. 22-26, 2012.
- [6] Lucio F. A. Campos, A. C. Silva, A. K. Barros, "Diagnosis of breast cancer in digital mammograms using independent analysis and neural network," CIARP, pp. 460-469, 2005.
- [7] De Vries Andreas, "Wavelets", FH Sudwestfalen University of Applied Sciences, Hagen, Germany, 2006.
- [8] Ben-Hur Asa, Weston Jason, "A user's guide to support vector machine", in Data Mining Techniques for the Life Science, pp 223-239, Humana Press, 2010.
- [9] Hsu Chih-Wei, Chang Chih-Chuang, Lin, Chih-Jen, "A practical guide to support vector classification". Department of Computer Science National Taiwan University, Taiwan, 2010.

#### AUTHORS PROFILE

KOHEI ARAI received BS, MS and PhD degrees in 1972, 1974 and 1982, respectively. He was with The Institute for Industrial Science and Technology of the University of Tokyo from April 1974 to December 1978 and also was with National Space Development Agency of Japan from January, 1979 to March, 1990. During from 1985 to 1987, he was with Canada Centre for Remote Sensing as a Post Doctoral Fellow of National Science and Engineering Research Council of Canada. He moved to Saga University as a Professor in Department of Information Science on April 1990. He was a counselor for the Aeronautics and Space related to the Technology Committee of the Ministry of Science and Technology from 1998 to 2000. He was a counselor of Saga University for 2002 and 2003. He also was an executive counselor for the Remote Sensing Society of Japan for 2003 to 2005. He is an Adjunct Professor of University of Arizona, USA since 1998. He also is Vice Chairman of the Commission A of ICSU/COSPAR since 2008.

INDRA NUGRAHA ABDULLAH was born at Bogor, Indonesia in June 1987. Finished his bachelor degree in Bogor Agricultural University and graduated from Saga University for master degree in the field of Information Science on March 2011. He is currently pursuing to get Ph.D. Degree from the same university with specialization in image processing area. Leaf identification becomes his interest in his latest degree.

HIROSHI OKUMURA was born at Kyoto, Japan in 1964. He received B.E.S.E. and M.E.S.E. degree from Hosei University in 1988 and 1990, respectively, and Ph.D degree on environmental engineering from Chiba University in 1993. He became a research associate at Remote Sensing and Image Research Center, Chiba University first in 1993. Next, he became a research associate and a lecturer at the Department of Electrical Engineering, Nagaoka University of Technology in 1995 and 2000, respectively. He is now an associate professor at the Department of Information Science, Saga University. His research interests are in image and speech processing and remote sensing.

# A Simulated Multiagent-Based Architecture for Intrusion Detection System

Onashoga, S. Adebukola, Ajayi, O. Bamidele and Akinwale, A. Taofik  
Department of Computer Science,  
Federal University of Agriculture, Abeokuta Ogun State Nigeria.

**ABSTRACT**—In this work, a Multiagent-based architecture for Intrusion Detection System (MIDS) is proposed to overcome the shortcoming of current Mobile Agent-based Intrusion Detection System. MIDS is divided into three major phases namely: Data gathering, Detection and the Response phases. The data gathering stage involves data collection based on the features in the distributed system and profiling. The data collection components are distributed on both host and network. Closed Pattern Mining (CPM) algorithm is introduced for profiling users' activities in network database. The CPM algorithm is built on the concept of Frequent Pattern-growth algorithm by mining a prefix-tree called CPM-tree, which contains only the closed itemsets and its associated support count. According to the administrator's specified thresholds, CPM-tree maintains only closed patterns online and incrementally outputs the current closed frequent pattern of users' activities in real time. MIDS makes use of mobile and static agents to carry out the functions of intrusion detection. Each of these agents is built with rule-based reasoning to autonomously detect intrusions. Java 1.1.8 is chosen as the implementation language and IBM's Java based mobile agent framework, Aglet 1.0.3 as the platform for running the mobile and static agents. In order to test the robustness of the system, a real-time simulation is carried out on University of Agriculture, Abeokuta (UNAAB) network dataset and the results showed an accuracy of 99.94%, False Positive Rate (FPR) of 0.13% and False Negative Rate (FNR) of 0.04%. This shows an improved performance of MIDS when compared with other known MA-IDSs.

**Keywords-** MIDS; CPM; Pattern-growth; Profiling

## I. INTRODUCTION

Computer networks, including the Internet, have grown in both size and complexity. The services they offer made them the main means to exchange data and optimal environment for e-businesses. They have consequently become the means to network attacks. Intrusion detection technology provides reasonable supplement to the intrusion prevention systems such as firewalls, audit trails, system log etc. It has been a research focus for more than two decades from the publication of John Anderson's paper in 1980 (Anderson, 1980). Intrusion Detection Systems (IDSs) detect some set of intrusions and execute some predetermined actions when an intrusion is detected (Wang, 2006). Intrusion Detection has been achieved by following two different strategies of analysis.

- Anomaly detection: relies on models of "normal" behaviour of a computer system. Behaviour profiles maybe focused on users, applications or networks. Anomaly detection compares the defined profiles against the actual usage

patterns to detect "abnormal" activity patterns. These patterns will be considered as intrusions.

- Policy detection: relies on a set of attack descriptions called attack signatures (Sasikumar & Manjula, 2011).

A Distributed IDS consists of multiple intrusion detection systems over a large network, all of which communicate with each other, or with a central server that facilitates advanced network monitoring, incident analysis, and inside attack data. Wrapping each of the components in IDS as mobile agent is aimed at effective intrusion detection in distributed environment. Intrusion detection in distributed environment requires data gathering, analysis and detection at every unit of the network and it has been established that mobile agent would perform well with this task (Sodiya, 2006). Agent is an entity being able to accomplish some work without manual intervention and supervision in certain condition and is able to migrate from host to host on a network under its own control. The agent chooses when and to where it will migrate and may interrupt its own execution and continue elsewhere on the network. An agent could also be static, that is, resides permanently on a platform performing one task or the other. In a distributed IDS system, each agent shares its data with other agents in the system (Oriola et. al, 2012).

Mobile Agents are considered to be an effective choice for many applications for several reasons. The ability for mobile agents to sense their environments and react dynamically to changes is useful especially in intrusion detection. As mobile agents, the IDS can evade attacks. The constant movement of these agents in a network among multiple hosts makes it difficult for an attacker to locate and disable them. A Multiagent system is a system in which several interacting, intelligent agents pursue some sets of goal, or perform some sets of tasks. Multiple Agent system can adopt the characteristic of mobility to carry out activities in a flexible and intelligent manner that is responsive to changes in the environment (Bradshaw, 1997). It consists of a number of agents, which interact with one another, typically by exchanging messages through some computer network infrastructure (Wooldridge, 2002).

This paper makes an attempt to propose solutions to having a better detection rate and to actualize the real implementation of a Multiagent system for intrusion detection in an environment by introducing an intelligent and flexible MultiAgent architecture for IDS (MIDS). MIDS is designed based on the following interests:

a) *Improving time-to-detection of MA-IDS.*

b) *Provide an architecture where real time attacks are efficiently detected.*

c) *Aims at reducing effectively, false alarm rates mining the closed frequent patterns of users' activities (Onashoga, et. al, 2009) for profiling.*

d) *Since the role of IDS is to monitor and ensure security of the network, the MA-IDS itself is a primary target of attacks. It then becomes important for IDS agents to operate in hostile environment and still exhibits a high degree of fault-tolerance and performance.*

The rest of the paper is organized as follows: Section 2 reviews past researches that have been done in the area of mobile agent based intrusion detection system. Section 3 details on the proposed architecture and its considerations for achieving a better detection rate, while section 4 describes the testbed implementation procedures and its performance analysis. Section 5 concludes the work.

## II. EXISTING RELATED RESEARCHES

Herrero & Corchado (2009), Kamaruzaman et. al. (2011) and Onashoga et. al. (2009) reviewed some related work on MA-IDSs with focus on the tasks, architecture and implementation of agents. In contrast, an extensive critical review of MA-IDS with focus on their architecture, techniques, strengths and weaknesses is done in this paper. This section details the reviews of recent related researches.

Sasikumar & Manjula (2012) proposed a 3-layer fault tolerant architecture. The architecture consists of Host and Net agents at the first layer, the mobile agents at the second layer and the Decision-making and Replication agents in layer 3. The Host Agent's function is to protect the host. When suspicious activities can't be decided, the Host Agent generates an Intrusion Detection event and transmits it to layer2. The role of the Net Agent is to detect network intrusions. It supervises the network traffic, records all suspected events in a data base and responds intrusions. It also installs mobile agent platform on it. The mobile agent is responsible for collecting information of an attack from the Host Agents or Net Agents for further analysis in layer3. The Decision-making Agent analyses the data collected by the mobile agent and passes the control to Replication agent, who in turn is responsible for replication and recovery management. The fault tolerance reported is the data analysis by agent and the pass of control to the replication agent. The techniques used is not reported. Also the security of the agents is not considered.

Oriola et. al. (2012) proposed a peer to peer architecture that integrates the concept of multiagent system and data mining. The architecture proposed has 3 levels namely: The first level which is the core of the system. It is at this level that the interaction and integration of static and decentralized multi-agent system and distributed data mining is established. The second level is made up of dedicated and specialized agents that cooperate and communicate to generate host based and network based intrusion detection system. At the highest level of composition, different intrusion detection systems are

involved. Their mode of cooperation, communication and detection capability are not reported..

Zeng and Duo (2009) followed a typical network-based application where there are more than one application servers, database servers and clients. The model designed consists of three agents namely: client agent, communication agent and server agent. Client agents are installed on a client workstation, and responsible for collecting extra user information and then send to server agents with the help of communication agents. Server agents run in the server where masquerade intrusion is to be detected. They process the message sent from client agents, read from and write to user model, server agents can make a decision on whether the current user is a legal one or not according to a predictive model. Communication agents monitor the client agent's request. After the received message is parsed, the useful message is forwarded to the server agents. The client agents collect user information such as operating system, log files, network card etc. Zeng and Duo (2009) adapted the use of Hidden Markov Model (HMM) to model user's activities on server. The algorithm makes sure that the likelihood of sequence with respect to the HMM increases after each iteration in the training. These training sets are constructed from the event database. However, a data mining algorithm is used to filter the events that seem abnormal, because abnormal user sequences are not allowed to be included in the training set. The strengths of this algorithm lie on (1) the focus of the model on detecting only one type of intrusion – masquerade attack (2) the model makes use of real time detection. The security of the agents is not reported.

DNIDS architecture proposed by Kuang (2007) consists of 5 components namely Sensors, Detectors, Alert Agents (AA), Maintenance Agents (MA), the Manager, and the Console. Sensors capture the network packets from a network segment and transform them into collection-based vectors. The Detector is a collection of CSI-KNN (Combined Strangeness and Isolation K-Nearest Neighbor) classifiers that analyze the vectors supplied by the sensors. The 3 agents are only designed for intrusion tolerance not for intrusion detection and are only installed on the administrative server. Detection rate of the architecture proposed is not reported in this work.

Abraham et.al (2007) proposed a hierarchical architecture with Central Analyzer and Controller (CAC) as the heart and soul of the DIDS. The CAC usually consists of a database and webserver which allows interactive querying by the network administrator for attack information/analysis and initiate precautionary measures. CAC also performs attack aggregation, building statistics, identify attack patterns and perform rudimentary incident analysis. The mode of data collection is not discussed but the algorithm is tested on the KDD cup 1999 dataset whose source is network based. The authors tested the model using different soft computing techniques which consists of neural network, fuzzy inference system, approximate reasoning and derivative free optimization techniques on a KDD cup dataset. The experiments have three phases namely: input feature reduction, training phase and testing phase. In the data reduction phase, important variables for real-time intrusion detection are selected by feature selection. In the training

phase, the different soft computing models are constructed using the Labeled data. The test data is then passed through the saved trained model to detect intrusions in the testing phase. The problem faced with hierarchical architecture is being solved by allowing a free communication between the layers. A well comparative analysis of the different soft computing algorithms with other machine learning techniques is being carried out which serves as references for researchers in the field. The full description of how the agents detect intrusions based on the soft computing algorithms proposed is not well discussed.

Sodiya (2006) proposed a two-level architecture coined MSAIDS. The first level is the Lower Level Detection (LLD), which has the data agents and processing agents. The data agents move around the nodes in the network to collect associated information. The 2 processing agents also known as node agents where Node-1 agent is responsible for construction of the first level database from the information collected and for data cleansing, classification and formatting. The Node-2 agent is responsible for data mining and first level intrusion detection and communicates the possibility of intrusions to the interface agent through the alarm agent. The Upper Level Detection (ULD) also known as confirmation level is involved in separate intrusion detection process. At the ULD, the lower level agents gather data from the data agents and inform the Controller and Protector (CP), which acts as the Facilitator agent about the nature of the data gathered. The CP also ensures proper communication and delivery of service among agents. The data gathered are then used to update the ULD database; the ULD does not check for intrusion if there is no signal from the LLD. The types of data collected are application messages, authentication events, system calls, TCP connections. An Apriori algorithm is modified to extract patterns by the first level and second level agents. MSAIDS maintains security of agents by using asymmetric cryptosystem of the Aglet's framework. In addition to this, agents' states are recorded and authenticated before they are initiated. Any suspected intrusion is reported by the Interface Agent to the Site Security Officer (SSO). The action to be taken by the SSO is not stated. In addition to securing mobile agents, the use of recorded state mechanism, which has been proved effective, is a plus in this work. The drawbacks identified are firstly, the activities at the ULD could still be integrated with the LLD to form one-level architecture and have the CP at the ULD since detection of intrusion at each level is still based on same algorithm. It took 0.14 seconds to report an intrusion at the LLD and 0.75 seconds at the ULD. And secondly, the architecture presented does not provide security for the database, which could be vulnerable to changes by attackers.

Wang et. al. (2006) designed a system framework which includes the Manager, who is the centre of controlling and adjusting other components. It maintains their configuration information. The manager receives intrusion alarms from host monitor mobile agent and executes intrusion responses using intrusion response mobile agent. It also consists the host monitor mobile agent that resides on every host in the network. If intrusions occur confirmatively, the host monitor MA will appeal to the manager and report the suspicious activity directly. After receiving the appeal, the manager distributes a data gathering MA patrolling other hosts in the network to gather information. If a distributed intrusion is found, the manager will assign an intrusion response MA to respond intelligently to every monitored host. The database of configuration stores the node configuration of detecting system. The data source of IDS is both host-based and network-based. The gathering part of data source is to record, filter and format the connection information of the monitored host and write them into the log. The types of data collected includes system log and some conserved audit records. The intrusion analysis mobile agent mainly analyses the log file in the monitored host system and compares them with the characters of known attack activities to find abnormal activity combined with different detection measures which were not mentioned. The framework's security is based on the security measures provided by Aglet. The intrusion response MA responds to the intrusion events that occur which can include tracking the intrusion trace to find the intrusion fountain, recording the intrusion events into database etc. It changes the hierarchical system structure of traditional distributed IDS. The major drawback lies at the control centre carrying out the major part of the intrusion detection, if the location of this centre is discovered, then the system collapses.

### III. PROPOSED ARCHITECTURE

This section presents a full description of Multi-agent based Intrusion Detection System (MIDS). MIDS's agents' architecture consists of both static and mobile agents. MIDS uses an algorithm named Closed Pattern Mining (CPM), which adopts a data mining descriptive model for user profiling. This is now followed by a full description of the components of MIDS.

#### A. Mids Architecture

The MIDS architecture, shown in Figure 1 adopts the data mining algorithm (CPM) for user profiling. It adopts a real time mode of detection in a network environment. MIDS architecture structure is into two parts:

- 1) *The IDS Control: resides on every host;*
- 2) *The Administrative Control: resides on the server.*

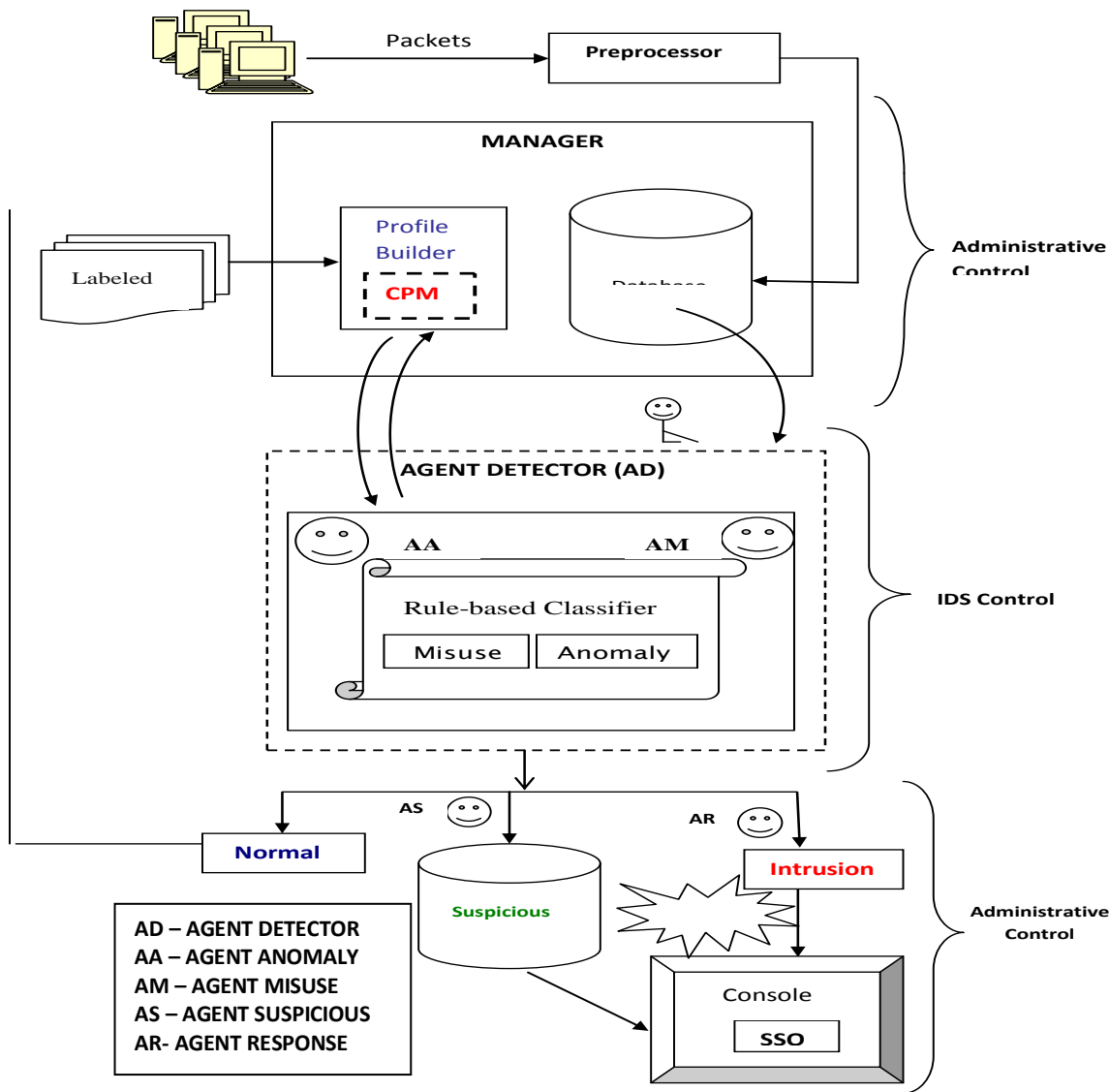


Fig. 1. Multiagent-based Intrusion Detection System (MIDS) Architecture

In general, the architecture consists of 3 major phases which involve the data gathering phase, the Detection phase and then the Response phase which is passed to the Site Security Officer (SSO).

Each of these phases is explained as below:

### 3.1.1 Data Gathering phase

The data gathering phase involves collection of data and profiling stage. The data collection is done on both the host and network. Each of the host has a sensor, a network sniffer is integrated in the sensor and is used to gather all network packets. As data streams travel back and forth over the network, the sniffer captures each packet and eventually decodes and analyzes its contents according to specifications. For example, *tcpdump*, a network debugging tool can serve as a sniffer and monitor the packets transmitted over a network. The preprocessor is responsible for accepting raw packet data and producing records. This component is capable of reading packets from the *tcpdump* file. The output produced by this component consists of records which are now stored in a

database. Record contains aggregate information for a group of packets.

In MIDS architecture, the roaming agent (RA) consists of three parts: the code, itinerary and results. It moves from host to host to gather data following a predefined itinerary established by the Manager. The Manager acts as the supervisor of all agents in the architecture. Each record gathered is now stored in the database. The profiling stage involves the use of CPM algorithm by mining only the closed patterns of users' activities.

### 3.1.2 Detection phase

The architecture makes use of the two approaches for detection: Anomaly and Misuse approach. This phase is the IDS Control part of the architecture. At this phase, the Agent Detector collects the newly arrived record and clones (using the clone() method) itself into "two": the Agent Misuse (AM) and Agent Anomaly (AA). The AA, who is in charge of anomaly detection takes this record and checks the Profile Builder (where CPM resides) for the user's profile. This is

done so as to know whether the behaviour is in line or deviates from the normal user's profile. On the other hand, the AM searches for any attack signature in the record based on the rules defined to check for an attack. See5 tool (RuleQuest, 2007) is used for rule classification. See5 is a GUI based software which is capable of classifying large volumes of data within a second depending on the speed and specification of computer processor. The rule-based classifier is used in this work so as to have an idea of how rules are being defined for misuse detection. The following are excerpts of the rules which the cloned agents now classifies the event as "Normal", "Suspicious", or "Intrusion":

*a) Suspicious*

An event is said to be suspicious if it slightly deviates from the normal behaviour of the user, that is, its item falls within a particular range, for example:

```
if (hot<3 || (failedLogin <=5 | srcByte <=100 |
destByte <= 50) && service == "hotspot")
{
    System.out.println ("DETECTOR >>
User: ["+id+"] Suspicious!");
    msg.sendReply(1);
}
```

This event is now transferred to the Agent Suspicious (AS) which first stores this in a database for monitoring and then passes it to the SSO through the console.

*b) Intrusion*

Some rules are also defined for categorizing intrusive events e.g. an event is said to be "intrusion" if it deviates entirely from the normal behaviour, that is, the values of its items passes the ones considered for "suspicious" or some discrete values are not seen. For example, in a system where the only network service used is "hotspot", any event that has a service aside this is taken as "intrusion".

*c) Normal*

Any other event outside the conditions in (a) and (b) is considered "Normal". The Agent Detector is responsible for passing the "Normal" user to the Profile Builder for update. The condition for classification of normal records is as shown in the example below:

```
if (hot==0 || (failedLogin <=3 && srcByte <=128 &&
destByte <=64) && service == "hotspot")
{
    System.out.println("DETECTOR >>
User: ["+id+"] Normal!");
    msg.sendReply(1);
}
```

### 3.1.2.1 CPM Algorithm

This section first describes the factors behind the development of CPM algorithm and then details the pseudocode of the algorithm. The Closed Pattern Mining (CPM) adopts the concept of FP-growth algorithm due to its advantages, by mining a prefix-tree called CPM-tree. CPM performs the closure checking on the fly with only one scan

over the dataset unlike in FP-growth algorithm where two scans are needed.

CPM tree is proposed to perform the closure checking of any real time intrusion. The CPM tree contains only the closed itemsets and its associated support count, unlike the FP-tree which contains all the information of the database.

The main steps of the CPM algorithm are as follows:

- 1) Perform a closure checking on the first specified number of transaction,  $T$ . (\* note that the number of transactions depends on some selected features).
- 2) Construct the CPM tree with each node containing only the closed itemsets and its associated support count which is a compact representation of the database (Note: every user has a node in the CPM tree).
- 3) When a new transaction arrives, the CPM algorithm checks whether itemset,  $X \sqsubseteq T$  is in the current closed itemsets for a particular user. If it is, it updates  $X$ 's support, otherwise, if  $X$  is a newly arrived closed itemset, the algorithm adds it as link to the existing node of that user in the CPM tree.
- 4) A transaction is deleted if within a time window, a particular transaction is not frequent. Then the node is pruned out in order to reduce the memory usage of the CPM tree.
- 5) The closed frequent itemsets (transaction) can be output any time at the Site Security Officer's request by traversing the CPM tree.

The CPM tree is used to maintain the current closed itemsets. Each node in the CPM tree stores a closed itemset, its current support information, and the links to its immediate parent and children nodes.

Pseudocode of CPM algorithm is illustrated below:

#### Algorithm 1: CPM – Addition

```
X_close = true; Cnew =  $\varnothing$ ;
procedure Add(X, C, Cnew)
    if (X  $\in$  C)
        for all (Y  $\subseteq$  X and Y  $\in$  C)
            Ys  $\leftarrow$  support(Y, C) + 1;
        end for
    if (X_close = true) return;
else
    if (support(X, C) > 0)
        if (Cnew =  $\varnothing$ )
            X0  $\leftarrow$  X;
            Cnew  $\leftarrow$  X;
            X_close = false;
            Xs  $\leftarrow$  support (X, C) + 1;
        else
            Xc =  $\varnothing$ ;
            for all ( K  $\supseteq$  X and K  $\in$  C)
                if (len(K) < len(M) then
                    M = K;
                end for
            Xc  $\leftarrow$  M;
```



```

if  $((X_c / X) \cap X_0 = \varnothing$  and  $X_c \neq \varnothing$ )
     $C_{new} \leftarrow C_{new} \cup X;$ 
     $X_s \leftarrow \text{support}(X, C) + 1;$ 
end if
end if
else
if  $(C_{new} = \varnothing)$  then
     $X_0 \leftarrow X;$ 
     $C_{new} \leftarrow X;$ 
     $X_s = 1;$ 
end if
end if
end if
for all  $(m \subset X$  and  $\text{Len}(M) = \text{Len}(X) - 1$ )
    call Add  $(M, C, C_{new});$ 
end for
if  $(X = X_0)$ 
     $C \leftarrow C \cup C_{new};$ 
     $\text{Support}(X, C) = X_s;$ 
end if
end procedure

```

### 3.1.2.1.1. Illustration of CPM algorithm

As an illustration, this part describes the use of closed frequent itemsets to construct anomaly detection. In profiling users' behaviour, the normal users are selected from the labeled data; and a user-id is the major key. Collect all the transactions for each user and find the closed patterns.

For example, the following transactions occur for users with *service*, *hot*, *failed login*, *src\_bytes*, *dst\_bytes*, *duration* as the 6 features picked respectively:

```

SP118 = {hotspot, 0, 1, 93, 15, 4:40 . . . }
SP118 = {hotspot, 0, 4, 13, 20, 3:15 . . . }
SP118 = {hotspot, 0, 0, 51, 41, 0:43 . . . }
SP172 = {hotspot, 0, 4, 26, 45, 8:55 . . . }
SP172 = {hotspot, 0, 2, 76, 52, 2:42 . . . }
SP144 = {hotspot, 0, 8, 71, 49, 6:20 . . . }
SP144 = {hotspot, 0, 4, 54, 2, 4:20 . . . }
SP144 = {hotspot, 0, 0, 92, 18, 6:81 . . . }

```

Applying CPM algorithm as detailed in section 3., with priority labels assigned to the features that could greatly contribute to having a normal activity e.g. *failed login*, *src\_bytes*, *dst\_bytes*. As an example, transaction *{hotspot, 0, 1, 93, 15, 4:40 . . . }* is stored in CPM tree for *SP118* being a superset of its first 2 transactions, giving a support of 2. The 3rd transaction is not left out as a transaction for the user.

Also the 2nd transaction for *SP172* is closed and then stored in the CPM tree with support of 2.

Lastly, the 3rd of *SP144*'s transaction is considered close with support of 2, in comparison with the 1st transaction, not leaving out the 2nd transaction with support of 1.

The CPM tree constructed for this example is as shown in Figure 2 with the nodes identified by the user-id.

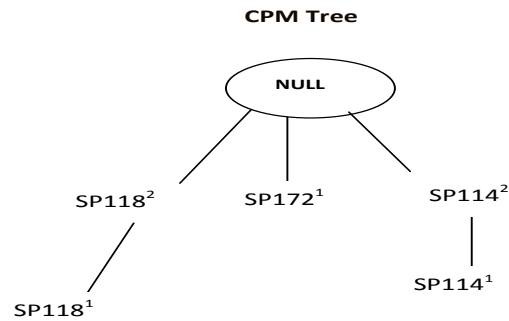


Fig. 2. The resulting Closed Pattern Mining (CPM) Tree for the illustration

### 3.2.2 Response phase

This phase is part of the Administrative control, but it could as well be on the host too. The Agent Response is responsible for alerting the SSO of every occurrence of intrusion based on real time module. The SSO now takes an active action which could be "Shut down the host", "Logout the user" e.t.c. Either AM or AA stores the "suspicious" events in a database for check in case of any reoccurrence (> 2), the attention of AR is then called to alert the SSO for an action to be taken.

### Console

The Console is an interface that allows control of agents, management of the list of monitored systems, and intrusions are reported through it.

### SSO

The Site Security Officer (SSO) is the network administrator who is in charge of the entire network environment and its resources. He/She takes an action when any alarm is raised.

### Database

This is where all the data gathered are stored. It also contains the records of both the normal events and suspicious events detected by the agents in charge of that task. This is being put in check by the Manager.

The critical component is the Manager agent who resides on the server, MIDS is designed in such a way that if at all the Manager is compromised, which implies that no agent would have access to the profile or even the database, then the AA is made to keep tracks of all the user it has checked for. If a new user now visits a host, the AA calls the attention of the RA to check for that user's information on the other hosts on the network. The RA is encoded with checking rules to identify the failure of the detector.

### B. Communication, Coordination and Security of MIDS' agents

All agents in this framework communicate and collaborate with peer agents, using a subset of the agent communication language and protocol, Knowledge Query and Manipulation Language (KQML). An agent's request for information or service is defined or encoded in KQML format and it is transported to the provider using ATP – Agents Transfer Protocol.

For the coordination and security of the agents in MIDS, on every host are the Static Agent (SA) and the IDS Control with its embedded agents. The Static agent (SA) ensures the security of the mobile agent platform. As part of the advantages of having SA on every host, is to stop the host from treating the agents as it likes, this problem is usually referred to as the *malicious host problem*. When an agent visits a host, the SA authenticates the agent before any interaction, when it is found to be from the right source it issues it a certificate, then it is allowed to perform its task. The notion of Digital Signature Algorithm is used in this case.

At the Administrative Control point, are the Manager, the Database and the Profile Builder. The Manager has the Agent Control list (ACL) which contains all information about the agents dispatched on the network; its movement, its identifiers and its state.

#### IV. IMPLEMENTATION OF MIDS

This section describes the implementation of MIDS architecture. Aglet Software Development Kit (ASDK) described in Lange and Oshima (1998) is used in this work. MIDS is implemented and tested over a UNAAB network dataset using java 1.1.8 and Aglet 1.0.3. The ASDK environment, developed by IBM provides mobility facilities to agent programs. It is written in Java, and includes primitives to create, move, communicate and dispose programs. A mobile agent in ASDK is known as an Aglet (contraction of agent + applet). The aglet migrates from one machine to another with the help of a server module, known as Aglets Server or Tahiti Server.

##### A. Testbed Implementation

In the test carried out, two hosts are established with Windows Vista operating system in a LAN to construct a distributed platform based on Aglets as earlier described. The

first host acts as the monitor host while the second one is the monitored host, each of these hosts has the UNAAB dataset.

UNAAB network log, which is a dataset downloaded from the local network connections of the University of Agriculture, Abeokuta, contains the network activities of users over a period of time. The labeled data consists of 5 weeks log of users' activities of 212644 records, where 201,540 are labeled as "normal" and 11104 as "intrusion". CPM is used on the labeled data for profiling. The features include ip-address, Protocol type, User-ID, Service, Hot, Scr\_bytes, Dst\_bytes, Failed\_logins, Duration, Period, Label etc. There are two main attack types found in this dataset, these are guess and sniff attacks.

Table 1 shows an example of network connection records in UNAAB network log with the features. Given a set of records, the CPM algorithm combined with the rules for classification can assign a label to describe each record in the unlabeled data.

The Tahiti server shown on Figure 3 offers a graphical user interface to run the agents described in this architecture and enables the loading of the MIDS's agents' classes for deployment. It thus provides the useful environment to run the implementation codes written in Java.

Once the Agent is loaded, the autonomous/mobility activities can be performed by the agent. In implementing MIDS, four classes are created: MIDSManager.java, MIDS\_AD.java, MIDS\_AA.java, MIDS\_AM.java.

##### B. Performance Evaluation of MIDS

The result displayed in Figure 4. The small pop-up shown in red is the alert displayed on detecting a "suspicious" event. The other window at the background is the console showing the activities of the mobile agents on execution.

TABLE I. Examples of connections found in UNAAB network log

User-ID	Service	hot	Src_bytes	Dst_byte	Failed_logins	...
SP 862	Hotspot	0	100	62	0	...
Admin	Hotspot	2	35	76	1	...
SP499	ftp	0	78	32	5	...
JP1042	Hotspot	1	54	20	0	...
SP535	http	0	8	78	0	...
...	...	...	...	...	...	...

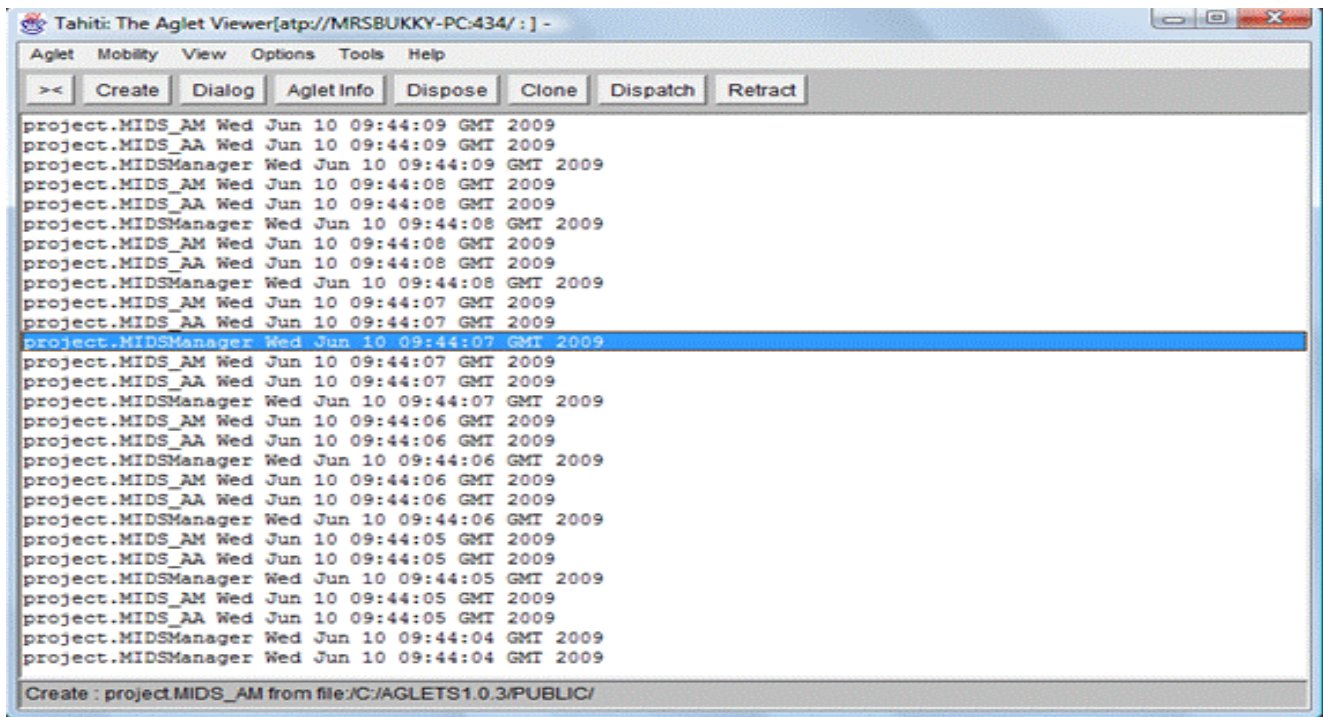


Fig. 3. An Interface showing the Tahiti Server of MIDS

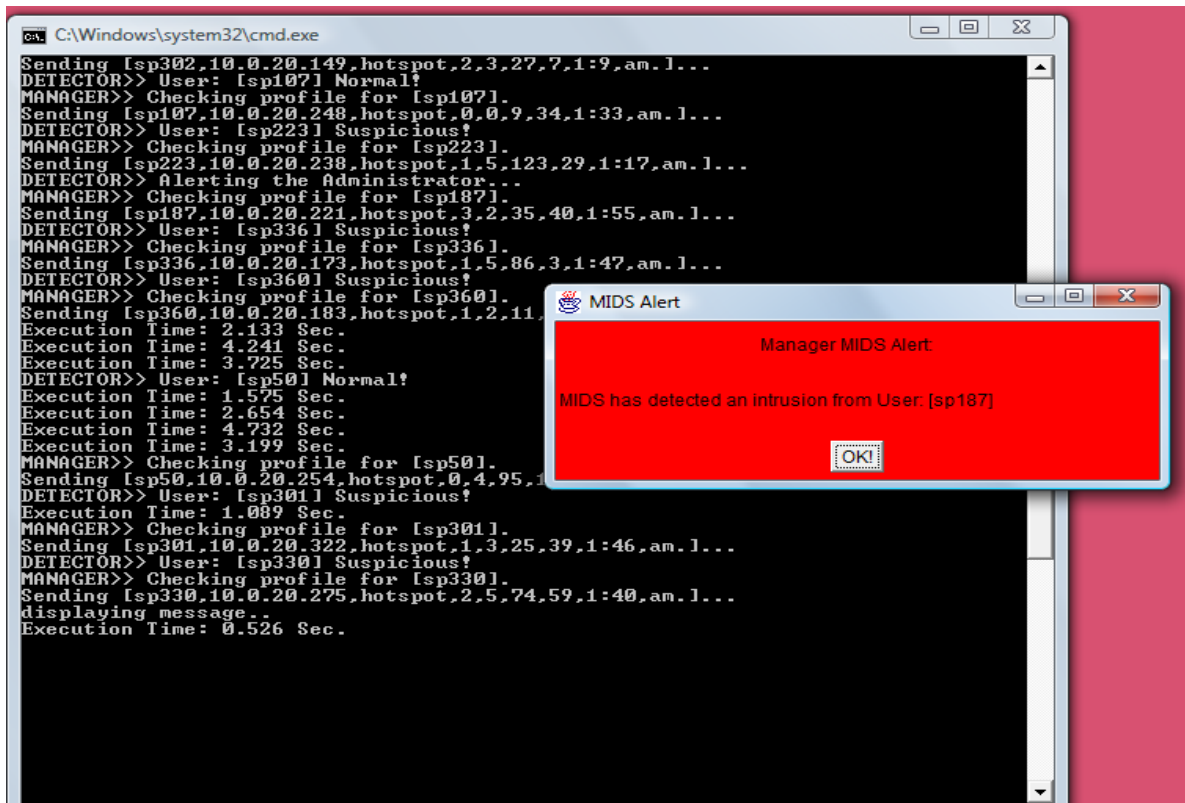


Fig. 4. Alert on detecting Intrusion

The records of the classification are taken by counts in order to identify the false alarm rates. The addition of the number of "suspicious" and "intrusions" are classified as

"intrusion". Table 2 shows the classification on the unlabeled data.

TABLE II. Results of MIDS on UNAAB network dataset

	Cases	False Positive Rate	False Negative Rate
<b>Normal</b>	201540	0.13%	99.87%
<b>Intrusion</b>	11104	99.96%	0.04%

Using the 4 metrics for evaluation of IDS, the following results are discovered: Accuracy = 99.94% ,

Detection rate = 99.96% ,False Positive Rate = 0.13%, and False Negative Rate = 0.04%

1) *Timing Result*

The performance in terms of time to detection and the mean time of reporting an intrusion are considered. This involves the system recording each time an intrusion is detected and then calculates the mean. It is found out that the mean time for reporting an intrusion is 0.67seconds. On the other hand, it took 0.89secs to report an intrusion in Sodiya (2006) while Eid (2004) recorded the overall trip for the agents in its architecture as 4.42 secs starting from activation of the sniffer to completion of the processing from one host to the other.

2) *Performance Analysis*

UNAAB dataset is divided into batches of 10%, 25%, 50%, 75%, 100%, the True Positive Rate and False Positive Rate are calculated as shown on Table 3 and depicted in Figure 5.

TABLE III. Comparison on batches of UNAAB network log

		BATCHES				
		10%	25%	50%	75%	100%
<b>MIDS</b>	<b>TPR (%)</b>	94.5	97.43	98.89	99.54	99.96
	<b>FPR (%)</b>	3.9	3.3	2.2	1.7	0.13

V. CONCLUSION

As network attacks become more alarming, exploiting systems faults and performing malicious actions, the need to provide effective intrusion detection methods increases. Distributed attacks are especially difficult to detect and require coordination among different intrusion detection components or systems. The idea of mobile and autonomous components intuitively seems useful in intrusion detection, hence the use

of multiagent system. A data mining approach is provided in this paper to enhance the detection performance of the agents deployed in the design. Experiments performed emphasize the aim of applying agents to detect intrusions.

ACKNOWLEDGEMENT

Our appreciation to the ICTREC staff for giving us access to the University network log.

REFERENCES

- [1] Anderson J. P. (1980). "Computer security threat monitoring and surveillance", Technical report, James P. Anderson co, Box 42, Fort Washington, February 1980.
- [2] Bradshaw, M. J. (1997). "An introduction to Software agents", In Jeffrey M. Bradshaw, Editor, Software agents, Chapter 1, AAAI press, The MIT press,1997.
- [3] Eid, M., Artail, H., Kayssi, A. and Chehab, A. (2004) "An Adaptive Intrusion Detection and Defense System based on Mobile Agents", Proceedings of the Innovations in Information technologies (IIT'2004), Oct, 2004, Dubai, UAE.
- [4] Kuang, L. V. (2007). "DNIDS: A Dependable Network Intrusion Detection System using the CSI-KNN", M.Sc. thesis, School of Computing, Queen's University,Ontario, Canada.
- [5] Lange, D. B. and Oshima, M. (1998). "Programming and Deploying JavaTM Mobile Agents with Aglets", Addison Wesley Longman, Inc.
- [6] Oriola, O., Adeyemo, A. B. & Robert, A.B.C. (2012). "Distributed Intrusion Detection System Using P2P Agent Mining Scheme", IEEE African Journal of Computing & ICT, Vol 5. No. 2, March, 2012 ISSN 2006-1781
- [7] Onashoga, S. A., Akinde, A. D. & Sodiya, A. S. (2009). "A Strategic Review of Existing Mobile Agent- Based Intrusion Detection Systems", Issues in Informing Science and Information Technology Volume 6, 2009
- [8] RuleQuest, (2007). Retrieved from <http://www.RuleQuest.com>
- [9] Sasikumar, R. & Manjula, D. (2011). "A Distributed Intrusion Detection System Based on Mobile Agents with Fault Tolerance", European Journal of Scientific Research, Vol.62 No.1 (2011), pp. 48-55
- [10] Sodiya, A. S. (2006). "Multi-Level and Secured Agent-based Intrusion detection System", Journal of Computing Science and Information Technology, vol. 14, no. 3.
- [11] Jain, P., Raghuvanshi, S. and Pateria RK (2011) "New Mobile Agent-based Intrusion Detection Systems for Distributed Networks", International Journal of Wireless Communication Volume 1, Issue 1, 2011, pp-01-04
- [12] Kamaruzaman, M., Shukran, M. A. M., Khairuddin, M. A. & Isa, M.R.M. (2011). "Mobile Agents in Intrusion Detection System: Review and Analysis". Modern Applied Science Vol. 5, No. 6; December 2011
- [13] Wang, W., Behera, S. R., Wong, J., Helmer, G., Honavar, V., Miller, L., Lutz, R., and Slagel, M. (2006). "Towards the Automatic Generation of Mobile Agents for Distributed Intrusion Detection System", Journal of Systems and Software, Vol 79, pp:1-14. [www.elsevier.com/locate/jss](http://www.elsevier.com/locate/jss).

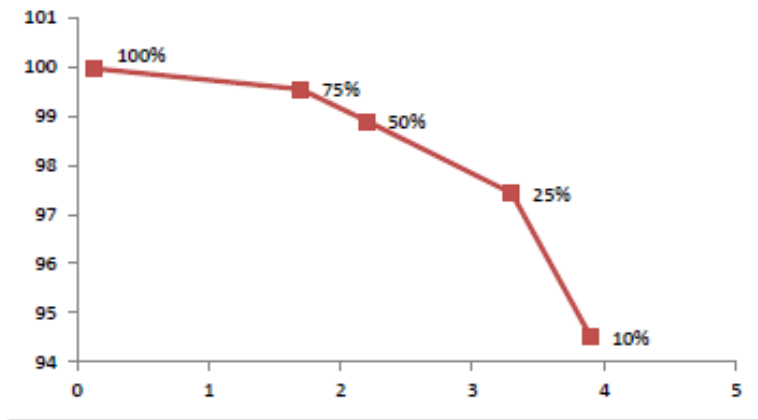


Fig. 5. Comparison of TPR (%) against FPR(%) on batches of UNAAB dataset

# Applying Inhomogeneous Probabilistic Cellular Automata Rules on Epidemic Model

Wesam M. Elsayed<sup>1</sup>

Department of Mathematics, Faculty  
of Science, Mansoura University,  
Mansoura, 35516, Egypt.  
Mansoura, Egypt.

Ahmed H. El-bassiouny<sup>2</sup>

Department of Mathematics, Faculty  
of Science, Mansoura University,  
Mansoura, 35516, Egypt.  
Mansoura, Egypt.

Elsayed F. Radwan<sup>3</sup>

Department of Computer Science,  
Faculty of Computer and Information  
Sciences Mansoura University,  
Egypt, P.O. Box: 35516

**Abstract**—This paper presents some of the results of our probabilistic cellular automaton (PCA) based epidemic model. It is shown that PCA performs better than deterministic ones. We consider two possible ways of interaction that relies on a two-way split rules either horizontal or vertical interaction with 2 different probabilities causing more of the best possible choices for the behavior of the disease. Our results are a generalization of that Hawkins et al done.

**Keywords**—Probabilistic Cellular Automata (PCA); Epidemic modeling; Optimization.

## I. INTRODUCTION

Because of the spread of diseases, a technical innovative model should be made to recover their time regions. Many researches tried to solve this problem based on medical disease feature, which suffer from unpredictable ones. Whilst a single infected host might not be significant, a disease that spreads through a large population yields serious health and economic threats. In this sense, mathematical epidemiology is concerned with modeling the spread of infectious disease in a population [see 2]. The aim is generally to understand the time course of the disease with the goal of controlling its spread. Traditionally, the majority of existing mathematical models to simulate epidemics are based on ordinary differential equations. These models have serious drawbacks in that they neglect the local characteristics of the spreading process and they do not include variable susceptibility of individuals. Specifically, they fail to simulate in a proper way (1) the individual contact processes, (2) the effects of individual behavior, (3) the spatial aspects of the epidemic spreading, and (4) the effects of mixing patterns of the individuals.

Mathematical modeling in epidemiology was pioneered by Bernoulli in 1760. Nevertheless, the work due to Kermack-McKendrick [7] can be considered as the starting point for the design of modern mathematical models. It consists of a SIR model (Susceptible-Infected-Recovered, SIR) which is a set of Ordinary Differential Equations.

Optimization methods have been developed for deterministic simulation models. However, they have not been done with more complex stochastic simulation models. For more details look in [2, 4, 5, 12]. Influenza is transmitted in a complex way from person to person. In addition, given an introduction of influenza into a population, the probability of a major epidemic and the possible size of an epidemic are high-

ly variable. Thus, the mathematical models for influenza epidemics should have a detailed contact structure and be stochastic. Besides, the epidemic process is non-linear since the incidence of new infections depends on the current number of both infectives and susceptibles in the population at a particular time. All of these factors make optimization based on traditional gradient methods, such as the Newton-Raphson method, difficult or even prohibitive. [8] Developed a stochastic approximation method whose convergence is guaranteed under mild conditions. The method, however, requires knowledge of the analytic gradient of the considered objective function [11]. However, in terms of simulation optimization, the drawback of these methods remains the unavailability of gradients. When trying to devise more realistic models we incorporate spatial parameters to better reflect the heterogeneous environment found in nature. An alternative to using deterministic differential equations is to use a two-dimensional cellular automaton (CA) to model location specific characteristics of the susceptible population together with stochastic parameters which captures the probabilistic nature of disease transmission. Cellular Automata model should be treated as a dynamical system that involves a random variable. As a result, the suggested model should be a stochastic dynamical model called probabilistic Cellular Automata model (PCA) which is an extension of CA. The state space remains the same as well as the local and synchronous character of the dynamic. The novelty is that each site updates its value randomly according to a probability distribution which depends on the neighboring sites. Also, we will apply non-uniform cellular automata where each cell satisfies the same or different rules according to which cell states are updated in a synchronous and local manner.

Usually, when a CA-based model is considered to simulate an epidemic spreading, individuals are assumed to be distributed in the cellular space such that each cell stands for an individual of the population as in our case.

In the case of our stochastic two-dimensional non uniform cellular automata model, we consider two possible ways of interaction so, we have two directions to get infected from other cells either horizontal or vertical interaction as each cell stands for an individual. This will reduce the possibility to get infection from others as in every direction there are only two neighbors affecting the central cell in every direction as seen in following sections. Stochastic optimization methods will

be used to model parameters for infectious diseases and population structures. Also, we append every rule with two factors namely certainty and coverage factors to show the non-uniform way where each cell affects another in its neighborhood and vice versa. This method of two-way split rules pave the way for more good choices of solutions as seen in section IV part B.

In this work we consider how we can model the spread of an epidemic using a two-dimensional cellular automaton using programming features of the matrix algebra package MATLAB to develop an implementation that simulates a simple model. By adding our new probabilities of getting infection either from horizontal or vertical motion to the program mentioned in [3]. Also, the effect of population vaccination can be considered in this model. A vaccination parameter  $V \in [0,1]$  must be considered in the objective function of the model. Such parameter stands for the portion of susceptible infected individuals at each time step which are vaccinated. But in the program, the user have the ability to vaccinate specific regions of the environment. This takes input from the user while the simulation is running, allowing vaccination strategies to be tested.

## II. PRELIMINARIES

### A. The Probabilistic Cellular Automata Model (PCA)

In this section, we describe the overall design of our automaton. The model is a two-dimensional grid of cells, each cell containing the same or different rules due to the fact that each epidemic can be in any one of four stages as in the SEIR model we introduced later (i.e. Susceptible, Exposed, Infected and Recovered). The susceptible individuals are those capable of contracting the disease; For many infections there is a period of time during which the individual has been infected but is not yet infectious himself; during this latent period the individual is said to be exposed. In this case we have the SEIR model in which the new class of exposed individuals (E) must be considered. The infectious individuals are those capable of spreading the disease; and the recovered individuals are those immune from the disease, either died from the disease, or having recovered, are definitely immune to it. So, different diagnosis of disease has different rules. The neighbors of any cell in the grid are the cell itself plus the four orthogonal adjacent cells (fig. 1) according to von Neumann.

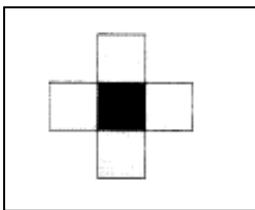


Fig. 1. The two-dimensional cellular automata cell's neighbors

Once the automaton was embedded in the grid, the cell as an individual finite state machine, began to follow the rule that is applied to it. A single cell cannot do much without interacting with other cells. The lattice starts out with an initial configuration of cells in which the following hold.

Each cell can take on one of the 4 different states:

- 1) Susceptible (i.e. healthy; designated as 0)
- 2) Exposed (designated as 1)
- 3) Infected (designated as -1)
- 4) Recovered (includes both survivors and deaths; designated as 2)

- It is supposed that the way of infection is the contact between the infected individual and the healthy individual.
- Once the healthy individuals have contracted the infection and have recovered from it, they acquire temporary immunity.

### B. Mathematical Formulation Of The PCA

Two-dimensional CA are discrete dynamical systems formed by a finite number of identical objects called cells, which are arranged uniformly in a two-dimensional space. Each cell is endowed with a state, belonging to a finite state set, that changes at every discrete step of time according to a rule, called local transition function. More precisely, a CA can be defined as a 4-uplet,  $A = (C, S, N, f)$ , where C is the cellular space formed by a two-dimensional array of  $r \times c$  cells, where r stands for rows and c for columns (see Fig. 2-(a)):  $C = \{(a, b), 1 \leq a \leq r, 1 \leq b \leq c\}$ . The state of each cell is an element of a finite set, S, in such a way that the state of the cell (a, b) at time t is denoted by  $S(a,b;t) \in S$ . The matrix  $C(t) = S(i, j; t)$  is called configuration of the CA at time t. Moreover,  $C(0)$  is the

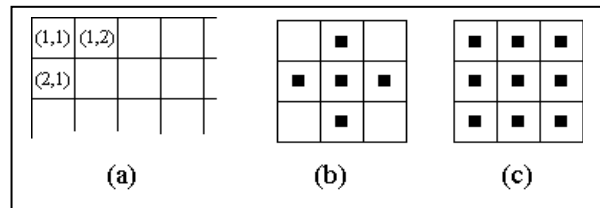


Fig. 2. (a) Cellular space (b) Von Neumann neighborhood (c) Moore neighborhood

initial configuration of the CA. The neighborhood of a cell(a,b) is the set of cells whose states at time t determine the state of the cell (a, b) at time  $t + 1$ , by means of the local transition function. Depending on the process to be modeled, one can choose an appropriate neighborhood. Nevertheless, the traditional neighborhoods considered are the Von Neumann neighborhood (see Fig. 2-(b)), and the Moore neighborhood (see Fig. 2-(c)). Note that the main cell is also considered in its neighborhood. A neighborhood is defined by means of a finite set of indices

$N = \{(x_i, y_i) : 1 \leq i \leq m\} \subset Z \times Z$  N: Neighborhood of a cell c, such that for every cell (a, b), its neighborhood,

$N_{(a,b)}$  is the set of m cells given by  $N_{(a,b)} = \{(a + x_i, b + y_i), \dots, (a + x_m, b + y_m) : (x_k, y_k) \in N\}$ .

Note that for Von Neumann neighborhood, we have  $N = \{(0,0), (-1,0), (0,1), (1,0), (0,-1)\}$ .

Cell's state [10]:

$$S_c(t+1) \in \{0, -1, 1, 2\} \quad (1)$$

$$f: S_c(t+1) \rightarrow S_c(t) \quad (2)$$

Where

$S_c$ : State of the cell at iteration  $t+1$

$f$ : Transition function (Determines how the cell's state can change).

As the cellular space is considered to be finite, boundary conditions must be taken into account in order to assure the well-defined dynamics of the CA.

### C. Probabilistic Analysis of Cellular Automata Rules

With each time step, the state of each individual cell changes according to a set of rules based on the states of the cell's neighbors. These rules can be either deterministic (certain) or stochastic (probability-based/uncertain). To determine this exactly we need to define two essential factors, if the decision rules have the form  $C \rightarrow D$ , meaning IF C THEN D, where C is the condition attribute, and D is the decision attribute of the decision rule then we have ,

The certainty factor of the decision rule  $C \rightarrow D$ , denoted by

$cer(C,D)$ , is defined as :

$$cer(C,D) = p(D/C) \quad (3)$$

Where  $cer(C,D) \in [0,1]$ . If  $cer(C,D)=1$ , then the given

decision rule is a deterministic or certain decision rule .

Otherwise,  $0 < cer(C,D) < 1$ , the given decision rule is a stochastic or uncertain decision rule.

The coverage factor of the decision rule  $C \rightarrow D$  in S, denoted by  $cov(C,D)$ , is defined as:

$$cov(C,D) = p(C/D) \quad (4)$$

In this work we consider a non-uniform case of cellular automata where different cells may contain different rules. At a given moment, only one rule is active for a cell and determines the cell's function. A non-active rules may be activated in next time steps.

Let any cell in the lattice be labeled by its position  $c=(i, j)$

where  $i$  and  $j$  are the row and column indices. A function

$S_c(t)$  is the state of cell  $c$  at time step  $t$ . The rules of the

model specify how the state  $S_c(t+1)$  is to be computed from

the states at time step  $t$  of it's neighbors

$\{(i-1, j), (i+1, j), (i, j-1), (i, j+1)\}$  as in fig. 3:

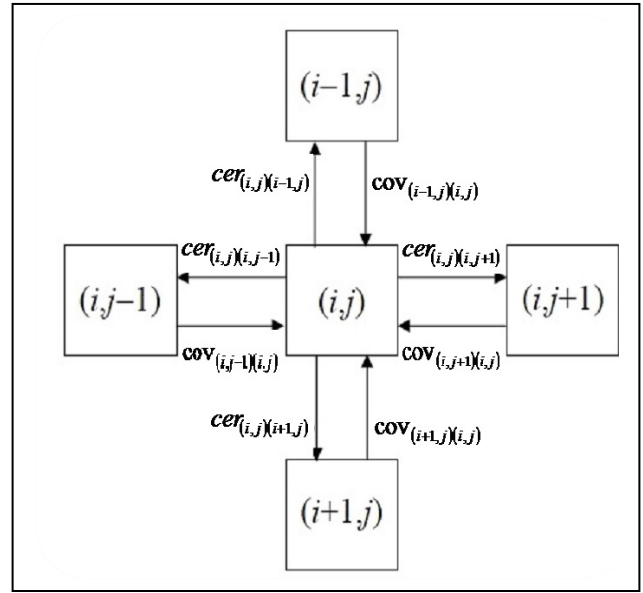


Fig. 3. Parameters of the transition rules.

Here we assume that there are two possible structures either horizontal or vertical interaction between cells each of them has different probability of infection respectively. A small probability 0.0001 of spontaneous infection is assumed. This represents the possibility of external infection e.g. infection due to traveling or imported objects [1].

In the horizontal case, the state of cell  $(i, j)$  depends only on the states of cells  $\{(i, j-1), (i, j+1)\}$  while during vertical interaction it's state depends on states of cells  $\{(i-1, j), (i+1, j)\}$ . So, the automata rules must be formalized for the two directions as follows:

5) For Horizontal interaction (with probability of infection  $P_h$ ):

$$a) \text{ If } S(i, j; t) = 0 \text{ and } S(i, j-1; t) = -1 \text{ or } S(i, j+1; t) = -1 \text{ then } S(i, j; t+1) = -1 \text{ with probability } P_h \quad (5)$$

$$b) \text{ If } S(i, j; t) = -1 \text{ then } S(i, j; t+1) = 2 \quad (6)$$

$$c) \text{ If } S(i, j; t) = 1 \text{ then } S(i, j; t+1) = 2 \quad (7)$$

$$d) S(i, j; t+1) = 1 \text{ (independent of it's interaction neighbors) with probability } 0.0001. \quad (8)$$

6) For Vertical interaction (with probability of infection  $P_v$ ):



a) If  $S(i, j; t) = 0$  and  $S(i, j-1; t) = -1$  or  $S(i, j+1; t) = -1$   
then  $S(i, j; t+1) = -1$  with probability  $P_v$  (9).

b) If  $S(i, j; t) = -1$  then  $S(i, j; t+1) = 2$  (10).

c) If  $S(i, j; t) = 1$  then  $S(i, j; t+1) = 2$  (11).

d)  $S(i, j; t+1) = 1$  (independent of its interaction neighbors) with probability 0.0001 (12).

If a cell is susceptible (0), the simulation module counts the number of infected cells that are its nearest neighbors. The simulation then calculates the probability the cell can avoid being infected  $(1-\beta)^m$ , where  $\beta$  is the infection rate (the probability a contact with an infected person is actually infectious) and  $m$  is the number of infected cells. Subtracting this value from 1 yields the probability of the cell being infected [10].

### III. THE OPTIMIZATION PROBLEM

The optimization problem is as follows: Given a limited quantity of influenza vaccine and a particular population structure and infection rate pattern for a single wave of pandemic influenza, what proportion of each stage should be vaccinated to minimize the impact of the epidemic? [ see :9]

We divide the population into four different cases: Susceptible, Exposed, Infected and Recovered that are indexed as  $i=1, \dots, 4$ . We let  $n_i$  be the number of individuals in class  $i$ , and the total population size is  $n = \sum_{i=1}^4 n_i$ . We let  $\beta$  be the infection rate, i.e. (the probability a contact with an infected person is actually infectious), where  $\beta$  either takes the value  $P_h$  or  $P_v$  depending on the movement direction. We let  $V$  be the total number of vaccine doses available before day one of the epidemic, and  $V_i$  the proportion of individuals in case  $i$  that is vaccinated. Thus, the total number of doses distributed is,

$$\begin{cases} Q = \sum_{i=1}^4 n_i V_i & \text{where,} \\ Q \leq V \end{cases} \quad (13)$$

since we cannot use more vaccine than there is available. We assume that each person vaccinated receives one dose of vaccine. Four different values of the vaccination rate are considered:  $V = 0, 0.2, 0.3, 0.4$ . Note that as  $V$  increases, the number of infected individual decreases. To reflect the impact of a single illness, we let  $w_i$  be the weight assigned to an illness in each case for minimization of the loss function. Then, the optimization problem is expressed as

$$\min \sum_{i=1}^4 \beta n_i w_i \quad (14)$$

Such that

$$\sum_{i=1}^4 n_i V_i \leq V \quad (15)$$

We concentrate on minimizing overall illness in the population as well as number of lives lost given a predetermined number of doses  $V$  of vaccine. We use weights of one, i.e.  $w_i = 1, i = 1, \dots, 4$  for minimizing illness objective function. The rules have been applied based on an optimization algorithm as illustrated in Fig. 4 showing the behavior of the epidemic through different probabilities.

*Pseudocode*

*Overall structure*

*Main function*

Get information from user and initialize variables  
Visualise state

Loop through generations:

- 1) Update count of infected neighbours for each cell
- 2) Update state of each cell based on number of infected neighbours
- 3) Visualize state
- 4) Stop

In this work we consider how we can model the spread of an epidemic using a two-dimensional cellular automaton. We will use programming features of the matrix algebra package MATLAB to develop an implementation that simulates a simple model [3] as shown in fig.4. We want to construct a model of an epidemic that will develop over a fixed  $N$  by  $N$  grid in a given number of generations. We apply a set of rules to each cell that will determine its fate in the next generation, for example whether a given cell will become infected or not. The probabilities of state changes are a set of predefined parameters. By studying the effects of varying these parameters we try to predict how the epidemic will develop over time will it eventually die out.

We apply the same strategy of vaccination used by [3] where the user have the ability to vaccinate specific regions of the environment. This takes input from the user while the simulation is running, allowing vaccination strategies to be tested. Since vaccination is not usually permanent but lasts for a period of time, it is implemented in much the same way as the temporary immunity that follows organism recovery. While the program is running, the user can click on the grid causing vaccination to be simulated at the clicked point.

```

Pseudo code for main program
Initialize constants to represent cell states (Susceptible,
Exposed, Infected, and Recovered)
Input N, the array size to use
Input  $P_h$  and  $P_v$ , the probabilities of becoming infected
during horizontal and vertical interaction
Input  $Q$ , the probability of becoming recovered.
Optionally input ca_state, the state matrix, from given
initial configuration
If no initial configuration was supplied:
    Initialize ca_state with all cells Susceptible
    Set randomly-selected cells near centre to Infected
Add a border of immune cells to ca_state
Visualize ca_state
Initialize infected_neighbours, the infected neighbour
count matrix
Loop through generations
    Loop through valid x-coordinates (2 to N+1)
        Loop through valid y-coordinates (2 to N+1)
            Update count of infected_neighbours(x,
y)
        End loop through y-coordinates
    End loop through x-coordinates
    Loop through valid x-coordinates (2 to N+1)
        Loop through valid y-coordinates (2 to
N+1)
            Update ca_state(x, y) based on in-
fected_neighbours(x, y)
        End loop through y-coordinates
    End loop through x-coordinates
    Visualize ca_state
End loop through generations
    
```

Fig. 4. Pseudo code for main program

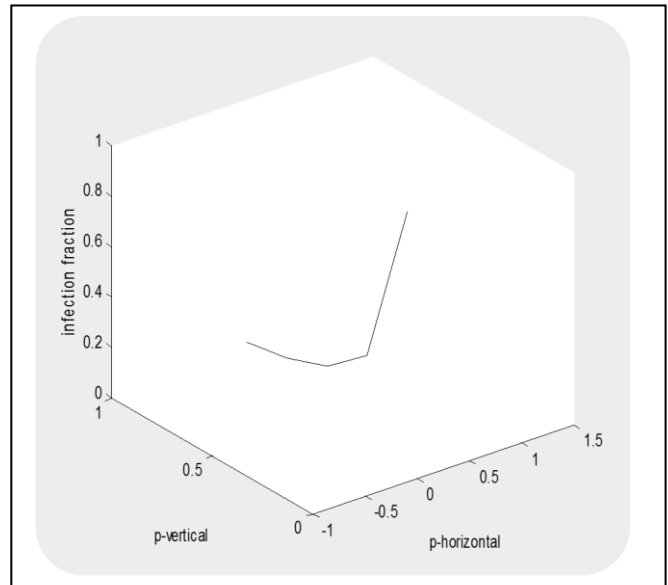
#### IV. SIMULATION AND ANALYSIS

##### A. Different scenarios based on varying $p$ -horizontal ( $P_h$ ) and $p$ -vertical ( $P_v$ )

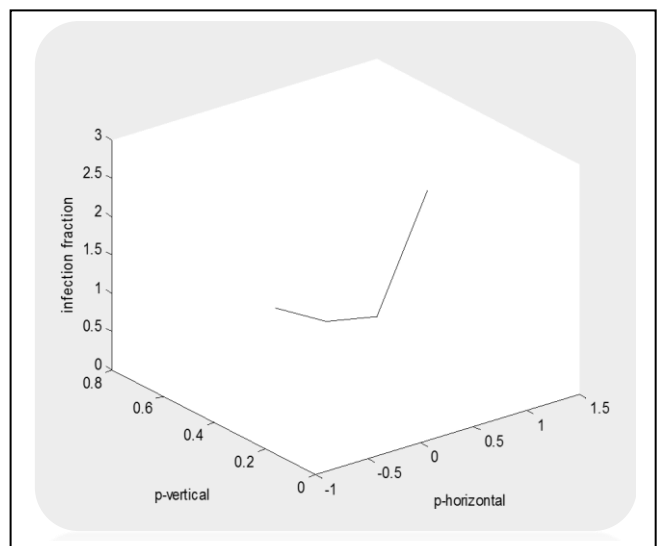
Because our cellular automaton is probabilistic (i.e. random numbers affect the chances of different scenarios arising,

even with fixed  $P_h$ ,  $P_v$  and  $Q$ ) it is necessary to run several simulations to obtain an approximate understanding of what should happen to the spread of the epidemic. We also need to test several different values of  $P_h$  and  $P_v$ . Initially, we will set  $Q$  as a constant 1 and vary  $P_h$ ,  $P_v$ . Thus an Infected cell will immediately become Recovered. We will test for  $P_h$ ,  $P_v \in \{0.1, 0.3, 0.5, 0.7, 0.9\}$ .

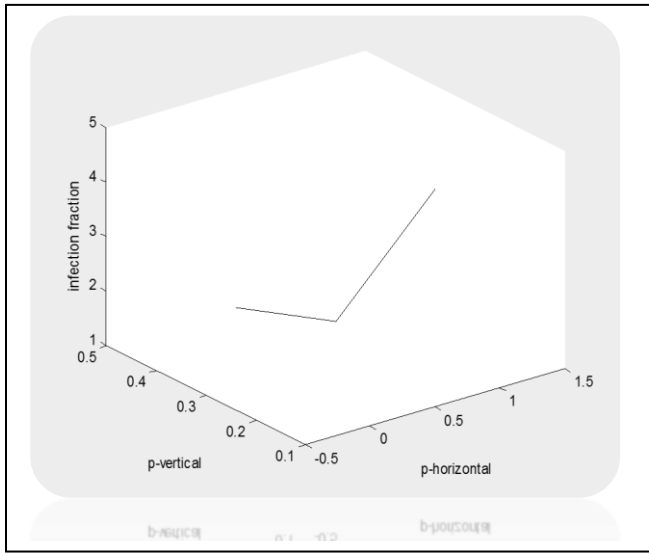
Case 1:  $P_h = 0.1$ ,  $P_v = \{0.1, 0.3, 0.5, 0.7, 0.9\}$ .



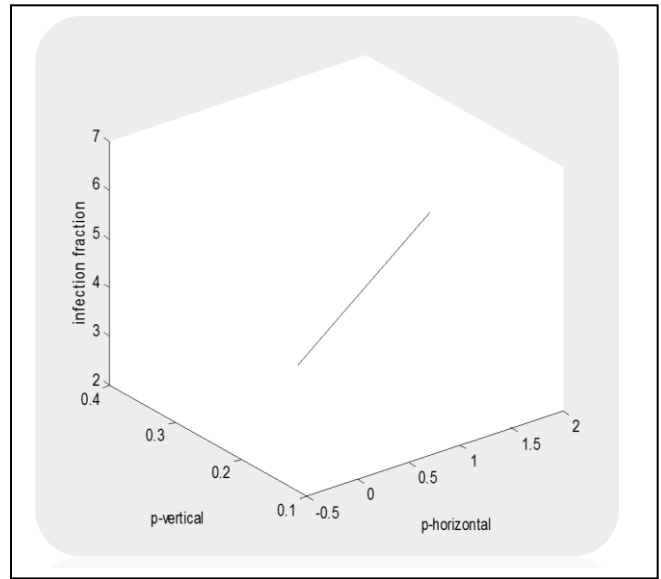
Case2:  $P_h = 0.3$ ,  $P_v = \{0.1, 0.3, 0.5, 0.7\}$ .



Case 3:  $P_h = 0.5$ ,  $P_v = \{0.1, 0.3, 0.5\}$ .



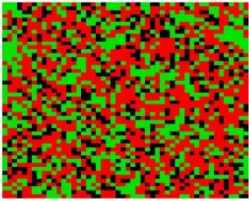
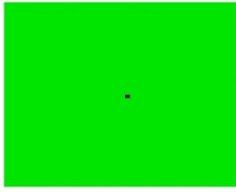
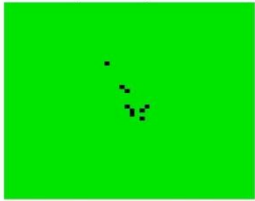
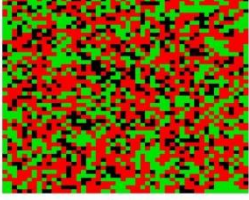

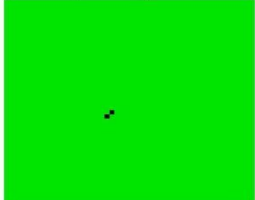
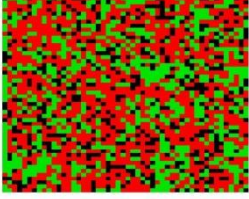
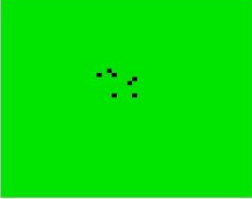
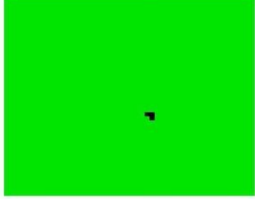
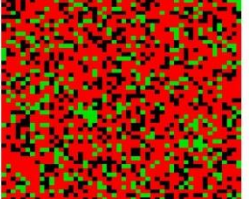
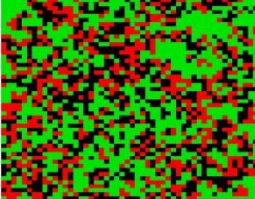
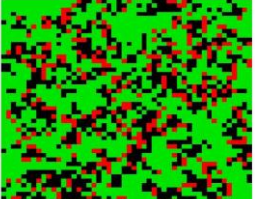
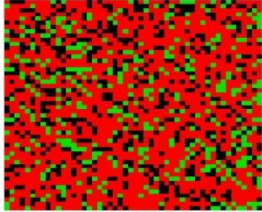
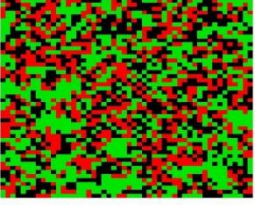
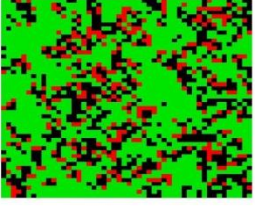
Case 4:  $p_h = 0.7, p_v = \{0.1, 0.3\}$ .

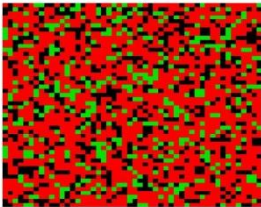
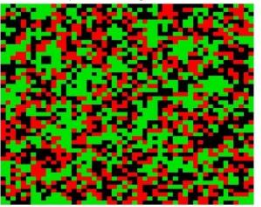
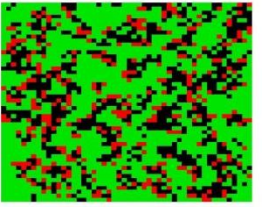
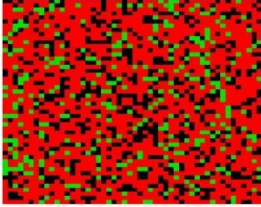
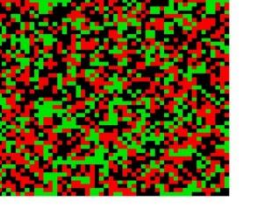



B. We run the simulations for 100 generations and observe the behavior of the disease in a grid of size  $50 \times 50$ .

TABLE I. Description of observed behaviour for a range of values of  $p_h, p_v$  and  $q$  (green is Susceptible, red is Infected, and black is Recovered)

$q$	0.2	0.6	1
$p_h, p_v$			
0.1, 0.1	 Epidemic simulation - generation 100 Chaotic pattern emerges rapidly. Almost all cells Infected at any one time.	 Epidemic simulation - generation 66 disease dies out followed by all cells Susceptible within approx 66 generations.	 Epidemic simulation - generation 5 disease dies out followed by all cells Susceptible within approx 5 generations.
0.1, 0.3	 Epidemic simulation - generation 100 Chaotic pattern emerges rapidly. Almost all cells Infected at any one time.	 Epidemic simulation - generation 16 disease dies out followed by all cells Susceptible within approx 16 generations.	 Epidemic simulation - generation 4 disease dies out followed by all cells Susceptible within approx 4 generations.

<p>0.1 , 0.5</p>	<p>Epidemic simulation - generation 100</p>  <p>Chaotic pattern emerges rapidly. Almost all cells Infected at any one time.</p>	<p>Epidemic simulation - generation 30</p>  <p>disease dies out followed by all cells Susceptible within approx 30 generations.</p>	<p>Epidemic simulation - generation 4</p>  <p>disease dies out followed by all cells Susceptible within approx 4 generations</p>
<p>0.1 , 0.7</p>	<p>Epidemic simulation - generation 100</p>  <p>Chaotic pattern emerges rapidly. Almost all cells Infected at any one time.</p>	<p>Epidemic simulation - generation 66</p>  <p>disease dies out followed by all cells Susceptible within approx 66 generations</p>	<p>Epidemic simulation - generation 9</p>  <p>disease dies out followed by all cells Susceptible within approx 9 generations</p>
<p>0.1 , 0.9</p>	<p>Epidemic simulation - generation 100</p>  <p>Chaotic pattern emerges rapidly. Almost all cells Infected at any one time.</p>	<p>Epidemic simulation - generation 14</p>  <p>disease dies out followed by all cells Susceptible within approx 14 generations</p>	<p>Epidemic simulation - generation 9</p>  <p>disease dies out followed by all cells Susceptible within approx 9 generations</p>
<p>0.3 , 0.3</p>	<p>Epidemic simulation - generation 100</p>  <p>Chaotic pattern emerges Spreads more quickly.</p>	<p>Epidemic simulation - generation 100</p>  <p>Chaotic pattern emerges Spreads slowly.</p>	<p>Epidemic simulation - generation 100</p>  <p>Chaotic pattern emerges Spreads more slowly.</p>
<p>0.3 , 0.5</p>	<p>Epidemic simulation - generation 100</p>  <p>Chaotic pattern emerges Spreads more quickly.</p>	<p>Epidemic simulation - generation 100</p>  <p>Chaotic pattern emerges Spreads rapidly.</p>	<p>Epidemic simulation - generation 100</p>  <p>Chaotic pattern emerges Spreads more slowly.</p>

0.3 , 0.7	 Chaotic pattern emerges Spreads more quickly.	 Chaotic pattern emerges Spreads rapidly.	 Chaotic pattern emerges Spreads more slowly.
0.5 , 0.5	 Chaotic pattern emerges Spreads more quickly.	 Chaotic pattern emerges Spreads rapidly.	 Chaotic pattern emerges Spreads slowly.

Note that: the figures shown in table1 will be a bit different every time we execute the program as the vaccine is given randomly by each user.

## V. CONCLUSION

These epidemic scenarios presented above provide an opportunity to demonstrate the visualization capabilities of a graphical CA model. When [3] use a single probability of infection, they got only two results in which all cells are in susceptible state. But, here when dividing the cellular space into two directions of motion with two different probabilities of infection, there are more optional values for  $P_h, P_v$  differ at which generation it is obtained as shown above in table1. We introduced a theoretical model to simulate the spreading of an epidemic. It is based on transferring the problem into parametric one and the rules into restrictions, obtaining the optimization problem (14). It is solved with the chosen values of  $P_h, P_v$  and  $q$  get the minimum value of the function which minimize the impact of the epidemic.

## VI. FUTURE WORK

PCA are lattice model of spatially extended systems with probabilistic local dynamical rules of evolution. It is difficult to analyze rigorously, so the computational simulation provide an alternative tool. So the future work is to develop an iterative Probabilistic Neural Networks with fully parallel probabilistic feedback dynamic. In addition, Parallel Genetic Algorithms can be incorporated by modifying the probabilities. PGA search through the space of parameters to calibrate the model to observe data. Whilst, PNN synthesis of approaches based on prior analysis and contextual information.

## ACKNOWLEDGMENT

We thank Prof. E. Ahmed, Mathematics Dept., Faculty of Science, Mansoura University, Egypt, for his comments. Also,

special thanks for MATLAB Developers, where matrix algebra package is used for implementing that simulation model.

## REFERENCES

- [1] Ahmed E., Agiza H.N. , (1998) On modeling epidemics. Including latency, incubation and variable susceptibility, *Physica A* 253 347-352.
- [2] Anderson, R., May, R., 1991. *Infectious Diseases of Humans: Dynamics and Control*. Oxford University Press, New York.
- [3] Andrew Hawkins, Danny Roff, Adam Gundry, 2005. *Cellular Automata and Spatial Epidemics*. November 25. <http://citeseerx.ist.psu.edu/viewdoc/download?doi=10.1.1.105.1458&rep=rep1&type=pdf>.
- [4] Greenhalgh, D., 1986. Control of an epidemic spreading in a heterogeneously mixing population. *Math. Biosci.* 80, 23–45.
- [5] Hethcote, H., Waltman, P., 1973. Optimal vaccine schedules in deterministic epidemic models. *Math. Biosci.* 18, 365–381.
- [6] Hoya White S., Marti'n del Rey A., Rodri'guez Sa' nchez G., (2007). Modeling epidemics using cellular automata. *Applied Mathematics and Computation* 186 193–202.
- [7] Kermack W.O., McKendrick A.G., *Proc. Roy. Soc. Edin.* (1927) A 115 700.
- [8] Robbins, H., Munro, S., 1951. A stochastic approximation method. *Ann. Math. Statist.* 22, 400–407.
- [9] Patel Rajan, Ira M. Longini Jr., M. Elizabeth Halloran, (2005) Finding optimal vaccination strategies for pandemic influenza using genetic algorithms. *Journal of Theoretical Biology* 234. 201–212.
- [10] Wang Jeffrey B., 2010. School's Out? Designing Epidemic Containment Strategies with a spatial stochastic method. <http://www.dancingdarwin.com/sca>.
- [11] Weisstein, E., 2004. Robbins–munro stochastic approximation. *MathWorld*; <http://mathworld.wolfram.com/Robbins–MonroStochasticApproximation.html>.
- [12] Wickwire, K.H., Guest, D., 1976. Optimal control policies for reducing the maximum source of a closed epidemic. *Math. Biosci.* 32, 1–14.

## AUTHORS PROFILE

Wesam Elsayed, Department of Mathematics, Faculty of Science, Mansoura University, Mansoura, 35516, Egypt

E-mail address: w\_mahmoud93@yahoo.com



Ahmed El-bassiouny , received his B.Sc. and M.Sc. from Mathematics Dept. Faculty of Science, Mansoura University, Egypt. He received his Ph.D. from University of Kiev, Soviet Union. He became a Lecturer at Mathematics Dept., Faculty of Science, Mansoura University, Egypt on

2004.

E-mail address: el\_bassiouny@mans.edu.eg



Elsayed Radwan, received his B.Sc. and M.Sc. from Mathematics Dept. Faculty of Science, Mansoura University, Egypt. He received his Ph.D. from Intelligent Lab., Graduate School of Engineering, Toin University of Yokohama, Japan. He became a Lecturer at Computer Science Dept., Faculty of Computer and Information Sciences, Mansoura University, Egypt on 2007. His areas of interest are Soft Computing, Evolutionary Computing, Pattern Recognition, and Cellular Neural Networks.

E-mail address: elsfradwan@yahoo.com

# Fusion of Saliency Maps for Visual Attention Selection in Dynamic Scenes

Jiawei Xu

School of Computer Science, University of Lincoln, Lincoln,  
LN6 7TS, United Kingdom

Shigang Yue

School of Computer Science, University of Lincoln, Lincoln,  
LN6 7TS, United Kingdom

**Abstract**—Human vision system can optionally process the visual information and adjust the contradiction between the limited resources and the huge visual information. Building attention models similar to human visual attention system should be very beneficial to computer vision and machine intelligence; meanwhile, it has been a challenging task due to the complexity of human brain and limited understanding of the mechanisms underlying the human attention system. Previous studies emphasized on static attention, however the motion features, which are playing key roles in human attention system intuitively, have not been well integrated into the previous models. Motion features such as motion direction are assumed to be processed within the dorsal visual and the dorsal auditory pathways and there is no systematic approach to extract the motion cues well so far. In this paper, we proposed a generic Global Attention Model (GAM) system based on visual attention analysis. The computational saliency map is superimposed by a set of saliency maps via different predefined approaches. We added three saliencies maps up together to reflect dominant motion features into the attention model, i.e., the fused saliency map at each frame is adjusted by the top-down, static and motion saliency maps. By doing this, the proposed attention model accommodating motion feature into the system so that it can responds to real visual events in a manner similar to the human visual attention system in a realistic circumstance. The visual challenges used in our experiments are selected from the benchmark video sequences. We tested the GAM on several dynamic scenes, such as traffic artery, parachuter landing and surfing, with high speed and cluttered background. The experiment results showed the GAM system demonstrated high robustness and real-time ability under complex dynamic scenes. Extensive evaluations based on comparisons with other approaches of the attention model results have verified the effectiveness of the proposed system.

**Keywords**—Global Attention Model; Saliency Map Fusion; Motion Vector Field

## I. INTRODUCTION

Human vision system can optionally process the visual information and adjust the contradiction between the limited resources and the huge visual information. Building attentions models similar to human visual attention system should be very beneficial to computer vision and machine intelligence; meanwhile, it has been a challenging task due to the complexity of human brain and limited understanding of the mechanisms underlying the human attention system.

The human visual system includes the eyes, the connecting pathways through to the visual cortex and other parts of the

brain. The visual pathway is the part of the central nervous system which gives organisms the ability to process visual detail. A complete visual pathway is consisted of the binocular vision field, temporal retina, ganglion ciliare, chiasma opticum, tractus opticus and so forth [1], while the lateral geniculate nucleus (LGN) is the primary relay center for visual information received from the retina of the eye. The LGN is found inside the thalamus of the brain. Most classical models of visual processing emphasize the lateral geniculate nucleus (LGN) as the major intermediary between the retina and visual cortex. Previous research revealed that the primary visual pathways begins in the retina, continues through the lateral geniculate nucleus (LGN) of the thalamus, and enters the first cortical way station in primary visual cortex (V1) [2]. This geniculostriate pathway is a fundamental part of early visual processing.

Human vision system is the evolved optical organ that can optionally process the vast and complex visual information with limited resources. By adopting visual mechanism in the research fields such as image processing pattern recognition and machine vision, the amount of processed information and computational resources can be reduced and the efficiency of information processing can be increased effectively. Therefore, the research of computational model for human visual attention [3][4] is a very attractive research area.

There are two interactive ways of attentional competition: **bottom-up** competition performs contrast in terms of pre-attentive features, whereas **top-down** biasing modulates attention based upon task instructions. Bottom-up and top-down contributions are combined together to decide which item is attended. Recent psychophysical research has shown that top-down factors play the dominant role in attentional competition [5]. In contrast to the well-developed computational models of bottom-up competition [6], the alternatives of top-down biasing have not been fully exploited. Starting from the Feature Integration Theory of Treisman and Gelade [7], Treisman hypothesized that simple features were represented in parallel across the field, but that their conjunctions could only be recognized after attention had been focused on particular locations. Recognition occurs when the more salient features of the distinct feature maps are integrated. Subsequently, Einhäuser et. al. (2006) [8] and Krieger, Rentschler, Hauske, Schill, and Zetzsche (2006) [9] suggested incorporating higher order statistics to fill some of the gaps between the predictive powers of current saliency map models. One way of doing this is adding more feature channels such as faces or text into the saliency map. This

significantly improves the accuracy of prediction (Cerf, Frady, & Koch, 2009) [10]. The extent to which such bottom-up, task-independent saliency maps predict human fixation eye movements [11][12] under free-viewing conditions remain under active investigation (Donk & Zoest, 2008 [13]; Foulsham & Underwood, 2008; Masciocchi, Mihalas, Parkhurst, & Niebur, 2009)[14]. Bottom-up saliency has also been adopted (Chikkerur, Serre, Tan, & Poggio, 2010 ) [15]; Navalpakkam & Itti, 2005 [16]; Rutishauser & Koch, 2007)[17] to mimic top-down searches.

However, these models have emphasized on the static images, in many real situations, there are moving objects in the visual scenes – the attention has to priorities and shift to those moving objects. In our daily life, it is hard to image the reality without motion exists. Motion is a property of objects by movement of a body of mass taken over time. Motion is natural or what man makes, or channels, to exert force, do work, travel, or to push and pull loads. In our paper we put our emphasis on the motion analysis and simulation in GAM. As human perception are environment-centralized [18] and evolved to cope with dynamic challenges. In biological visual systems, visual pathways are specialized in dealing with the motion cues and optical ‘changes’ [19][20][21][22]. Hereby we consider fusion motion features onto the multi-channels saliency map to facilitate fast response of the attention model to motion cues in an interactive environment. Unlike the previous research on visual attention model [23][24][25][26], our proposed model will behave more like a human visual attention system in real scenes as we discussed below.

The key inspiration of the proposed attention model can be tracked to the medial temporal area in the biological fields. The medial temporal (MT) area [27] is involved primarily in the detection of motion. Motion features have been studied in the previous model [28][29][30][31], however, both of them are not well integrated or reflected in current models. Motion features extraction is a kind of specific form of dimensionality reduction. In this paper, we decomposed the motion into angular movements and scalar transformation as they are the basic and generic motion vector in the space. They are the simplest motion patterns in the real world. These vectors comprise the motion vector field and thus lead to the motion saliency maps when we set a temporal dimensional field beforehand. At the later stage, the motion saliency map is integrated into the static saliency map and top-down saliency map together to form a final fused saliency map. With the motion feature integrated into the saliency map, the proposed attention model will be able to respond to motion feature naturally. Furthermore, motion feature is a dominant factor in the complex dynamic scenes and we mimic the real circumstance after adopting the motion cues into the model.

The rest of the paper is organized as follows. In Section II we propose an efficient fusion attention framework. The top-down saliency map, static saliency map, motion saliency map and model fusion are described in Section III. The experimental results and performance evaluation are reported in Section IV. Finally, Section V concludes the paper.

## II. THE PROPOSED ATTENTION MODEL

Studies of attention models can be categorized according to the two attributes mentioned previously. The first attribute is based on the spatial contrast analysis; the second attribute is based on the frequency domain analysis. The following sections elaborate on the visual attention model and describe our proposed attention model briefly. The details of the proposed model will be further illustrated in section 3.

### A. Related work on visual attention model

Recent work on computational models of visual attention are generally classified into four parts with different aims, they are salience map, temporal tagging, emergent attention and selective routing, respectively. A majority of computational models of attention follow the structure adapted from the Feature Integration Theory (FIT) [7] and the Guided Search model. Koch and Ullman [32] proposed a computational architecture for this theory and Itti [33][34] were among the first ones to fully implement and maintain it. The main idea here is to compute saliency in each of several features (e.g., color, intensity, orientation; saliency is then the relative difference between a region and its surrounding) in parallel, and to fuse them in a scalar map called the “saliency map”. Le Meur et al. adapted the Koch-Ullman’s model to include features of contrast sensitivity, perceptual decomposition, visual masking, and center-surround interactions. Some models have added features such as symmetry [35], texture contrast [36], curvedness [36], or motion [37] to the basic structure. For example, a computational model of visual attention is an instance of a model of visual attention, and not only includes a formal description for how attention is computed, but also can be tested by providing image inputs, similar to those an experimenter might present to a subject, and then seeing how the model performs by comparison. We put our emphasis on the saliency region detection with the combination of prior knowledge and feature extraction to get a relatively realistic and logical situation.

In addition to the mentioned models, several motion models of visual saliency have been developed over the past years. In Hou’s model [38], the motion saliency map is obtained through the multi reference frames, and enhanced by spatial saliency information. In Raj’s model [39], he advised the statistical saliency model to include motion as a feature. These models do improve the motion features under complex scenes. However, these models consider the motion cues as a separate channel and do not fused it into the simulated human visual system well. In our model, we not only computed the motion cues as a part of saliency map before the fusion stage, and also consider the prior knowledge or task-driven stimuli, and static saliency map into the final weighted saliency fusion. This process can lead to a better accuracy to the ground-truth saliency map which is indicated by our human eyes compared with other previous models. We described our model as below.

### B. The Proposed System Overview

Figure 1 illustrates the framework of our system. The system is composed of four modules, video preprocessing, feature pooling, saliency map acquisition and final saliency map fusion.



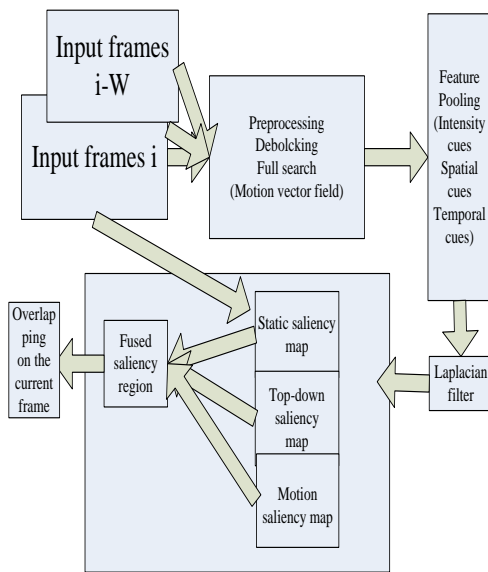


Fig. 1. System overview

In video preprocessing module, the input video is segmented into  $8 \times 8$  blocks. Then the full search between the previous  $W$  frame, which  $W$  is setting by our different users, generate all the motion vectors by observing the moving components on the HSV channel, with RGB turning into HSV beforehand.

The feature pooling module chooses the selected cues from all  $W$  frames. Our proposed idea is composed by three channels, which are motion intensity, spatial cues and temporal cues, respectively. After using Laplacian filter, which carries the isotropic properties, we can smooth the processing images and get a refine results before getting the motion saliency map.

The saliency map acquisition module contains three layers, the static saliency map is obtained from the Itti and Koch bottom-up attention model, which the top-down saliency map is generated by the AIM model [40], our motion saliency map is an important role on the later stage of final fusion module.

The final saliency map module is to combine all the saliency maps by giving the fusion weight and variance as we describe in the later part. The attention region is detected and we overlapped it on the current frame, remember that the  $W$  is a human-supervised frame rate setting before our proposed model.

In the following sections, we will illustrate our attention model in details.

### III. ATTENTION SALIENCY MAPS

#### A. Top-down Saliency Map

This section first presents an overview of the top-down saliency map and its underlying assumptions. It goes on to explain in the details of the different components and their functions. The processing architecture of the system is shown in Figure 2.

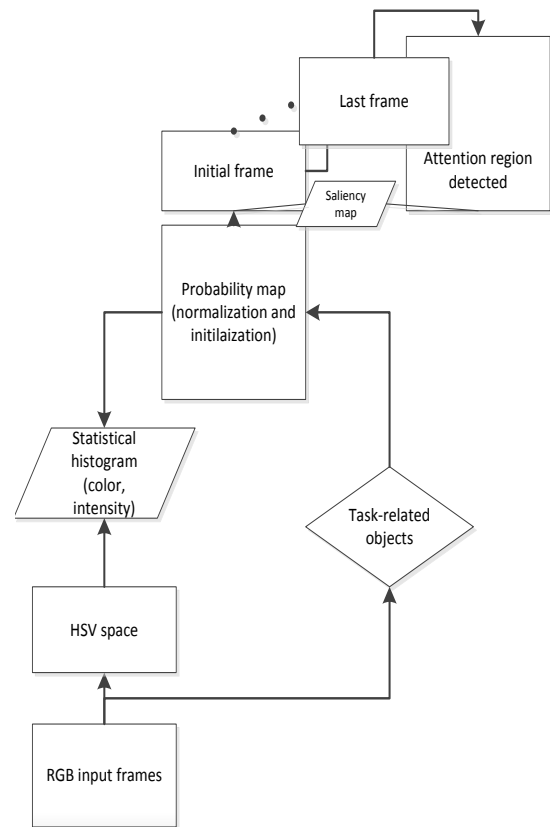


Fig. 2. The scheme of top-down saliency map

As shown in the Figure 2, the system consists of the several units which are all implemented in the systems. The web camera input might be produced by a motorized pan-and-tilt camera simulating a moving eye. Here we adopt a stationary camera image and only simulate the eye movements. The work space that the eye can explore is an area formed by  $352 \times 288$  RGB pixels. We convert the input frames into HSV which can enlarge the color contrast in spatial dimension. After obtaining the statistical histogram and designating the attention region, we can get the probability map (PM) [41], we adopt normalization and initialization to search the attention regions on each frame. The saliency map is a key process of our flowchart, which combines a number of visual feature maps into a combined map that assigns a saliency to every location in the visual field (Itti, Koch and Neibur, 1998). Each feature map is typically the result of applying some simple visual operator to the input image. For example, a feature map could consist of an activity pattern that may code for intensity, color, motion or some other visual cues. The result of summing the different feature maps is that the saliency map will code for locations in the image with many features.

Here, the saliency map selects the region of interest (ROI) by evaluating the possible area in the initial frame. Alternatively speaking, our model is based on the task-related visual searching. Variants of the task are obtained by positioning a certain number of distractors. The saliency region is detected by the following algorithm:

Algorithm 1 Top-down Saliency Map
i. Initialize proposed algorithm: (a) select the target region; (b) calculate the color histogram of each frame; (c) obtain the probability model of the object's features; (d) set the initial position.
ii. Process next frame: (a) read next frame; (b) set the previous frame's target center to the current frame's one; (c) set the searching window's width and height by half of the minimum bounding rectangle's width and height; (d) calculate the joint histogram; (e) obtain candidate model
iii. Tuning the weights on the probability map.
iv. Compute the next location of the target candidate by assuming the 10 pixels bias.
v. Compute the deviation to the tolerance range, if the current frame iteration stops, the current position is the saliency center and the algorithm goes back to step ii. Otherwise, to adjust the target position and to go back to step iii in order to continue the current frame's iteration.

As the algorithm implements, we can obtain our attention area by giving the attention region we assumed before, which can be formally called a semi-supervised top-down saliency map. In next stage, we need the static saliency map as one of the components before the saliency map fusion.

### B. Static Saliency Map

As we mentioned in the previous section, the first attribute is based on the spatial contrast analysis. Different spatial locations compete for saliency within each map, such that only locations which locally stand out from their surround can persist. All feature maps feed, in a purely bottom-up manner, into saliency map, which topographically codes for local conspicuity over the entire visual scene. The second attribute is based on the frequency domain analysis. Recently, a simple and fast algorithm, called the spectrum residual (SR), was proposed based on the Fourier Transform [42]. The paper argues that the spectrum residual corresponds to image saliency. Following this, the Phase spectrum of the Fourier

Transform (PFT) was introduced, which achieved nearly the same performance as the SR [43]. On the other hand, the choosing of perceptive unit differentiates the existing attention analysis methods. The perceptive unit can be chosen as pixel, image block, region or object. A pixel/block contains little perceptive information. Comparatively, an object contains much perceptive information but is difficult to be obtained because object detection is still an open problem in the area of computer vision. In color images, an object is composed of one or more regions. In other words, a region is a unit between a pixel/block and an object. It contains more perceptive information than a pixel/block and can be obtained by image segmentation, which is much easier than object detection. So, in our work we adopt region as perceptive unit. This choice also enables the proposed method to analyze visual attention at multi-scales for the adaptive size of region. Since our purpose is to obtain the image patches which can be used as perceptive unit, image segmentation is simplified by performing color quantization using K-Means. Then the neighboring pixels of same color are regarded as a region. The saliency of each region can be calculated by using equation (1):

$$Sal(k) = \log p(f(k)) \sum_{i=1}^{\kappa} d(f(k), f(i)) * G_{\kappa}(i, k) \quad (1)$$

where  $\kappa$  is the total number of regions in the image.  $G_{\kappa}$  is the DoG function of region  $\kappa$ , of which the radius is the same with the region.  $f(k)$  is the feature of region  $\kappa$  and  $p(f(k))$  is its probability calculated by using the color quantization result.  $d(f(k), f(i))$  is the distance between features. It is evaluated in our work by using Gaussian distance. An example of static saliency calculation is illustrated in Figure 4.

### C. Motion Saliency Map

In this section, we introduce the architecture of motion attention model and hereby this is the key contribution of our work. We intergrated this element into our model as previous approaches [44][45][46] are not well considered or simplified this part. Here, we start our research based on AVI video stream. However, we only select the uncompressed video clips to keep the information fidelity. As shown in figure 1, we can obtain approximate motion information from the motion vectors. In each frame, the spatial layout of motion vectors would compose a field called Motion Vector Field (MVF)[47][48]. If we consider MVF as the retina of eyes, the motion vectors will be the perceptual response of optic nerves. We set 3 types of cues, intensity cues, spatial coherence cues, and temporal coherence cues, when the motion vectors in MVF go through such cues, they will be transformed into three kinds of feature maps. We fuse the normalized output of cues into a saliency map by linear combination, and it will be tuned by the weight as describe in section 3.4. Finally, the image processing methods are adopted to detect attended regions in saliency map image, where the motion magnitude and the texture are normalized to [0, 255]. The selection of texture as value, which follows the intuition that a high-textured region produces a more reliable motion vector,

provides this method a significant advantage that when the motion vector is not reliable for camera motion, the V component can still provide a good presentation of the frame. After transforming the RGB to HSV color space, motion saliency can be calculated using the segmentation result of section. An example of saliency map and motion attention is illustrated in Figure 3. Figure 3(a) is the corresponding motion saliency map based on 9 dimensional MVF, while figure 3(b) is the result provided on 2 dimensional MVF. According to our assumption, there will be three cues at each location of macro block  $MB_{i,j}$ . Marco block is a basic unit of motion estimation in video encoder and it is consisted by an intensity pixel and two chromatic pixel blocks. Hereby we adopt 16\*16 Marco block due to the computational burden. Then the intensity cues can be obtained by computing the magnitude of motion vector

$$I(i, j) = \sqrt{dx_{i,j}^2 + dy_{i,j}^2} / MaxMag \quad (2)$$

here  $(dx_{ij}, dy_{ij})$  indicate two components of motion vector, and  $MaxMag$  is the maximum magnitude in MVF. The spatial coherence cues induces the spatial phase consistency of motion vectors has high probability to be in a motion object. By contraries, the area with inconsistent motion vectors is possible to be located near the edges of objects or in the still condition. First, we calculate a phase histogram in spatial window with the size of  $m*m$  pixels at each location of Marco block. The bin size of each is 10 degree, as we segment the 360 degree into 36 intervals, which means from 0 degree to 10 degree we regard it as a same angle. Then, we measure the phase distribution by entropy as following:

$$C_s(i, j) = -\sum_{t=1}^n p_s(t) \log(p_s(t)) \quad (3)$$

$$p_s(t) = SH_{i,j}^m(t) / \sum_{k=1}^n H_{i,j}^m(k)$$

where  $C_s$  donates spatial coherence,  $SH_{i,j}^m(t)$  is the spatial phase histogram whose probability distribution function is  $p_s(t)$ , and  $n$  is the number of histogram bins. Similarly, we define temporal phase coherence within a sliding window with the size of  $W$ (frames). It will be the output of temporal coherence cues as expressed below:

$$C_t(i, j) = -\sum_{t=1}^n p_t(t) \log(p_t(t)) \quad (4)$$

$$p_t(t) = TH_{i,j}^W(t) / \sum_{k=1}^n TH_{i,j}^W(k)$$

where  $C_t$  denotes temporal coherence,  $TH_{i,j}^W(t)$  is the temporal phase histogram whose probability distribution function is  $p_t(t)$  and  $n$  is still the number of histogram bins. Moreover, we increase the frame number as a temporal dimension and the output is easier to distinguish the difference. The result indicates the attended region can be more precise if

we elongate the frame number as shown in figure 5. The Laplacian filter is to remove the impulse noise generated by the input frames. Hereby we adopt the median filter can also preserve the edge information and sharpen the image details. We adopt 3\*3, 7\*7..., 25\*25 window slides at the experiment stage, but finally we utilize 3\*3 window as the convenience of later computation.

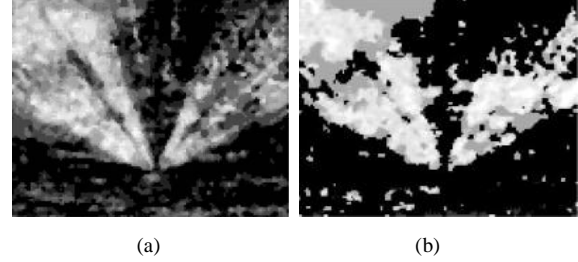


Fig. 3. the saliency map results from video set 1, as we can see more information fidelity from (a) but poor information from (b), the left one donates  $n=1-10, 2-11, \dots, 10-20$ , which means 9 motion vector fields in summation, while the right one only aggregates  $i=1-3, 2-4, 3-5$ , only computes 2 motion vector fields.

Generally, the intensity cue reveals the highly moving objects. The spatial cues indicate the different motion objects in spatial, while the temporal cues donates the variability of one object in the temporal dimensional. Also, the motion orientation weights the motion saliency map and affect the results on a critical extent. For example, when we capture a 135 degree motion on a motion saliency map consisted by most of 45 degree motion vector. This is quite singular and obvious to our human vision system, which means a high tuning weight on the next stage.

In figure 4, we demonstrate one of our experiment results, here  $W$  in equation 4 is set to 23, which means 23 frames constructs a motion vector field. The first column indicates the first frame and the  $W$  frame from the top to bottom, respectively. The second row illustrates the top-down saliency map by using AIM and the static saliency map from the Itti & Koch model, which the bottom figure shows the motion saliency map proposed by our model and the right most is our final fused saliency map.

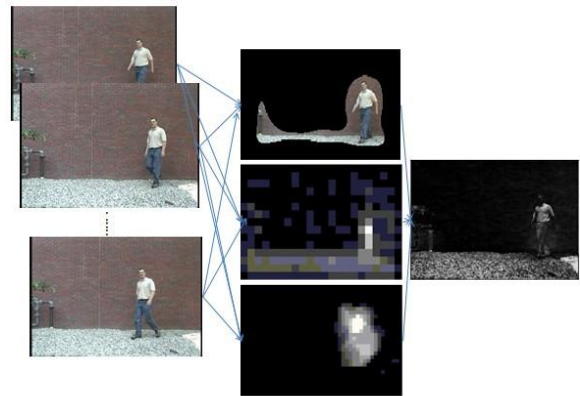


Fig. 4. The first column indicates the first frame and the  $W$  frame from the top to bottom respectively. The second row illustrates the top-down saliency map by using AIM and the static saliency map from the Itti& Koch model, which the bottom figure shows the motion saliency map proposed by our

model and the right most is our final fused saliency map

#### D. Saliency Map Fusion

After multi-channel analysis, we obtain three saliency maps including static saliency map, motion saliency map and top-down saliency map. Suitable fusion of the maps produces the final attention map. Map fusion can be performed with linear and nonlinear methods. In our work we adopt linear method for simplicity and with adaptive coefficients to fit different types of videos. Considering that our goal is to detect Region of Interest (ROI) from the saliency/novelty maps, we model this progress as binary classification and use the variance between classes to determine the fusion coefficients. Saliency map is first classified with the method of maximum variance between classes. Let  $Var_s$  be the result variance between classes:

$$Var_s = (n_1(\mu_1 - \mu)^2 + n_2(\mu_2 - \mu)^2) / n \quad (5)$$

where  $n_1$  and  $n_2$  are the number of samples of the two classes,  $n$  is the total number of samples.  $\mu_1$  and  $\mu_2$  are the means of two classes,  $\mu$  is the mean of all the samples. In equation 6, let  $Var_s$  donates for the variance on static saliency maps,  $Var_{motion}$  and  $Var_{top-down}$  be the variances between classes of motion saliency map and top-down saliency map respectively. Then the fusion weight for static saliency maps is

$$W_s = Var_s / (Var_s + Var_{motion} + Var_{top-down}) \quad (6)$$

The weights for motion saliency map and top-down saliency map are similarly calculated. We obtained  $w_M$  and  $w_N$  for the weight of motion saliency map and top-down saliency map. Hereby  $M_s$ ,  $M_M$  and  $M_N$  indicate the static saliency map, motion saliency map and top-down saliency map respectively. Finally, the fused attention map is computed as

$$AM = w_s M_s + w_M M_M + w_N M_N \quad (7)$$

with the above equation, motion features will be integrated as a part of fused saliency map, as attention is mostly guided by motion cues in dynamic scenes. The top-down saliency map is also fused into the fusion stage. The static saliency map is calculated in the final saliency map based on the bottom-up computational attention model.

The motivation behind the evaluation is to find an efficient and robust fusion method that not only extracts all useful information, but also reduces the impact of false findings.

After applying the proposed maps fusion method, we selected the points higher than the threshold; the threshold is obtained from the subtraction from each consecutive block

3\*3. The higher value we get, the more probability of attention region it is, since it implies the higher differences between foreground and background. After we get the labeled points on each frame, if the points occupy on a relatively concentrated area, we then assumed it as the region of interests. To indicate the region of interests, we will add a red circle with the radius of 64 pixels to indicate ROI on each frame. In the experiments and evaluation section, we will test the proposed attention model with various video sequences.

The effect of saliency fusion stage is to make our model more close to the real human visual system. As human visual system is affected by exogenous and endogenous stimuli, our model considers the **top-down** and **bottom-up** mechanism to link a bridge for both biological and artificial vision systems.

#### IV. PERFORMANCE EVALUATION

To demonstrate the effectiveness of the propose attention model, we have extensively applied the method on several types of video sequences from the benchmarks. The detail of the testing videos is given in Table 1.

##### A. Data Set and Experimental Results

We applied our system on different types of videos to verify its feasibility and generality. The dataset are from [49][50][51][52], as detailed in Table 1, includes surfing player, parachute landing, outdoor, traffic artery and other video sequences with high or low motion features.

TABLE I. Testing Videos

No.	Video	Subjects	Frames
1	Surfing player	Surfing player	25
2	Glider	Glider pilots	30
3	Traffic artery	Vehicles	108
4	Toll station	Tollbooth collector	258
5	Parachuter landing	Parachuter	33

The first testing set contains video sequences with prominent motions. The video are mainly focusing on the motion surfing player.

In this case, the motion saliency map plays an important role in the feature fusion, when the spatial and temporal cues do not take a large percentage on the equation (4). Hereby the value of the variables in our model is described as the following in the Table 2.

We apply our proposed algorithms to these video clips and the most relevant region of interest will be found out and highlighted with a red circle. All the results are shown in the figures below. As the image size of each frame is 640 by 480 pixels, the circled region of interest can be relatively small as you will notice, for example, in Figure 6.

TABLE II. PARAMETER SETTING

$n = 25$	$n_1 = 9$	$n_2 = 2$	$W_N = 0.3$
$\mu_1 = 4.5$	$\mu_2 = 1$	$\mu = 12.5$	$Var_s = 27.3$
$Var_{motion} = 29.1$	$Var_{top-down} = 24.6$	$w_s = 0.34$	$W_M = 0.36$

The second test video clip is about mostly dynamic scenes that recorded a parachute player descending in the atmosphere. Our model also proves its robustness and efficiency in this experiment. With the motion vector fusion in the attention model, our accuracy reaches 87% since it contains rich entropy and the weight factor is relatively high. The variables change a little due to different total frames and number of samples. We have not listed all the parameters as the table 2 because the effects of saliency maps are quite similar. And interest region is also detected and indicated using a red circle with radius of 64 pixels. The circle is relatively small due to higher resolution of these images (640\*480).

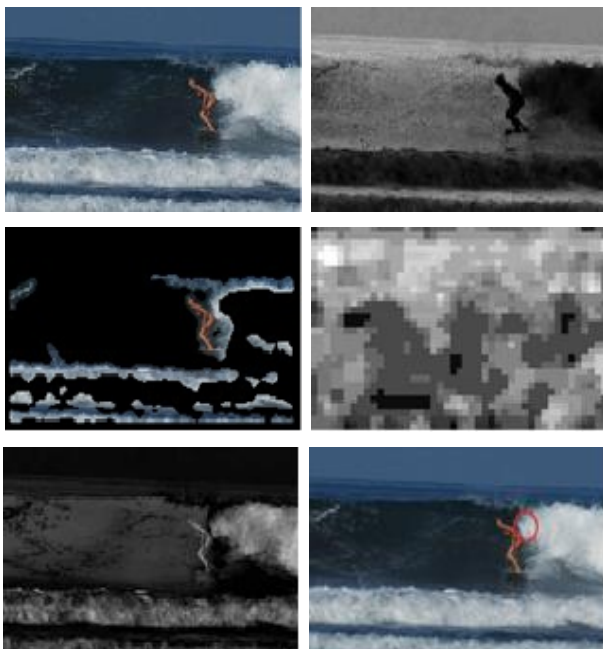


Figure 6. Testing Video 1: the illustration of one example results using our proposed model, the first left image indicates the original video, the right image shows the static saliency image; the left image on the second row shows the top-down saliency map while the right one is the motion saliency map. The third row of the left image is the fused saliency map while the right one is the attention region, red circle indicates our detected attention region by using the fusion of saliency map. The total detected frames are about 25 frames with nearly 16 frames accurately detected.

On the test video 3, the traffic artery with multiple objects contains in the frame. We can accurately detect the approaching vehicles in the video sequences – as shown in the example images in the following Figure 7. The interest region indicated by the red circle is very small, as the size of the images is 960 by 540. On video clip 4 and 5, the accuracy is 74.8% and 78.7%, respectively, which is a satisfactory result overall. The images size in video clip 4 and 5 are 352 by 288 and 640 by 480, respectively.

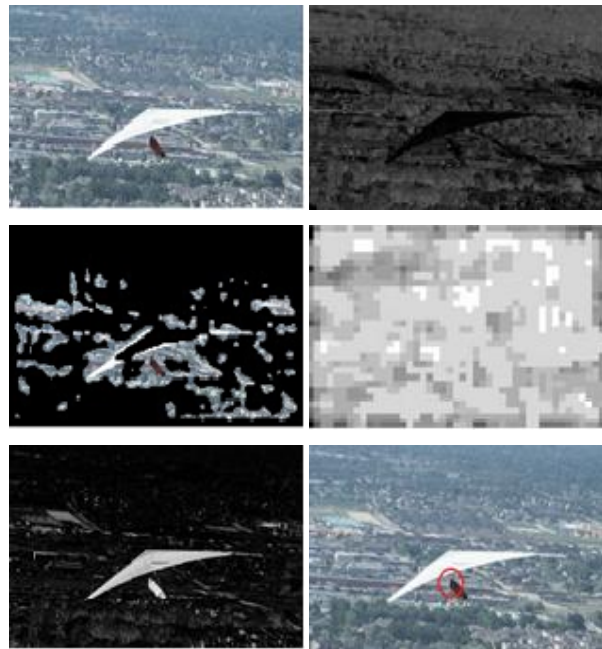
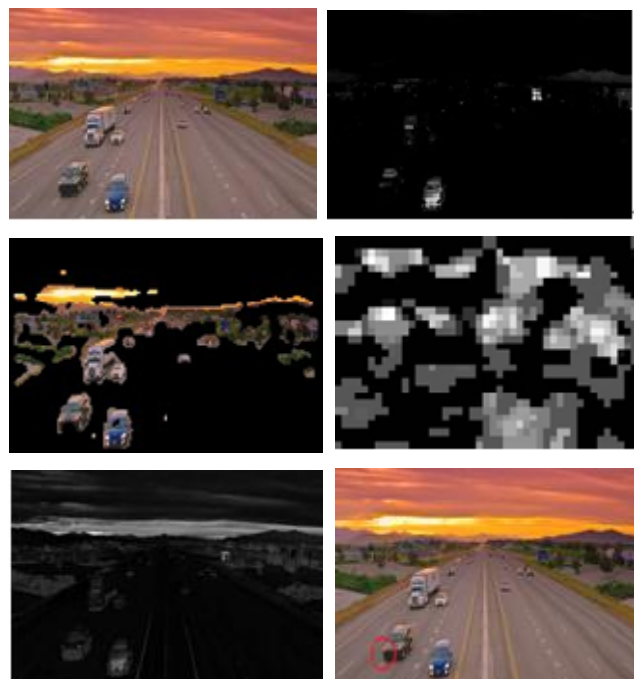
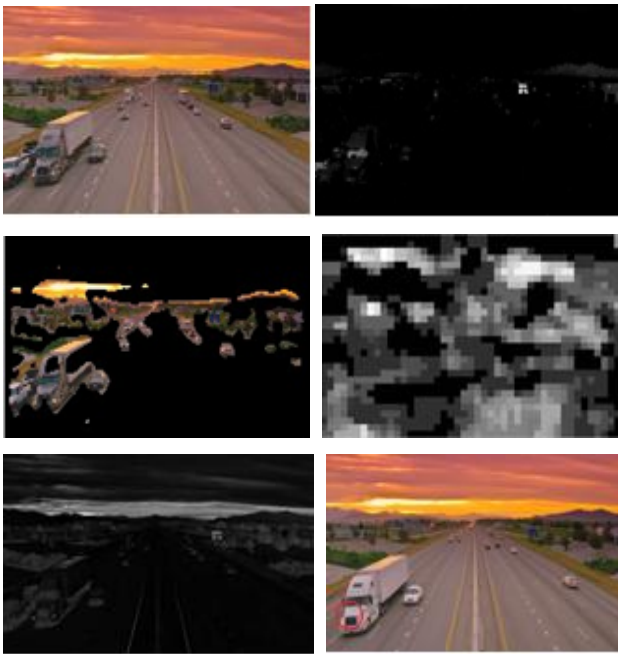


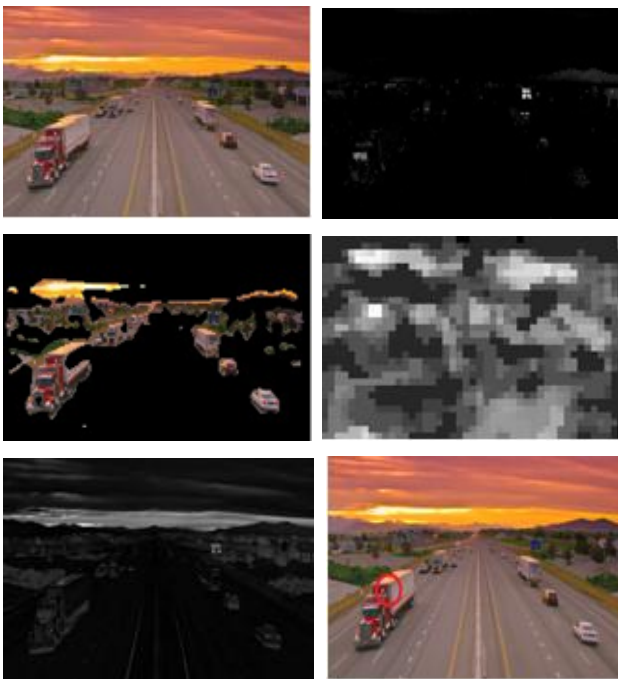
Figure 7. Testing Video 2: the illustration of one example results using our proposed model, the first left image indicates the original video, the right image shows the static saliency image; the left image on the second row shows the top-down saliency map while the right one is the motion saliency map. The third row of the left image is the fused saliency map while the right one is the attention region, red circle indicates our detected attention region by using the fusion of saliency map. The total detected frames are about 30 frames with nearly 19 frames accurately detected.



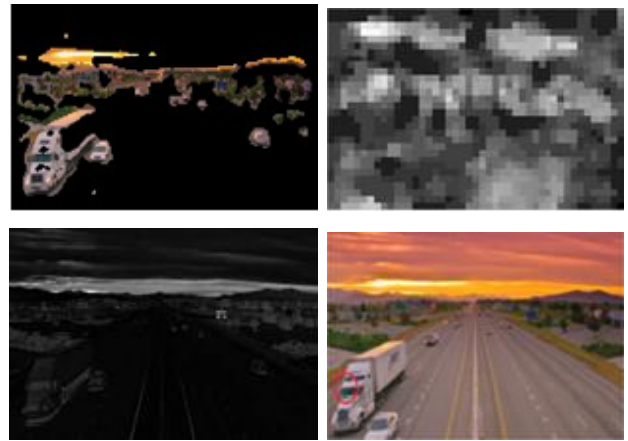
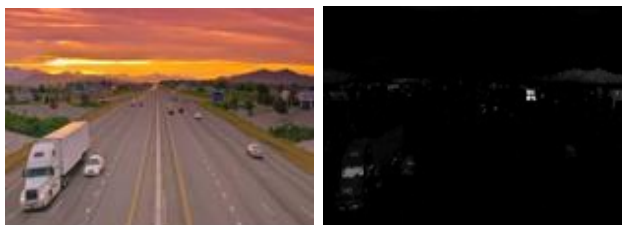
(Group A, selected from the video frame 7)



(Group B, selected from the video frame 31)



(Group C, selected from the video frame 78)



(Group D, selected from the video frame 93)

Figure 8. Testing Video 3: the illustration of four examples results using our proposed model, the first left image indicates the original video, the right image shows the static saliency image; the left image on the second row shows the top-down saliency map while the right one is the motion saliency map. The third row of the left image is the fused saliency map while the right one is the attention region, red circle indicates our detected attention region by using the fusion of saliency map. The total detected frames are about 108 frames with nearly 95 frames accurately detected. Hereby we randomly select 4 frames results to illustrate our results. They are the frames at 7,31,78 and 93, respectively.

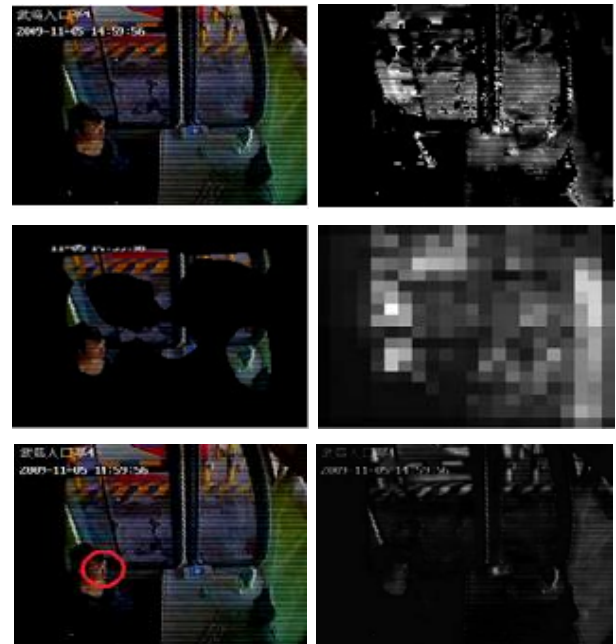


Figure 9. Testing Video 4: the illustration of one example results using our proposed model, the first left image indicates the original video, the right image shows the static saliency image; the left image on the second row shows the top-down saliency map while the right one is the motion saliency map. The third row of the left image is the fused saliency map while the right one is the attention region, red circle indicates our detected attention region by using the fusion of saliency map. The total detected frames are about 258 frames with nearly 193 frames accurately detected.



Figure 10. Testing Video 5: the illustration of one example results using our proposed model, the first left image indicates the original video, the right image shows the static saliency image; the left image on the second row shows the top-down saliency map while the right one is the motion saliency map. The third row of the left image is the fused saliency map while the right one is the attention region, red circle indicates our detected attention region by using the fusion of saliency map. The total detected frames are about 33 frames with nearly 26 frames accurately detected.

### B. Comparison and Evaluation

In order to further verify the proposed method, we compared our approach with several state-of-the-art methods. We measured the overall performance of the proposed method with respect to precision, recall, and O-measure, and compared them with the performance of existing competitive automatic salient object segmentation methods, such as Itti & Koch's method [53][54], AIM [40] and Achanta's method [55].

According to the standard evaluation methods, precision is the percentage that the detected saliency map divided on the non-ground-truth saliency map as been predicted. Recall is a measure of the percentage provided that the detected saliency map divided on the ground-truth saliency map as been predicted. The highest percentage of precision indicates the real attention as the test participants assumes them as the attention region. The recall is similar as the false positive. O-measure is a special method which predicts the overall performance of the model. The O-measure used in this study is calculated from:

$$O_{\Omega} = \frac{(1+\Omega^2) \text{precision} * \text{recall}}{\Omega^2 * \text{precision} + \text{recall}} \quad (8)$$

Here we use  $\Omega = 0.25$  in our experiments to weigh precision than recall. For all three performance measures, a high percentage is indicating a better performance.

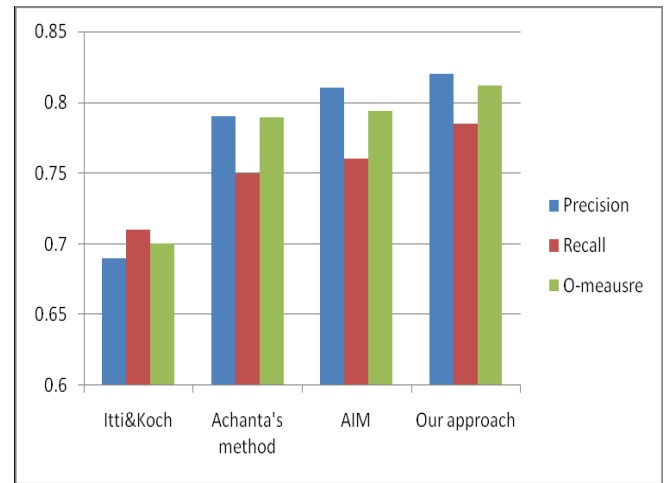


Figure 11. Performance comparison between the proposed method and the state-of-the-art methods. The vertical axis indicates the percentage of precision, recall and O-measure index, the horizontal axes is the approaches proposed and our model.

As shown in Figure 11, we compared the precision, recall and O-measure among the methods of Itti & Koch [53][54], Achanta [55], AIM [40] and proposed model. The proposed method outperformed the state-of-the-art attention models in all three performance measures- precision, recall, and O-measure.

### V. CONCLUSION AND FUTURE WORK

In this paper, we proposed a novel automatic approach to detect attention region from video sequences. We designed a motion saliency map by using the motion vector field, which shows a high entropy and motion vector on the specific region.

The saliency map fusion can extensively balance the low-level and high-level features and optimize them to the maximum extent as the experiments going. Our experiments demonstrated that the saliency model outperforms other models with respect to performance measures.

This paper has addressed the bottom-up cues into the saliency model, however, in human visual system, top-down attention and the combination of the bottom-up and top-down cues play significant role in the emergence of high level intelligence [56].

It is also believed that the ability to respond to motion cues is vital for not only low level animals such as insects [57], but also import in the emergence of complex human brains. We will further integrate more motion cues into the attention model, and will implement these models to robots for efficient human robot interaction in the future.

### ACKNOWLEDGEMENT

Thanks to all of the collaborators whose modeling work is reviewed here, and to the members of school of computer science, at the University of Lincoln, for discussion and feedback on this research. This work was supported by the grants of EU FP7-IRSES Project EYE2E (269118), LIVCODE (295151) and HAZCEPT(318907).

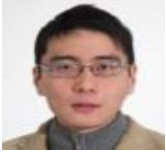
REFERENCES

- [1] L. Ferman, H. Collewin, A. Van Den Berg, A direct test of Listing's law-I. Human ocular torsion measured in static tertiary positions, *Vision Research* 27 (1986) 929-938.
- [2] E. Proeto, U and Peter A.Tass, Timing of V1/V2 and V5+ activations during coherent motion of dots: An MEG study, *Neuroimage* 37(2007)1384-1395.
- [3] A. Oliva, A., Torralba, A., Castelhana, M.S., & Henderson, J.M. Top down control of visual attention in object detection. *IEEE Proceedings of the International Conference on Image Processing, 2003, Vol I, 253-256.*
- [4] D. Parkhurst, Modeling the role of salience in the allocation of overt visual attention, *Vision Research, 2002.*
- [5] C. Rentschler, , Fixations in natural scenes: Interaction of image structure and image content, *Vision Research* 46 (2006) 2535-2545.
- [6] G. Kreiman, T. Serre and T. Poggio. On the limits of feed-forward processing in visual object recognition. *Cosyne, February 2007.*
- [7] A. Treisman, A M, Gelade, G. A feature-integration theory of attention. *Cognitive Psychol*, 1980, 12(1): 97-136.
- [8] R.Einhäuser et al. Differences of monkey and human overt attention under natural conditions, *Vision research*, 46, 1194-1209, 2006.
- [9] C. Rentschler, , Fixations in natural scenes: Interaction of image structure and image content, *Vision Research* 46 (2006) 2535-2545.
- [10] M. Cerf, P. Frady, C Koch, Faces and text attract gaze independent of the task: Experimental data and computer model, *Journal of Vision*, 9(12):10, 1-15, 2009.
- [11] A. Oliva, Contextual guidance of eye movements and attention in real-world scenes: The role of global features on object search, *Psychological Review*, 113, 766-786.
- [12] A.Castelhana, M.S., & Henderson, J.M. Incidental Visual Memory for Objects in Scenes. *Visual Cognition*, 2005,12, 1017-1040.
- [13] H. Donk, M. & van Zoest, W. Effects of salience are short-lived. *Psychological Science*, 19 (7), 733-739, 2008.
- [14] CM Masciocchi , S Mihalas , D Parkhurst , Niebur E. Everyone knows what is interesting: salient locations which should be fixated, *Journal of Vision*, vol. 9 no. 11 article 25, 2009.
- [15] S. Chikkerur, T. Serre, C. Tan and T. Poggio. What and where: A Bayesian inference theory of attention. *Vision Research (Special issue on "Mathematical Models of Visual Coding")*. 55(22), pp. 2233-2247, Oct 2010.
- [16] V. Navalpakkam, L. Itti, Optimal cue selection strategy, In: *Advances in Neural Information Processing Systems*, Vol. 19 (NIPS\*2005), pp. 987-994, Cambridge, MA: MIT Press, 2006.
- [17] U. Rutishauser, C. Koch, Probabilistic modeling of eye movement data during conjunction search via feature-based attention, *Journal of Vision*, 7(6):5, 1-20, 2007.
- [18] YF Ma, L Lu, HJ Zhang, M Li, "A user attention model for video summarization" *ACM Multimedia'02.*
- [19] S Yue and Rind F. Claire, "Postsynaptic organizations of directional selective visual neural networks for collision detection," *Neurocomputing* (in press), DOI: 10.1016/j.neucom.2012.08.027.
- [20] S Yue and Rind F. Claire, "Visually stimulated motor control for a robot with a pair of LGMD visual neural networks.", *IJAMechS*, (2012)
- [21] HY Meng , A Kofi, S Yue, H Andrew, H Mervyn, P Nigel, H Peter "Modified Model for the Lobula Giant Movement Detector and Its FPGA Implementation," *Computer Vision and Image Understanding*, 2010, vol.114(11), pp.1238-1247. ISSN 1077-3142, doi:10.1016/j.cviu.2010.03.017.
- [22] S. Yue and Rind F. Claire, "Collision detection in complex dynamic scenes using a LGMD based visual neural network with feature enhancement," *IEEE Transactions on Neural Networks*, 2006, vol.17(3), pp.705-716.
- [23] J. J. Clark, "Spatial attention and saccadic camera motion," in *Proc. IEEE Int. Conf. Robot. Autom.*, Leuven, Belgium, 1998, pp.3247-3252.
- [24] M. Z. Aziz and B. Mertsching, "Fast and robust generation of feature maps for region-based visual attention," *IEEE Trans. Image Process.*, vol. 17, no. 5, pp. 633-644, May 2008.
- [25] R Bodor, B Jackson, and N. Papanikoloupolos, ; "Vision-based human tracking and activity recognition", *XI Mediterranean Conf. on Control and Automation*, 2003.
- [26] J. Tsotsos and A Rothenstein (2011), "Computational models of visual attention", *Scholarpedia*, 6(1):6201. doi:10.4249/scholarpedia.6201.
- [27] K.Tanaka, H.Saito, G. Analysis of motion of the visual field by direction, expansion/contraction, and rotation cells clustered in the dorsal part of the medial superior temporal area of the macaque monkey. *Journal of Neurophysiology*, vol. 62 no. 3, 626-641, 1989.
- [28] C. Alais, D., & Blake, R. (1999). Neural strength of visual attention gauged by motion adaptation. *Nature Neuroscience*, 2(11), 1015-1018.
- [29] A. Cyrus Arman, "Effects of feature-based attention on the motion aftereffect at remote locations", *Vision Research*, 46 (2006) 2968-2976.
- [30] P. Anandan, "Measuring visual motion from image sequences," *Ph.D.thesis*, Univ. of Mass., May 1987.
- [31] AC Huk & DJ Heeger , Pattern-motion responses in human visual cortex, *Nature Neuroscience*, 5:72-75, 2001.
- [32] L. Itti, C. Koch, and E. Niebur, A Model of Saliency-Based Visual Attention for Rapid Scene Analysis, *IEEE TRANSACTIONS ON PATTERN ANALYSIS AND MACHINE INTELLIGENCE*, VOL. 20, NO. 11, NOVEMBER 1998.
- [33] L. Itti, C. Koch, Feature Combination Strategies for Saliency-Based Visual Attention Systems, *Journal of Electronic Imaging*, Vol. 10, No. 1, pp. 161-169, Jan 2001.
- [34] [34] L. Itti, C. Koch, E. Niebur, A Model of Saliency-Based Visual Attention for Rapid Scene Analysis, *IEEE Transactions on Pattern Analysis and Machine Intelligence*, Vol.20, No. 11, pp. 1254-1259, Nov 1998.
- [35] G. Kootstra, A. Nederveen, and B. de Boer. Paying attention to symmetry. *BMVC*, 2008.
- [36] R. Valenti, N. Sebe, and T. Gevers. Image saliency by isocentric curvedness and color. *ICCV*, 2009.
- [37] L. Itti, N. Dhavale, and F. Pighin. Realistic avatar eye and head animation using a neurobiological model of visual attention. *SPIE*, 2003.
- [38] [38] X. Hou and L. Zhang, "Saliency detection: A spectral residual approach," in *IEEE Conf. Computer Vision and Pattern Recognition*, 2007.
- [39] Raj, Alvin Statistical Saliency Model incorporating motion saliency and an application to driving Massachusetts Institute of Technology. Dept. of El.
- [40] L. Bruce, N.D.B., Tsotsos, J.K., Attention based on information maximization. *Journal of Vision*, 7(9):950a, 2007.
- [41] M. DeGroot, *Optimal Statistical Decisions*, McGraw-Hill, (1970).
- [42] C. Guo, Q. Ma, and L. Zhang, "Spatio-temporal saliency detection using phase spectrum of quaternion fourier transform," in *IEEE, Conf. Computer Vision and Pattern Recognition*, 2008.
- [43] J Li, Visual Saliency Based on Scale-Space Analysis in the Frequency Domain, *IEEE Transactions on Pattern Analysis and Machine Intelligence*, Vol. 6, No. 1, January 2007.
- [44] J. J. Clark, "Spatial attention and saccadic camera motion," in *Proc. IEEE Int. Conf. Robot. Autom.*, Leuven, Belgium, 1998, pp.3247-3252.
- [45] M. Z. Aziz and B. Mertsching, "Fast and robust generation of feature maps for region-based visual attention," *IEEE Trans. Image Process.*, vol. 17, no. 5, pp. 633-644, May 2008.
- [46] TZ Lauritzen , M D'Esposito, DJ Heeger , MA Silver . Top-down flow of visual spatial attention signals from parietal to occipital cortex, *Journal of Vision*, 9(13):18, 1-14, 2009.
- [47] X. Hou and L. Zhang, "Saliency detection: A spectral residual approach," in *IEEE Conf. Computer Vision and Pattern Recognition*, 2007.
- [48] C. Guo, Q. Ma, and L. Zhang, "Spatio-temporal saliency detection using phase spectrum of quaternion fourier transform," in *IEEE, Conf. Computer Vision and Pattern Recognition*, 2008.
- [49] <ftp://ftp.cs.rdg.ac.uk/pub/PETS2001/>
- [50] <http://cim.mcgill.ca/~ljjian/database.htm>
- [51] [http://vision.ucsd.edu/~bbabenko/project\\_miltrack.shtml](http://vision.ucsd.edu/~bbabenko/project_miltrack.shtml)
- [52] <http://people.csail.mit.edu/tjudd/research.html>
- [53] L. Itti, Quantitative Modeling of Perceptual Saliency at Human Eye Position, *Visual Cognition*, Vol. 14, No. 4-8, pp. 959-984, Aug-Dec 2006.
- [54] R. J. Peters, L. Itti, Beyond bottom-up: Incorporating task-dependent influences into a computational model of spatial attention, In: *Proc. IEEE Conference on Computer Vision and Pattern Recognition (CVPR)*, Jun 2007.
- [55] R. Achanta and S. Süsstrunk, Saliency Detection for Content-aware Image Resizing, *IEEE International Conference on Image Processing*, 2009.



- [56] M. Begum and F. Karray, "Visual attention for robotic cognition: a survey," *IEEE Transactions on Autonomous Mental Development*, vol.3(1), pp92-105, 2011.
- [57] S. Yue and F.C. Rind, "Redundant neural vision systems - competing for collision recognition roles," *IEEE Transactions on Autonomous Mental Developments*, 2013 (in press) (DOI 10.1109/TAMD.2013.2255050).

AUTHORS PROFILE



**Jiawei Xu** received the B.S. and M.S. degrees in computer engineering from Shanghai University of Engineering Science and Technology, Shanghai, China, 2007 and Hallym University, Korea, 2010, respectively. Now he is a PhD student in the School of Computer Science, University of Lincoln, UK. His research interests include computer vision, human attention models, and visual cortex modeling. He was a pattern classification engineer in JTV Co.Ltd, Beijing during the year of 2011.



**Shigang YUE** is a Professor of Computer Science in the Lincoln School of Computer Science, University of Lincoln, United Kingdom. He received his PhD and MSc degrees from Beijing University of Technology (BJUT) in 1996 and 1993, and his BEng degree from Qingdao Technological University (1988). He worked in BJUT as a Lecturer (1996-1998) and an Associate Professor (1998-1999). He was an Alexander von Humboldt Research Fellow (2000, 2001) at University of Kaiserslautern, Germany. Before joining the University of Lincoln as a Senior Lecturer (2007) and promoted to Reader (2010) and Professor (2012), he held research positions in the University of Cambridge, Newcastle University and the University College London(UCL) respectively. His research interests are mainly within the field of artificial intelligence, computer vision, robotics, brains and neuroscience. He is particularly interested in biological visual neural systems, evolution of neuronal subsystems and their applications – e.g., in collision detection for vehicles, interactive systems and robotics. He is the founding director of Computational Intelligence Laboratory (CIL) in Lincoln. He is the coordinator for several EU FP7 projects. He is a member of IEEE, INNS, ISAL and ISBE.

# Web-based Expert Decision Support System for Tourism Destination Management in Nigeria

Yekini Nureni Asafe  
Computer Technology Department  
Yaba College of Technology  
Lagos, Nigeria

Adetoba Bolaji  
Computer Technology Department  
Yaba College of Technology  
Lagos, Nigeria

Aigbokhan Edwin Enaholo  
Computer Technology Department  
Yaba College of Technology  
Lagos, Nigeria

Oluwafemi Olubukola  
Hospitality, Leisure and Tourism Management  
Yaba College of Technology  
Lagos, Nigeria

**Abstract--** The use of Information Technologies have played and currently playing prominent roles in many organizations, such as business, education, commerce. The tourism industry has witnessed the use and application of various computer-based systems in carrying out one or more activities or operation. But currently there is no computer-based system tourist destination to integrate the tourists (from outside Nigeria) and tourists center within Nigeria, so that tourists can make a pre destination plan and decision before venturing into tourism journey to the country Nigeria. The authors of this paper proposed the design of web-based Expert Decision System (WEDSS), to provide tourist to Nigeria and its environ essential data and tools to managing their tours and to base all the decisions concerning to queries on the, tourist centers and hotels based on the following issue; climate, road conditions, cultural aspects, lodging, health facilities, banking, etc. of the location to be visited on sound and rational bases. Web-Based Tourist Decision Support System (WEDSS) for Nigeria will be developed to allow the tourist to find their route in Nigeria and ask for information about sights, accommodations and other places of interest which are nearby to him to improve the convenience, safety, efficiency of travel and enhance tourism attraction of tourists.

**Keyword-Tourism; Tourism Destination; Decision Support System; Web-Based; Lagos; Abuja; Nigeria**

## I. INTRODUCTION

For many countries, either developed or developing, tourism is a very important source of foreign currency earnings and employment. Links between tourists and tourism destination is key success factors for integrated tourism development. Tourism is travel for recreational, leisure, or business purposes. The World Tourism Organization defines tourists as people "traveling to and staying in places outside their usual environment for not more than one consecutive year for leisure, business and other purposes". [1] Tourism has become a popular global leisure activity. In 2011, there were over 983 million international tourist arrivals worldwide, representing a growth of 4.6% when compared to 940 million in 2010. [2][3]. some kind of traveling have been categorized has tourist travel by international communities.

Theirs possibility that somebody a tourists has never been to the place he or she wish to visit before, and he or she has no relative or friends in the place. For example academician from Canada to present an academic paper in a conference to be held in Lagos Nigeria and there is no available information on geographical location of Nigeria, her economy etc. This person has to decide on how to locate the country Nigeria and available tourist center for leisure, tourist attraction, to sleep overnight etc. The so called tourist has prepared to Visit the country Nigeria for the conference. At a stage he or she has to decide on where to stay, visit and enjoy some tourist attraction within the period of the conference. The successful completion of this stage can be assisted by an Expert Decision Support System (EDSS) developed to analyses the perspectives and planned strategies of this tourism stakeholders.

This paper discusses the model, operation and suitability of a Web-based EDSS for integration of tourist and tourist centers in Nigeria. The paper concludes by assessing the usefulness of the web-based EDSS for tourism planners, and suggests areas for future research.

## Objective

Objective of this study is to design a web-based decision support system for integration of tourists and tourists center within Nigeria, so that tourists can make a pre destination plan and decision before venturing into tourism journey.

## Scope of study

The scope of this study is limited to federal republic of Nigeria

## II. BACKGROUND TO THE STUDY

The use of ICTs application is a relevant opportunity for growing and strengthening tourism industry, and for the development of destinations economies overall. Specifically ICTs application have the potential to improve destination management [12], [13]: developing and reinforcing local

tourism and tourism-related entrepreneurship and activities; developing genuine tourism offerings that rely on local productions and traditions (for ex. food, furniture, handicrafts and constructions); enabling direct promotion and commercialization of local tourism offerings in international markets reducing dependence on big foreign intermediaries. Basically ICTs allow destinations to improve online presence (i.e. visibility and participation to Internet market) and offline connectivity (i.e. collaboration, clustering as well as inter sectorial linkages among local public and private tourism and tourism-related actors) required to compete in nowadays global tourism market.

More specifically the beneficial effects of ICTs are to be found in the opportunity to reduce the traditional disadvantages of small operators. First ICTs provide direct, cheap and effective access to (actual and potential) customers. At the same time ICTs make profitable to use multiple distribution channels and target niche markets [10], [13], [14]. Which is almost impossible for SMEs to reach, serve and even to identify?

Tourism in Nigeria centers is largely depends on events, due to the country's ample amount of ethnic groups, but also includes rain forests, savannah, waterfalls, and other natural attractions.[1] The industry, unfortunately, suffers from the country's poor electricity, roads, and water quality.[2] Tourist sites in Nigeria include festivals and cultural celebrations (such as Durbar festivals), the nation's national parks (such as Old Oyo, Yankari, and Cross River National Parks), and other geographical sites (such as Aso Rock, Abuja.)

The tourism industry is regulated by the Ministry of Culture, Tourism and National Orientation, a Nigerian government ministry. [3] In an attempt to raise the profile of the country's tourism sector, a beauty pageant, the Miss Tourism Nigeria Pageant, was created in 2004.[4] The winners in 2004, 2005, and 2006 have been, respectively, Shirley Aghotse,[5] Abigail Longe,[4] and Gloria Zirigbe.[6] The World Travel and Tourism Council estimates revenue related to tourism and travel in Nigeria will exceed 10 billion \$USD in 2007, and will account for approximately 6% of the gross domestic product.[7]

Tourism in Nigeria has witnessed some development since 1999, when Nigeria transits in to civil rule, The Federal Ministry of Culture and Tourism came into being in June 1999, following the harmonization of the Culture and Tourism as a Ministry by the present Administration. Its creation by a democratic Administration represents an important contribution of the President Olusegun Obasanjo's Administration towards the growth of the Culture and Tourism sub-sector. The vision of the Ministry is to position Culture and Tourism as leverage for economic growth and development in Nigeria. [8]

With the evolution of Internet technologies web-based tools for tour planning can now be easily made available, implemented and become a valuable resource for the traveling community and tourists. Decision Support System provides tools for persuasion and a vocabulary and discipline that facilitate negotiations and coordination across the organizational boundaries. Bousset et al [9]

### III. RESEARCH METHODOLOGY

Case study area for this research work is Nigeria, a country in Africa continent. This study area was divided into three cardinal point of reference.

Southwest with particular references Lagos State, The choice of Lagos state is based on its relevance in economy development of the country Nigeria, been the former federal capital and economy nerve center of Nigeria and is made up several tourist centers, which includes; Monuments & Buildings - National Art Theatre, Iganmu, The Remembrance Arcade, Peacock, Lekki Conservation Centre, Lekki Conservation Centre, Lagos Central Mosque, Slave Port, Badagry, Glover Memorial Hall, First Storey Building in Nigeria, Slave Jetty, Badagry, Early Missionary Cemetery, Canon Gun, Instrument of Slave Abolition & War, Slave Market, Badagry, Christ Cathedral, CMS, Tafawa Balewa Square, Shitta\_Bay Mosque etc., Hotels and Restaurant; - federal palace hotel, sharaton hotel, airport hotel etc,

Southeast with particular reference to Anambra state, The choice of Anambra is based on its population as the second most densely populated state in Nigeria after Lagos State, and also some cultural diversity with monumental tourist attraction.

Northern Region with particular reference to Abuja, the federal capital territory. The choice of Abuja is based on its relevance as meeting point of all Nigerians, the seat of power, tourist attraction like zuma rock, and availability of modern hotels and Inns.

#### Data Collection

The data for this work come from three sources. Firstly, documentation from Lagos state ministry of tourism from which we gathered data on various tourists' centers and hotels within Lagos State and its environs. Secondly, The Federal Ministry of Culture and Tourism from which we gathered, data on various tourist attractions center within the nook and cranny of the nation. Thirdly, visitation to the 30 selected tourists center (excluded hotels and inn), and forty five hotels (fifteen from each of selected states i.e. Abuja, Lagos and Anambra) to be include in our EDSS database.

### IV. PROPOSED DESIGN OF WEDSS

#### Description of Proposed System

Proposed Web-based expert decision support system is a set of computer-based tools; provides tourist with interactive capabilities to enhance his understanding and information basis about considered tourism destination through usage of models and data processing, which in turn allows reaching decisions by combining personal judgment with information provided by these tools.

The proposed web-based EDSS will use artificial intelligence techniques to solve problems, and the architecture will be divided into three levels as shown in figure 2.

The basic data to be included in the database are the selected data as in tourist centers and hotels obtained from

data been collected earlier. The proposed system will be designed to give allowances for updating of the database system. The proposed system will be using following technologies; internet based communication tools to enable tourist/s to connect to the system anywhere in the world, e-mail tool that will enable the user to communicate with people

or management of tourist centers. The users (tourists) will communicate with the system via a communication layer as shown in figure 1, figure 2 describe the organization of the proposed WEDSS. The database management system lies on the database server, a server that is isolated in order to avoid hacker's attacks and also provides satisfactory response times.

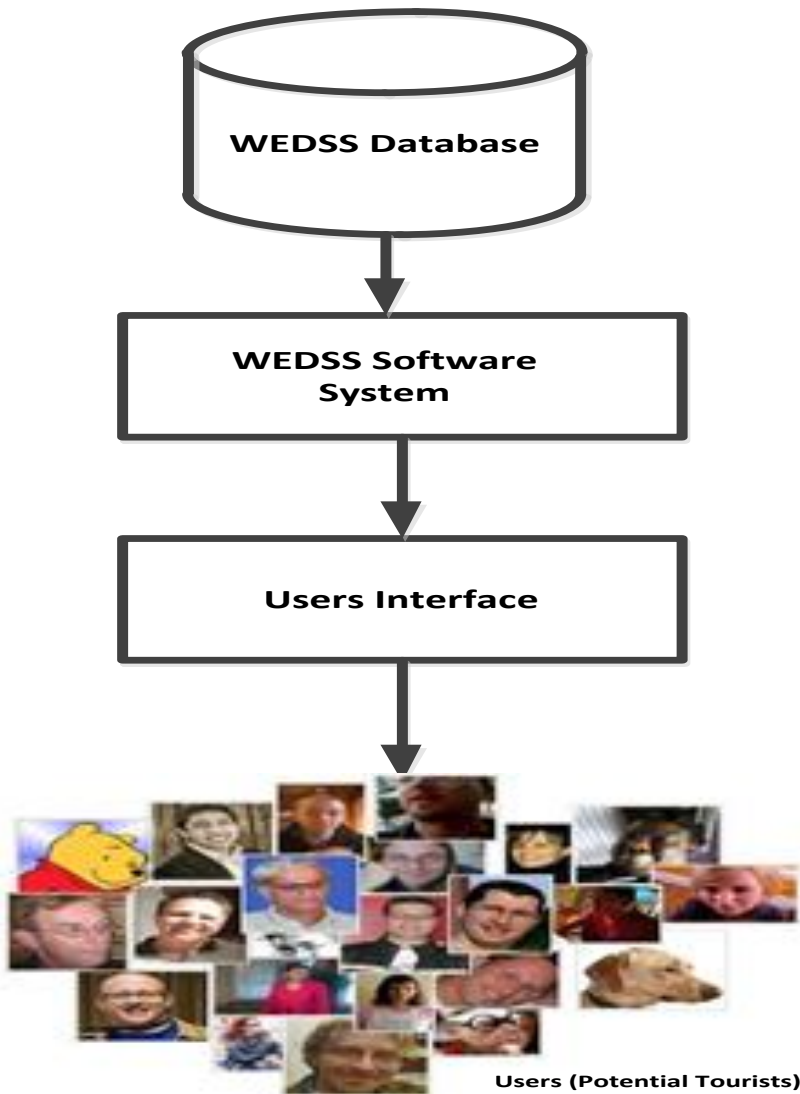


Fig. 1 Components of WEDSS

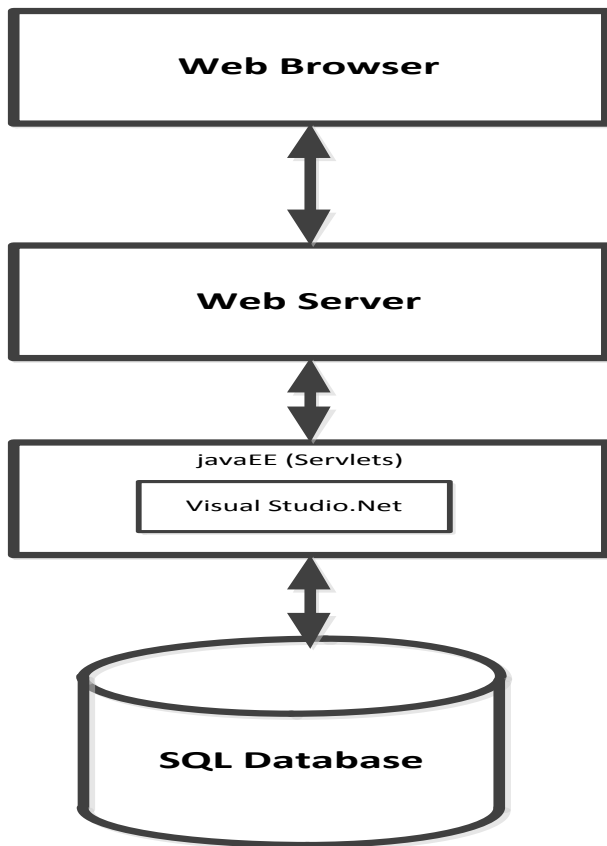


Fig. 2 Organization of WEDSS

Database: The tourism data was gathered under various categories, which constitute various tables in the designed database following a relational database model format. The database will be developed using MySQL

#### V. CONCLUSION

In this study; WTDSS (Web-Based Expert Decision Support System) intended to provide tourism information for tourists visiting the Nigeria will be developed. The development of WEDSS will have all necessary and required data to publishing on the web. The data will be stored in a data base and contain historical, cultural, geographical, and other relevant data for tourism destination. Since this system is web-based, users (tourists) who has technical possibilities to connect with the Web can have unlimited access to various information required for tourism destination in other to make a decision. The developed WEDSS will provide the tourists vital information to answer the fundamental questions such as near-by facilities, finding route, searching places of interest etc. in Nigeria. Using this kind of system increases convenience and efficiency in tourism activities by providing information for decision support in order to save money, manpower and time.

#### Advantages of proposed system

ICTs application are changing significantly the ways in which traditional destination management activities (i.e., Planning, Development, Marketing, Promotion, Delivery,

Management, Coordination and Monitoring of destination's offering) are being carried out.

The same can be said for planning and development as well as for almost all the other destination management activities. So ICTs application can produce a number of benefits for Tourism destination management activities in terms of:

- Enable potential tourists to make pre-plan before embark on tourist.
- Reducing costs, for instance lowering the need to print and distribute promotional material.
- reducing times needed for undertaking activities, for instance the collection and analysis of tourism data, while at the same time increasing their effectiveness (e.g. augmenting periodicity without additional costs).
- increasing quality, for instance with the introduction of authorization processes enabling distributed editing of tourism contents, ensuring up-to-dating as well as precision and truthfulness of information provided;
- increasing effectiveness, for instance through the delivery of targeted promotional campaigns for specific high-value segments or even individuals (using CRM applications) or using web-based learning systems for vocational training, ensuring a wider diffusion of knowledge and competences

REFERENCES

- [1] Archibong, Maurice (2004-03-18). "Nigeria: Gold mine waiting to be tapped". The Sun Online (The Sun Publishing Ltd.). Retrieved 2012-12-13.
- [2] Nigeria starts taking tourism sector seriously". afrol.com (afrol News). Retrieved 2013-01-21.
- [3] Honourable Minister of Culture, Tourism and National Orientation". UNESCO.org. UNESCO. Retrieved 2012-06-21
- [4] Ekunkunbor, Jemi (2012-10-22). "Beauty queens have duties to perform- Barrister Nike Agunbiade". Vanguard online (Vanguard Media Limited). Retrieved 2013-01-11.
- [5] Abuja beckons new Miss Tourism Nigeria". The Sun Online (The Sun Publishing Ltd.). 2001-10-05. Retrieved 2007-06-21.
- [6] Ekunkunbor, Jemi (2006-12-24). "Winning Miss Tourism is more than an Xmas gift — Gloria Zirigbe". Vanguard online (Vanguard Media Limited). Archived from the original on 2007-01-15. Retrieved 2007-06-21.
- [7] Nigeria". Wttc.org. World Travel and Tourism Council. Retrieved 2007-06-21.
- [8] <http://www.nacd.gov.ng/ministry%20of%20culture%20and%20tourism.htm>
- [9] Bousset, J. P., Skuras, D., Tesitel, J., Marsat, J. B., Petrou, A., Fiallo-Pantziou, E., Kusova, D. and Bartos, M., "A Decision Support System for Integrated Tourism Development: Rethinking Tourism Policies and Management Strategies", *Tourism Geographies*, vol. 9(4), 2007, pp. 387–404.
- [10] Buhalis, D., "Information technologies as a strategic tool for economic, cultural and environmental benefits enhancement of tourism at destination regions", *Progress in Tourism and Hospitality Research*, 3(1), 71–93, 1997.
- [11] Buhalis, D., *eTourism: Information Technology for Strategic Tourism Management*. Financial Times/Prentice Hall, London, 2003.
- [12] UNCTAD, *The Information Economy Report 2005*, New York and Geneva, pp. 142-186, 2005
- [13] UNWTO, *Using Cluster-Based Economic Strategy to Minimize Tourism Leakages*, Madrid, 2003
- [14] Werthner, H. and Klein, S. *Information Technology and Tourism - A challenging relationship*. Springer-Verlag. Wien-New York, 1999.

AUTHORS PROFILE

**Yekini Nureni Asafe**, obtain his academic degree from Lagos State College of education Ijanikin (NCE Physics Education), Lagos State University Ojo (Bsc Computer electronics and engineering), and University of Lagos (Msc Computer Science). He is an academic Staff in the department of computer technology, yaba college of technology, lagos nigeria. He is a member of Nigeria Computer Society (NCS), Member International Association of Engineers (IAENG) and Member International Association of Computer Science and Information Technology (IACSIT)

**Adetoba Bolaji**, obtain her academic degree from, Obafemi Awolowo University, Ile-ife (Bsc Computer Sciences), University of Lagos (Msc Computer Science), She is an academic Staff in the department of computer technology, yaba college of technology, lagos nigeria. She is currently a researcher in the department of computer science university of Abeokuta Nigeria. She is a member of Nigeria Computer Society (NCS), Computer Professional Council (CPN).

**Aigbokhan Edwin Enaholo**, obtain her academic degree from, University of Benin, (Bsc Computer Sciences), University of Lagos (Msc Computer Science), he is an academic Staff in the department of computer technology, yaba college of technology, lagos nigeria. He is currently a researcher in the department of computer science university of Lagos Nigeria. He is a member of Nigeria Computer Society (NCS), Computer Professional Council (CPN).

**Olufemi Olubukola** (HND, MRT, TTC), she has a wide experience in hospitality and hotel management. She is currently a principal lecturer in the department of Hospitality Leisure and Tourism Management, Yaba College of Technology, Lagos Nigeria. She is a member of Nigeria Hotel and catering Institute, Hospitality and Tourism Management Association of Nigeria.

# Category Decomposition Method for Un-Mixing of Mixels Acquired with Spaceborne Based Visible and Near Infrared Radiometers by Means of Maximum Entropy Method with Parameter Estimation Based on Simulated Annealing

Kohei Arai

Graduate School of Science and Engineering  
Saga University  
Saga City, Japan

**Abstract**—Category decomposition method for un-mixing of mixels (Mixed Pixels) which is acquired with spaceborne based visible to near infrared radiometers by means of Maximum Entropy Method (MEM) with parameter estimation based on Simulated Annealing; SA is proposed. Through simulation studies with spectral characteristics of the ground cover targets which are derived from spectral library and actual remote sensing satellite imagery data, it is confirmed that the proposed method works well.

**Keywords**—category decomposition; mixed pixel; satellite remote sensing; maximum entropy method; simulated annealing; spectral library

## I. INTRODUCTION

Linear models for un-mixing are based on: (1) a maximum likelihood method (Settle, 1996 [1]; Matsumoto et al., 1991 [2]); (2) a least squares method with constraints (Chang, 2003 [3]; Arai et al., 1995 [4]); (3) spectral feature matching (Mazer, 1988 [5]); (4) a partial space projection technique (Chang et al., 1998 [6]; Arai et al., 2002 [7]); (5) a rectangular partial space method (Harsanyi et al., 1994 [8]). Other than these, there is standard method; Principal Component Analysis (PCA) based un-mixing. In essence, the PCA based method is almost identical least square method without constraint. The least squares method with constraints estimates a mixing ratio vector based on an end-member's spectral feature vector, using the generalized inverse matrix or the least squares, where the convex combination conditions act as a constraint. The spectral feature matching method searches and selects two or more spectral features out of many in a spectral database, and compares the mixing ratios and the spectral feature of the mixed pixel: mixel of interest.

Further studies of un-mixing methods are required for appropriate end-member determination, improvement of accuracy, reduction of processing time, etc. This paper mainly focuses on the improvement of un-mixing accuracy, and estimation of accuracy of mixing ratio.

Un-mixing methods based on partial space projection (Chang, et al., 1998 [6]; Arai et al., 2002 [7]), and rectangular partial space (Harsanyi et al., 1994 [8]), can make the spectral features of a target category more conspicuous, by mapping and combining the spectral feature of the mixel with a subspace that intersects perpendicularly with the other spectral features. The methods can also perform dimensionality reduction. Moreover, the un-mixing method based on an orthogonal subspace has a comparatively good accuracy of un-mixing, and is widely used. Furthermore, it is equivalent to un-mixing based on maximum likelihood, and also to the method of least squares.

Independent component analysis (ICA) is a technique that decomposes a given mixel into highly independent components in the spectral feature space (Parra et al., 2000 [9]). Specifically, it is assumed that a mixing ratio can express the spectral features of a mixel by taking into consideration an end-member's spectral features and their variation. The statistical model for a component and the ratio of each component are estimated by unsupervised learning. Therefore, it is a method that uses ICA with constraints. Moreover, since the orthogonal subspace method becomes ideally independent in the spectral feature after projection, it is also equivalent to ICA. For this reason, this paper shall examine un-mixing method based on the orthogonal subspace.

The subspace method with learning process has already been proposed as an image classification technique (Erkki, 1983 [10]). The basic idea is as follows: if the coordinate-axis of the subspace in the orthogonal subspace method is rotated, then classification accuracy will be improved, resulting in an appropriate angle for a high classification performance; the spectral features of a pixel are then mapped and classified into the orthogonal subspace of this optimal coordinate-axis angle.

The following section describes the proposed category decomposition (un-mixing) method based on Maximum Entropy Method: MEM with parameter estimation by using Simulated Annealing: SA followed by some experiments. Then conclusion is described together with some discussions.

## II. PROPOSED METHOD

### A. Conventional Method

Mixed pixel: Mixel is defined as the pixel which is composed with plural ground cover materials. Also un-mixing is defined as the method which allows estimation mixing ratios of the ground cover materials in the Mixels in concern. In particular for hyper-spectral radiometer data, un-mixing can be done utilizing spectral feature of the ground cover materials with a consideration of atmospheric influences. Figure 1 shows example of the spectral characteristics of the ground cover materials which are included in the Mixels in concern. There are specific absorption characteristics to the ground cover materials. Specific absorption characteristics can be observed with hyper-spectral radiometers. Absorption wavelength intervals, depth of the absorption, and center wavelength of absorption can be used as spectral absorption characteristics and also used as features for discrimination of types of ground cover materials and also for un-mixing.

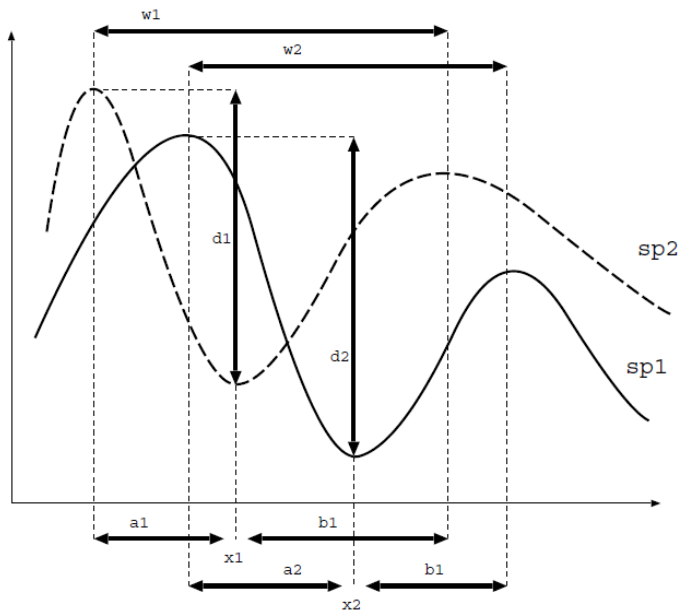


Fig. 1. Example of the spectral characteristics of the ground cover materials

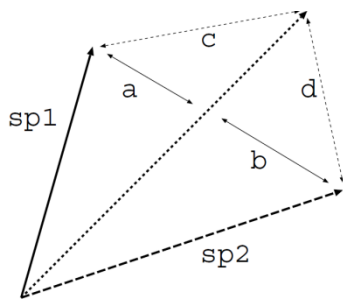


Fig. 2. Feature vectors of the spectral characteristics of ground cover materials

Figure 2 shows the vectors, sp1 and sp2 of the end member of the ground cover materials together with the unknown vector of the Mixel in concern (dotted line). Mixing ratios of sp1 and sp2 can be estimated with the ratio of c and d.

There is another conventional method so called ‘‘SVD method’’. Hyper-spectral data represented by vector  $Y$  can be expressed as follows:

$$Y = \begin{bmatrix} y_1 \\ y_2 \\ \vdots \\ y_n \end{bmatrix} = \begin{bmatrix} m_1 \\ m_2 \\ \vdots \\ m_m \end{bmatrix} \begin{bmatrix} z_{11} & z_{12} & \dots & z_{1n} \\ z_{21} & \dots & \dots & z_{2n} \\ \vdots & \vdots & \vdots & \vdots \\ z_{m1} & \dots & \dots & z_{mn} \end{bmatrix} = mZ \quad (1)$$

where  $m$  denotes mixing ratio vector of each ground cover target no.1 to  $m$ , while  $Z$  denotes the spectral characteristics of the ground cover target such that if the inverse matrix of  $Z$  is existing then the mixing ratio vector can be estimated as follows,

$$m = YZ^{-1} \quad (2)$$

It is, however, not always true that the inverse matrix exists. In order to solve this problem, regularization techniques with constraints, a prior information, etc., have been proposed. One of those is the generalized inverse matrix, or so called ‘‘Moore-Penrose’’ inverse matrix that is derived from Singular Value Decomposition (SVD). If  $Y$  is expressed with SVD as follows:

$$X = u^t Y v \quad (3)$$

where  $u$  and  $v$  are orthogonal vectors, then the Moore-Penrose generalized inverse matrix  $Y^+$  is expressed by the following equation:

$$Y^+ = v^t Y u \quad (4)$$

Therefore, if  $u$  and  $v$  can be calculated then the generalized inverse matrix can also be calculated. This method is referred to the conventional SVD based method hereafter.

### B. Proposed Un-Mixing Method

The proposed un-mixing method is based on Maximum Entropy Method: MEM which is described in the next section. MEM allows finding maximum probability of the unknown vectors of the Mixels in concern with a possible combination of ground cover materials. The basic idea of the proposed un-mixing method is that mixing ratios of the ground cover materials in the Mixels in concern can be estimated at the maximum probability of the unknown vectors of Mixels in concern. The maximum probability is equal to maximum entropy. Therefore, MEM can be utilized for this process.

Through maximizing process, unknown parameters have to be determined. The unknown parameters are in both sides of the equation. Therefore, iteration process is required to determine the unknown parameters. Although there are many iteration methods, Most Steepest Descent method, Conjugate Gradient method, etc., there is only one method, Simulated Annealing: SA method that gives a global optimum solution. The other methods give local minima, not the global optimum. Therefore, SA is used for parameter determination.

### C. Maximum Entropy Method

Maximum Entropy Method: MEM is used for learning processes for maximizing combined entropy in two layered neural network



$$y_i = g(\sum_{k=1}^2 w_{ik} x_k - \theta_i) \quad (5)$$

$$g(v) = 1 - e^{-v} / 1 + e^{-v} \quad (6)$$

where  $x, y$  notes input and output signals, or images while  $w$  denotes weighting coefficients of two layered neural network.  $\theta$  denotes a threshold.  $g(v)$  is called sigmoid function.

The combined entropy can be expressed with the equation (7).

$$H(y) = \langle \ln(|J|) \rangle - \langle \ln(p(x)) \rangle \quad (7)$$

where  $J$  denotes Jacobian matrix as shown in equation (8)

$$J = \det \begin{pmatrix} \partial y_1 / \partial x_1 & \partial y_1 / \partial x_2 \\ \partial y_2 / \partial x_1 & \partial y_2 / \partial x_2 \end{pmatrix} \quad (8)$$

Because the second term of the equation (7) is constant, the following equation (9) has to be maximized.

$$I = - \langle \ln(|J|) \rangle \quad (9)$$

It used to be said that blind separation can be done by Maximum Entropy Method (MEM) theoretically if the mixed voice sounds is distributed as Generalized Gauss Function (GGF) and if the mixing ratio of the target voice sounds is greater than a certain level. It, however, used to be distributed as non-GGF distribution and the mixing ratio of the target voice sounds is not so high. Then it becomes difficult to separate the target voice sounds from the mixed voice sounds signals. In order to fit the distribution of mixed voice sounds to GGF distribution, the method using high frequency component of MRA is proposed [11].

In general, if the wavelet transformation is applied to the target voice sounds and the other voice sounds individually, then irregularly distributions are used to be obtained for low frequency component. Turns out, high frequency component derived from the wavelet transformation for the mixed voice sound signals shows GGF distributions. Therefore high frequency component of the target voice sounds become separable to the other voice sounds because learning converged neural network may output the high frequency component of the target voice sounds and the other voice sounds if the high frequency components of the target voice sounds and the other voice sounds are input to the neural network. Thus the histogram of the high frequency component of the mixed voice sounds after the wavelet transformation is followed by the GGF distribution after the learning process of the neural network is converged.

If low frequency components of the target voice sound and the other voice sound signals are input to the neural network, the low frequency components of the target voice sound and the other voice sound are output from the neural network after the learning process is converged results in the target voice sound is reconstructed based on inverse wavelet transformation because the mixing ratio of the target voice sound and the other voice sound is not changed.

The separability of the proposed method depends on how the histogram of the high frequency component is similar to the GGF distribution and the kurtosis of the histogram. In

general, the GGF likeness is not so bad while the kurtosis is not so good. The blind separation method proposed here is to improve the separability through enhancement and improvement the GGF likeness and the kurtosis.

#### D. Simulated Annealing

Simulated annealing utilizes Metropolis algorithm (Metropolis *et al.* 1953 [12]), in which some trades that do not lower the mileage are accepted when they serve to allow the solver to "explore" more of the possible space of solutions. Such "bad" trades are allowed using the criterion that

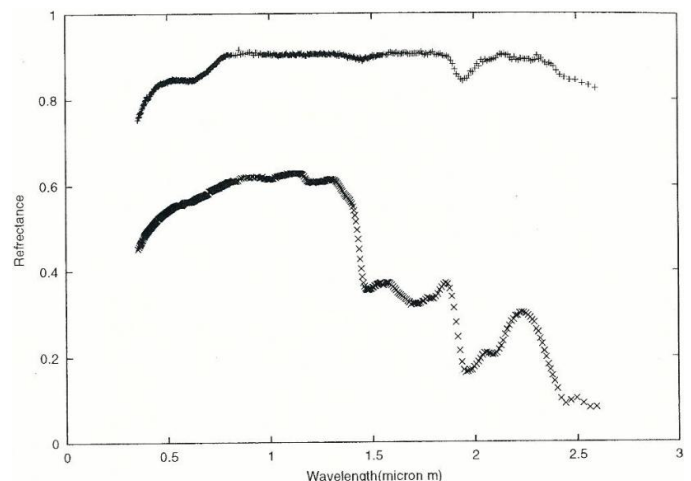
$$e^{-\Delta D/T} > R(0, 1), \quad (10)$$

where  $\Delta D$  is the change of distance implied by the trade,  $T$  is a "synthetic temperature," and  $R(0, 1)$  is a random number in the interval  $[0, 1]$ .  $D$  is called a "cost function," and corresponds to the free energy in the case of annealing a metal. In the case of the temperature parameter would actually be the  $kT$ , where  $k$  is Boltzmann's Constant and  $T$  is the physical temperature, in the Kelvin absolute temperature scale. If  $T$  is large, many "bad" trades are accepted, and a large part of solution space is accessed. Objects to be traded are generally chosen randomly, though more sophisticated techniques can be used.

### III. EXPERIMENTS AND SIMULATIONS

#### A. Simulation Method

From the Unites State of America Geological Survey: USGS web site so called "Spectral Library", spectral characteristics (surface reflectance) can be retrieved for huge number of ground cover materials. In the library, two ground cover materials which show a good correlation between both spectral characteristics are chosen. Also two ground cover materials which show a poor correlation between both are selected. Moreover, ground cover materials which show a middle level of correlation are used. These are shown in Figure 3. 437 spectral channels ranged from 500 nm to 2500 nm of wavelength region of spectral characteristics are used.



(a) Poor Correlation (R=0.0009)

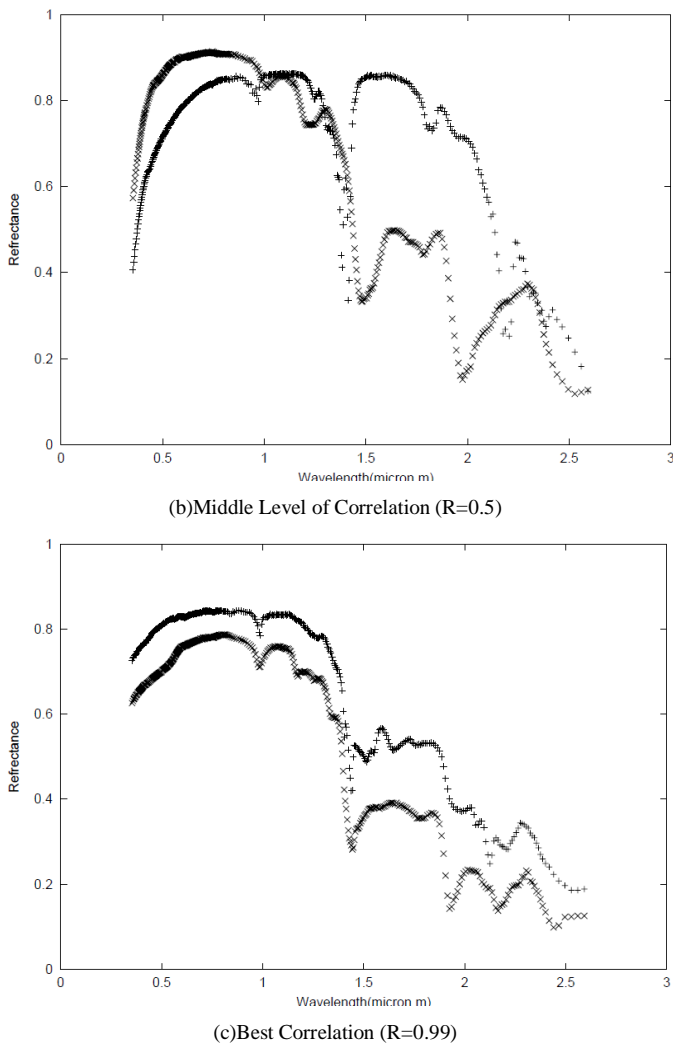


Fig. 3. Examples of the selected two ground cover materials of spectral characteristics which show a good a middle level and a poor correlation between both spectral characteristics

Using these spectral characteristics, un-mixing by means of the proposed MEM based un-mixing method is attempted with changing mixing ratio as well as additive noises. 0.5 of mixing ratio of Mixels are generated for simulation study.

Root Mean Square Error: RMSE between designated and estimated mixing ratios is evaluated. The RMSE is evaluated for both the conventional SVD based method and the proposed method.

### B. Simulation Method

RMS error of the un-mixing error between designated mixing ratio and estimated mixing ratio is evaluated as function of additive normal distributed noises which is generated using random number generator with zero mean and standard deviation of “noise” based on Messene Twister for the three cases of correlation, poor, middle level and maximum.

The evaluation results are shown in Figure 4. Figure 4 (a) shows relation between RMS and noise standard deviation for the poor correlation case while Figure 4 (b) shows that for the

middle level of correlation case. Meanwhile, Figure 4 (c) shows that for the case of maximum correlation.

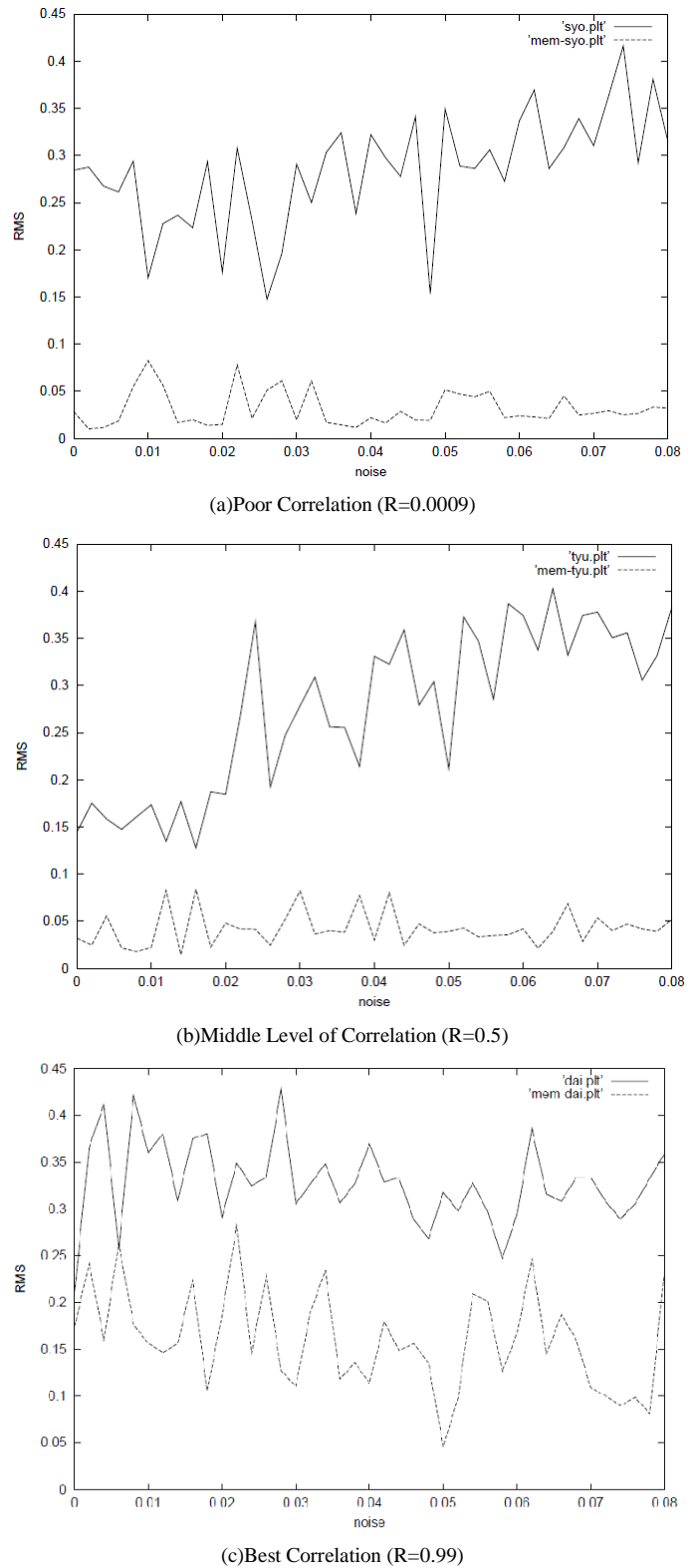


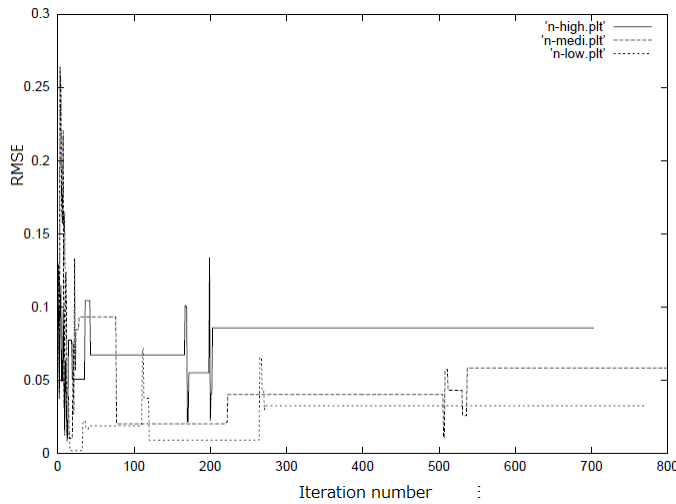
Fig. 4. RMS error

Figure 4 shows RMS errors for conventional SVD method and the proposed MEM based method. As shown in Figure 4,

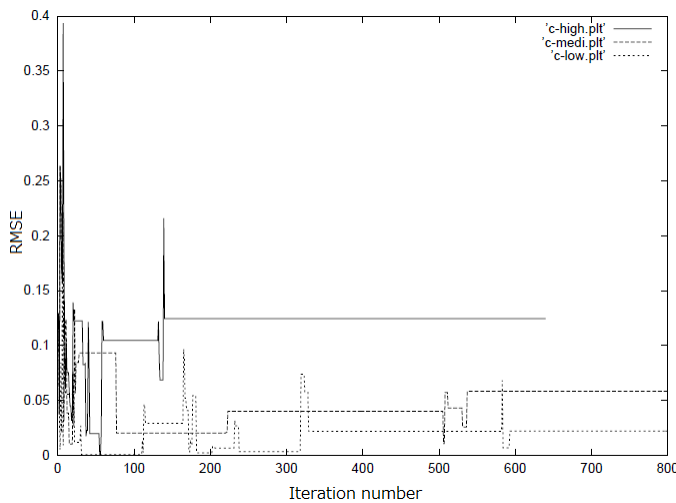
RMS error of the proposed MEM based method is always lower than that of the conventional SVD based method. Therefore, it is said that the proposed un-mixing method is superior to the conventional method.

It also shows that RMS error depends on correlation. Namely, it is hard to estimate mixing ratio when the Mixel is composed with highly correlated spectral characteristics of ground cover materials for both the conventional and the proposed un-mixing methods.

Convergence processes for the iteration are shown in Figure 5. Figure 5 (a) shows noise dependency on RMS error while Figure 5 (b) shows correlation dependency on RMS error. Much longer time is required for convergence process for greater noise and highly correlated ground cover materials.



(a)Noise dependency



(b)Correlation Dependency

Fig. 5. Convergence processes for the iteration of the proposed MEM based method for a various noises and correlation between ground cover materials of the Mixels for simulation study

In accordance with the number of categories which is changed from the poorly correlated ground cover materials from two to 10, RMS error the proposed MEM based method

is increased as shown in Figure 6. Correlation coefficients of 10 of combinations of ground cover materials are as follows,

- 0.990
- 0.893
- 0.796
- 0.676
- 0.589
- 0.465
- 0.329
- 0.202
- 0.096

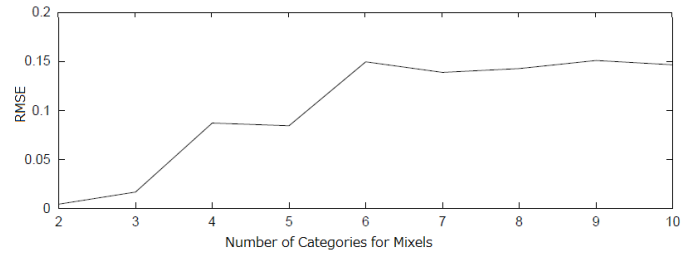
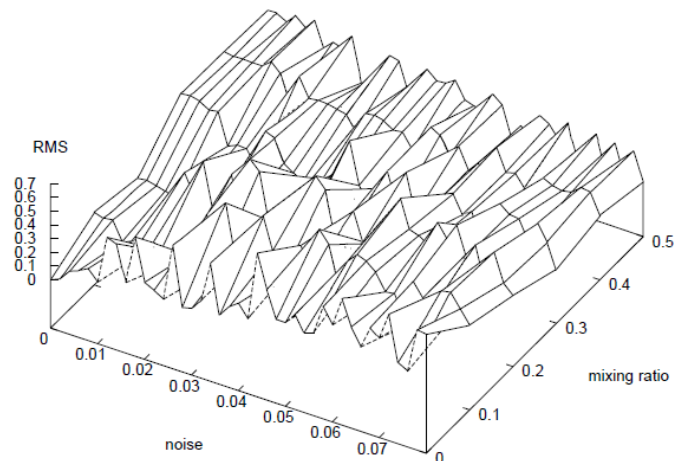


Fig. 6. Relation between the number of categories (ground cover materials) and RMS error for the proposed MEM based un-mixing method.

The relation of Figure 6 shows that RMS error is increased with increasing of the number of ground materials from two to six, then it is gradually increased form the number of ground materials is six. This trend is almost same for the other cases of middle level of correlation as well as highly correlated ground cover materials.

RMS error also depends on mixing ratio. Figure 7 shows relation among RMS errors for the proposed MEM based method (a) and the conventional SVD based method (b), noise, and mixing ratio. RMS errors of the proposed un-mixing method are almost lower than those of the conventional method. RMS error decreases in accordance with increasing of mixing ratio. Also RMS error increases in accordance with increasing of noise.



(a)Proposed Method

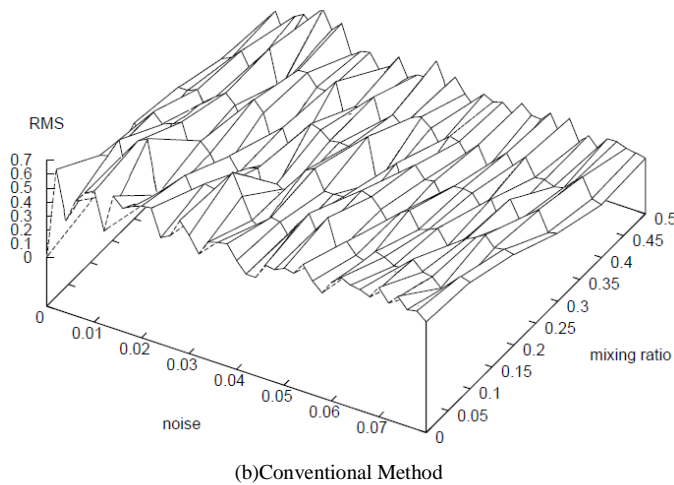


Fig. 7. Relation among RMS errors for the proposed MEM based method (a) and the conventional SVD based method (b), noise, and mixing ratio.

#### IV. CONCLUSION

Category decomposition method for un-mixing of mixels (Mixed Pixels) which is acquired with spaceborne based visible to near infrared radiometers by means of Maximum Entropy Method (MEM) with parameter estimation based on Simulated Annealing; SA is proposed.

Through simulation studies with spectral characteristics of the ground cover targets which are derived from spectral library and actual remote sensing satellite imagery data, it is confirmed that the proposed method works well.

Through simulation studies with USGS provided spectral reflectance, it is found that RMS error depends on mixing ratio. In particular, relation among RMS errors for the proposed MEM based method and the conventional SVD based method, noise, and mixing ratio shows that the proposed method is superior to the conventional method. RMS error decreases in accordance with increasing of mixing ratio. Also RMS error increases in accordance with increasing of noise

#### ACKNOWLEDGMENT

The author would like to thank Mr. Hiroyuki Nakaota for his effort to conduct experiments.

#### REFERENCES

- [1] Settle J.J., On the relationship between spectral unmixing and subspace projection, *IEEE Trans., Geosci. Remote Sensing*, 34, 1045-1046, 1996.
- [2] Matsumoto M., H. Fujiku, K. Tsuchiya and K. Arai, Unmixing by means of maximum likelihood classification, *J. of Japanese Society for Photogrammetry and Remote Sensing*, 30, 2, 25-34, 1991.
- [3] Chang C.I., *Hyperspectral Imaging: Techniques for spectral detection and classification*, New York: Kluwer Academic, 2003.
- [4] Arai K., Y. Terayama, Y. Ueda, and M. Moriyama, Adaptive least square method for estimation of partial cloud coverage within a pixel, *International J. of Remote Sensing*, 16, 12, 2197-2206, 1995.
- [5] Mazer A.S., M. Martin, et. al., Image processing software for imaging spectrometry data analysis, *Remote Sensing of the Environment*, 24, 1, 201-210, 1988.
- [6] Chang C., X. Zhao, M.L.G. Althouse, and J.J. Pan, Least squares subspace projection approach to mixed pixel classification for hyperspectral images, *IEEE Trans. Geosci. Remote Sensing*, 36, 3, 898-912, 1998.
- [7] Arai K., H. Chen, Unmixing based on subspace method with learning process, *Proceedings of the 33rd General Conference of Remote Sensing Society of Japan*, 2002.
- [8] Harsanyi J.C. and C.I. Chang, Hyperspectral image classification and dimensionality reduction: An orthogonal subspace projection approach, *IEEE Trans. Geosci. Remote Sensing*, 32, 4, 779-785, 1994.
- [9] Parra L., K.R. Muller, C. Specce, A. Ziehe, and S. Sajda, Unmixing hyperspectral data, *Advances in Neural Information Processing Systems*, 12, 942-948, 2000.
- [10] Erkki O., *Subspace methods of pattern recognition*, Research Studies Press Ltd., 1983.
- [11] Arai, K., *Lecture Note on Wavelet Analysis*, Kindai-Kagaku-sha Publishing Co. Ltd., 2006.
- [12] Metropolis N., A.W. Rosenbluth, M.N. Rosenbluth, A.H. Teller, and E. Teller. "Equations of State Calculations by Fast Computing Machines". *Journal of Chemical Physics*, 21(6):1087-1092, 1953.

#### AUTHORS PROFILE

**Kohei Arai**, He received BS, MS and PhD degrees in 1972, 1974 and 1982, respectively. He was with The Institute for Industrial Science and Technology of the University of Tokyo from April 1974 to December 1978 also was with National Space Development Agency of Japan from January, 1979 to March, 1990. During from 1985 to 1987, he was with Canada Centre for Remote Sensing as a Post Doctoral Fellow of National Science and Engineering Research Council of Canada. He moved to Saga University as a Professor in Department of Information Science on April 1990. He was a councilor for the Aeronautics and Space related to the Technology Committee of the Ministry of Science and Technology during from 1998 to 2000. He was a councilor of Saga University for 2002 and 2003. He also was an executive councilor for the Remote Sensing Society of Japan for 2003 to 2005. He is an Adjunct Professor of University of Arizona, USA since 1998. He also is Vice Chairman of the Commission "A" of ICSU/COSPAR since 2008. He wrote 30 books and published 322 journal papers